CARBON PARTITIONING IN ENGINEERED CYANOBACTERIUM FOR THE STUDY OF FEEDBACK INHIBITION OF PHOTOSYNTHESIS

By

Bradley William Abramson

A DISSERTATION

Submitted to
Michigan State University
in partial fulfillment of the requirements
for the degree of

Cell and Molecular Biology-Doctor of Philosophy

2018

ABSTRACT

CARBON PARTITIONING IN ENGINEERED CYANOBACTERIUM FOR THE STUDY OF FEEDBACK INHIBITION OF PHOTOSYNTHESIS

By

Bradley William Abramson

Cyanobacteria have promising potential to generate valuable compounds from light energy and atmospheric carbon dioxide (CO_2). Many strains have been engineered to express pathways to generate a variety of products from pharmaceuticals to biofuels. Even with cyanobacteria's high photosynthetic efficiencies most strains remain economically inviable. Many strains are grown in bioreactors where ample light and CO_2 are provided, however, photosynthetic conversion of carbon and light to useful compounds is limited. I propose photosynthesis is feedback limited, or sink limited, and the mechanisms of feedback inhibition can be alleviated in a *Synechococcus elongatus* PCC7942 strain engineered to export sucrose. By inducing expression of sucrose permease, in various salt conditions, the amount of sucrose can be tuned, which allowed us to measure a transient increase in the operating efficiency of PSII proportional to the rate of sucrose export. Concomitantly, an oxidized electron transport chain and lowered PSI acceptor side limitation were observed. These two photosynthetic parameters could be consequences of increased carbon fixation since the ratio of RbcL to PSII increases as well as greater accumulation of RbcS-GFP following sucrose export. These data suggest that sucrose export leads to greater carbon fixation and as a consequence increase light use efficiency within PSII. Furthermore, using this knowledge, we created strains that could partition carbon from growth and division to bioproduction and observed greater total and specific productivities for sucrose production. The ideas herein aid in the understanding of bioproduction strain inefficiencies and novel avenues for future genetic engineering for increased bioproduction.

ACKNOWLEDGEMENTS

This work would not have been possible without the careful guidance of Dr. Daniel Ducat. His thoughtful insights and a willingness to let me branch out on projects have made me a better scientist. Danny fostered a friendly lab environment and the close friendships developed in the lab are important on those days you have to fight for incubator space. Thanks to all my wonderful Ducat lab mates!

I must thank my guidance committee members for their careful critique of my research along the way, Dr. Christoph Benning, Dr. Beronda Montgomery, Dr. David Kramer and Dr. Federica Brandizzi. I hope my future research results in collaborations with all of you! There are no words for how much I enjoyed my time at the PRL. The community of scientists and friends I've made will endure for a lifetime. Likewise, the Cell and Molecular Biology program and the BioMolecular Science program made it possible to start my academic career. I also have to thank the Michigan State Archery organization, when I moved here they made MSU feel like home.

I cannot thank my friends and family enough for all the support they have given me through the years, Harold, Jane, Andrew, Torie. Torie you are my favorite! Obviously, I have to thank Dr. Meredith Frie for being the original awesome opossum.

And finally, to all the pets I had during my graduate career. To my fish, thanks for providing tranquility. To my bed bugs, thanks for keeping me up all night so I could study for prelims. To Stafford, it was fun while it lasted pupper. To Thalia, thanks for not barking and peacefully sleeping while I write this.

TABLE OF CONTENTS

LIST OF FIGURES

KEY TO ABBREVIATIONS

B6f, Cytochrome B6f

CA, Carbonic anhydrous

CB, Calvin-Benson

CEF, Cyclic electron flow

CCM, Carbon concentrating mechanism

CBR, Carboxysome reporter strain

CscB, Sucrose permease

DHAP, Dihydroxyacetone phosphate

FNR, Ferredoxin-NADPH reductase

Fd, Ferrodoxin

G3P, Glyceraldehyde 3-phosphate

glgC, glycogen synthase gene

HC, high carbon

LC, low carbon

M35, the short chain of CcmM running on a gel at 35kda

M58, the long chain of CcmM running on a gel at 58kda

PHB, Polyhydroxybutyrate

PBS, Phycobilisome

PC, Plastocyanin

PQ, Plastoquinone

NDH, NADPH oxidoreductase

SPS, Sucrose Phosphate Synthase

ΦII, Quantum yield of PSII

IPTG, Isopropyl β-D-1-thiogalactopyranoside

PET, photosynthetic electron transport

P700, PSI primary electron donor

qP, photochemical quenching

QY, Maximum realized quantum efficiency of PSII

rETR, relative electron transfer rate

ROS, Reactive oxygen species

rubisco, Ribulose-1,5-bisphosphate carboxylase/oxygenase

RuBP, Ribulose 1,5-bisphosphate

SPS, Sucrose phosphate synthase

SSLD, rubisco small-subunit-like-domain

Suc-Ex, Sucrose exporting strain containing CscB and SPS

Theo, Theophylline

2PG, 2-phosphoglycolate

3PGA, 3-phosphoglycerate

CHAPTER 1: INTRODUCTION

Cyanobacteria are single-celled photosynthetic organisms inhabiting most environments on Earth. These photosynthetic prokaryotes have diverse cell morphologies, and some cyanobacteria have linked cells, forming filaments or colonies, and some are free floating as single cells in freshwater or saltwater environments (Nozzi, Oliver and Atsumi, 2013). Some species also have the ability to fix atmospheric nitrogen. However, all cyanobacteria can perform photosynthesis, the cellular process whereby light and CO_2 are utilized to produce sugars for cell metabolism. Similarly, cyanobacteria have recently been the focus of research due to their potential to generate valuable compounds through metabolic processes utilizing light energy and atmospheric carbon dioxide (CO_2). This study focuses on a particular freshwater strain called *Synechococcus elongatus* PCC 7942 (hereafter *S. elongatus*), and the study of the interplay between metabolic engineering efforts and the unexpected consequences for upstream photosynthetic processes.

S. elongatus is a cyanobacterium that has inner and outer membranes as well as thylakoid membranes where photosynthetic electron transport (PET) takes place, aiding in the production of NADPH and ATP. The NADPH and ATP that is produced through the photosynthetic light reactions is used for cellular metabolism and, importantly, for carbon fixation through the Calvin-Benson (CB) Cycle. As an obligate phototroph the process of photosynthesis provides *S. elongatus* with sufficient ATP and NADPH for growth and division in the absence of other organic carbon sources. As discussed later, the carbon and energy derived from photosynthesis can be diverted in engineered strains to produce high-value products.

Engineered photosynthetic strains have the potential to provide human civilization with novel compounds while not competing with arable land in addition to lowering atmospheric carbon by using freely-available solar energy (Nozzi, Oliver and Atsumi, 2013; Hays and Ducat,

2014). Currently, most engineered strains are economically impractical because bioproduction yields are not high enough to offset cultivation and harvesting costs. Strains have been engineered to produce a wide variety of metabolites with various photosynthetically derived energy and carbon demands. While multiple strategies have been put forward to rationally engineer cyanobacterial strains for bioproduction, some of the most efficient strains have a final product designed to be exported to the extracellular space or strains producing volatile compounds that can freely diffuse out of the cell. One hypothesis is that photosynthesis is inhibited by an accumulation of excess photosynthate, termed sink limitation, and that consumption of excess photosynthate through heterologous pathways can increase photosynthetic capacity. This dissertation will discuss how sink limitation occurs in cyanobacterial strains and show sink limitation of photosynthesis can be relieved by exporting sucrose (Figure 1.1).

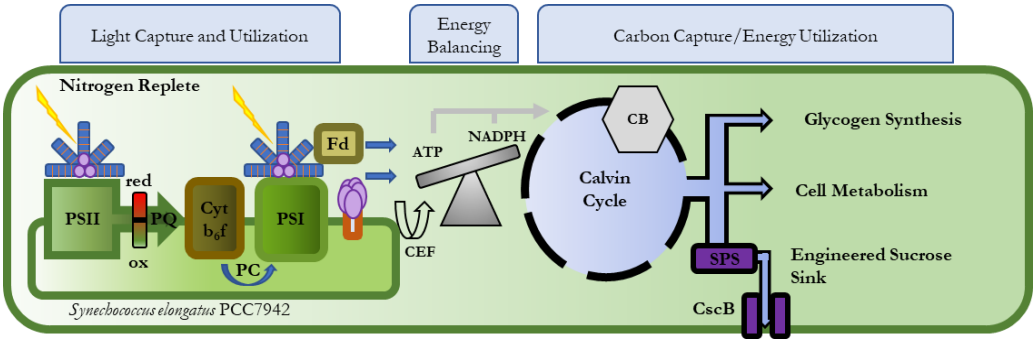

FIGURE 1.1: OVERVIEW OF PHOTOSYNTHETIC METABOLISM IN S. ELONGATUS.
See text in Chapter 1 for full description of photosynthetic production of sucrose. See "KEY TO ABBREVIATIONS" for extended names of complexes. Importantly, the engineered strain in this study expresses sucrose phosphate synthase (SPS) and sucrose permease (CscB) when IPTG is added to the medium which allows inducible control of photosynthetically-derived sucrose to be exported.

Overview of photosynthesis

Photosynthesis is the cellular process whereby numerous macromolecules, metabolites, minerals and cofactors aid in the absorption of light and fixation of CO_2 to generate carbohydrates. The carbohydrates are metabolized to sustain cellular functions (*e.g.*, as future energy reserves at night) and as the building blocks for other biomolecules, including proteins, nucleotides, and lipids. It is not uncommon for photosynthetic reactions to be categorized into the light (photon capture and conversion to transient energy pools) and dark (use of transient energy pools to fix CO_2) reactions. However, it is important to understand that both processes occur simultaneously in the light and that regulation between the two is critical, as discussed below.

Light driven electron transport

The light reactions in cyanobacteria start with light capture by the light harvesting phycobilisomes and transfer to Photosystem II (PSII) or light can be absorbed by PSII itself. Subsequent to light absorption, low-potential electrons are removed from water and transferred

through a series of protein complexes, Cytochrome b_6f (b_6f) and Photosystem I (PSI). The first step in PSII is exciton trapping by the primary chlorophyll pair, P680 in PSII, which raises the energy level of the electron. Excited electrons in P680 suffer several fates, including transfer to other electron carriers for photochemistry, dissipation as heat, or a return to a non-excited ground state through the release of a photon of light. These competing exciton fates are in direct competition and by measuring the yield of chlorophyll fluorescence, one can determine the yield or efficiency of photosynthesis.

PSII utilizes solar radiation to induce a charge separation event which oxidizes water to reduce an electron carrier chain within the PSII complex while transferring protons to the lumen and releasing molecular oxygen (O_2). The electrons are transferred through several internal PSII electron carriers, notably, to a terminal bound quinone in PSII, Q_A. Q_A transfers two electrons to the membrane-soluble plastoquinone (PQ), a PSII interacting, electron carrier (Messinger *et al.*, 2009) to reduce Plastoquinone (PQ; oxidized form) to plastoquinol (PQH_2; reduced form). Plastoquinol can then disengage from the binding pocket of PSII and diffuse through the membrane to bind the cytochrome b_6f complex.

Extensive research disentangling the mechanisms of PQH_2 mediated electron transfer to the cytochrome b_6f complex has resulted in a complex process termed the Q-cycle, which has been reviewed elsewhere (Cramer, Hasan and Yamashita, 2011; Tikhonov, 2014) One of the main tasks of the cytochrome b_6f complex is to oxidizePQH_2 and transfer the electrons to plastocyanin (PC) (Cramer, Hasan and Yamashita, 2011). The series of electron transfer events in one Q-cycle leads to the net translocation of 4 protons from the thylakoid lumen to the cytosol for each PQH_2 oxidized, and the

reduction of 2 plastocyanin proteins. Plastocyanin is a copper containing protein located in the lumen of the thylakoid and it can diffuse to the donor side of PSI.

Much like PSII, PSI holds a special chlorophyll pair, termed P700, which absorbs an additional quantum of light to induce a charge separation event furthering electron transfer events within the PET chain. Similar to the excitation of PSII, the light harvesting phycobilisome can absorb light and transfer an exciton to the primary reaction center in PSI. Light excitation of P700 induces a charge separation event generating $P700^{*}$ and leading to transfer of an electron to the primary bound electron acceptor (A_0) leaving $P700^{+}$ (oxidized form) and A_0^{-} (reduced form). $P700^{+}$ regains missing electrons by accepting an electron from reduced plastocyanin in the thylakoid lumen. A_0^{-} transfers electrons through the PSI electron transport chain to reduce a cytosolically localized oxidized ferredoxin (Fd_{ox}) becoming (Fd_{red}). Finally, ferredoxin-$NADP^{+}$ oxidoreductase (FNR) catalyzes the oxidation of two Fd_{red} and reduction of $NADP^{+}$ to NADPH yielding two Fd_{ox} which can diffuse back to PSI for future reductions. The electrons on Fd_{red} can also participate in a number of other redox reactions within the cell or be donated back into the PET chain to contribute to cyclic electron flow (CEF), which is discussed later. NADPH is the main reductant produced through photosynthesis that can be used for many cellular reactions, including in the CB cycle.

The proton gradient generated through water splitting activity of PSII and the Q-cycle both aid in the accumulation of protons in the thylakoid lumen relative to the cytosol. This gradient of protons stores potential energy across the thylakoid membrane which can be separated into a gradient composed of differential proton concentrations (ΔpH) and charge gradients ($\Delta\Psi$) across the thylakoid membrane. The gradient is utilized by ATP synthase, a large complex embedded in the thylakoid membrane that allows protons to flow through while

harnessing proton flux to generate ATP from ADP and pyrophosphate (Pi) within the cytosol. The two main products of the light reactions are therefore, ATP and NADPH, which can be subsequently used to power downstream biochemical reactions.

Redox homeostasis and energy balance

Although often described as the light and dark reactions of photosynthesis, the two processes are concurrent, requiring careful balancing of ATP and NADPH production and the cellular process that consume these metabolites. If ratios of ATP:ADP or NADPH:$NADP^+$ drastically decrease, cellular processes requiring these metabolites will become limited. However, photosensitization of PSII can occur if electron carriers within PSII become over-reduced. The short lifetime of reduced electron carriers within PSII can lead to redox reactions with molecular oxygen. The likelihood of redox chemistry with molecular oxygen increases as PSII electron carriers remain reduced due to a lack of electron acceptors in the downstream PET chain (e.g. PQ). Therefore, as photosynthetic electron transfer becomes limited or the PET chain becomes over-reduced, PSII is more likely to become photosensitized and reduce molecular oxygen generating toxic Reactive Oxygen Species (ROS) within the cell (Pospísil, 2009).

The redox status of critical electron carriers within the cell can quickly change in response to light and can be directly sensed to regulate the activity of a number of metabolic pathways, thus avoiding energetically wasteful futile cycles (Michelet *et al.*, 2013). As an electron carrier involved in both photosynthesis and respiration, the redox status of the PQ pool is a critical indicator in cyanobacteria (Cameron, 2011; Schuurmans *et al.*, 2014, Mullineaux, 2014a). Since PQ is central to vital to several cellular processes tight regulation of the redox status of the PQ pool is maintained (Schuurmans *et al.*,

2014). If the PQ pool becomes too reduced, then the likelihood of electron transfer from Q_a within PSII to PQ decreases, accelerating the rate of electron transfer to oxygen and ROS accumulation (Pospísil, 2009). If PQ is too oxidized there is insufficient reduction of PSI, which limits the cell of reducing power by limiting NADPH production.

The redox-regulated state transition is one mechanism to distribute energy between PSII and PSI to maintain PQ redox homeostasis (Mullineaux and Allen, 1990; Campbell and Oquist, 1996). The mechanisms and protein complexes involved in state transitions are vastly different in cyanobacteria and plants although the concept of partitioning energy to the photosystems is conserved. For the sake of this dissertation I focus on the cyanobacterial state transition. In cyanobacteria, the phycobilisome (PBS) captures light and distributes absorbed excitation energy to PSII (State I) or PSI (State II) (Mullineaux and Allen, 1990). By distributing energy to PSII more electrons can be inserted into the PET chain reducing PQ, whereas greater energy partitioned to PSI will withdraw electrons from the PET chain thereby oxidizing the PQ pool. Ultimately, the redox status of the PQ pool determines the "State" and energy partitioning by the phycobilisome (Mullineaux and Allen, 1990; Mao *et al.*, 2002). In general, *S. elongatus* is in State II in the dark and State I in the light (Tsimilli-Michael, Stamatakis and Papageorgiou, 2009). However, the molecular mechanisms leading to the cyanobacterial state transition remain unclear (Chukhutsina *et al.*, 2015; Ueno *et al.*, 2016).

The stoichiometry of ATP/NADPH produced in the photosynthetic linear electron transfer reactions can be different than the ATP/NADPH needed for carbon fixation. CEF is one mechanism whereby the ATP/NADPH ratio can be altered. In cyanobacteria, the linear flow of electrons produce roughly 1.2 ATP/NADPH compared with the need of 1.5ATP/NADPH to complete the CB cycle (Kramer and Evans, 2011; Maarleveld *et al.*, 2014). Therefore, more ATP

must be produced per NADPH produced. To accomplish this, Fd_{red} can inject electrons back into the electron transport chain upstream of b_6f (Battchikova *et al.*, 2011). This allows b_6f to increase the number of protons transferred to the lumen per electron transferred through the PET chain, increasing the ratio of ATP/NADPH produced. Likewise, a pseudo-CEF pathway can alter the ATP/NADPH ratio produced through a NAPDH dependent reduction of cytosolic O_2 back to H_2O, therefore producing ATP without producing reductant, termed the water-water cycle (WWC) (Allahverdiyeva *et al.*, 2013). These processes are dynamic, and the exact ATP/NADPH ratio can be met depending on cellular demands (Mullineaux, 2014b).

Finally, a direct link between redox status and enzymatic activity is mediated through redox-mediated disulfide bond protein linkages which alter metabolic flux through key pathways (Trost *et al.*, 2006; Michelet *et al.*, 2013). When cytosolic redox carriers become more oxidized, protein thiol groups can become covalently linked by a disulfide bond (Trost *et al.*, 2006). However, when the photosynthetic redox carriers are in a relatively reduced state they may transfer electrons (e.g., through thioredoxins) to disulfide bonds, breaking the covalent disulfide bridges. In contrast, formation of covalent bonds between cysteines can restrict the degrees of freedom in protein conformational states, while reduced cystines do not limit the flexibility in the amino acid backbone. The switch between these two conformational states within a single protein can activate or inhibit the enzymatic activity, and several CB cycle proteins are redox-regulated by disulfide bonds either directly or indirectly (Michelet *et al.*, 2013).

Calvin cycle and carbon capture

The ATP and NADPH produced in the light reactions are utilized in many cellular processes, yet substantial amounts of the ATP and NADPH are consumed to fix CO_2 in the CB the CB cycle. The first step in carbon fixation is through the enzyme Ribulose-1,5-bisphosphate carboxylase/oxygenase (rubisco) which catalyzes the carboxylation of Ribulose 1,5-bisphosphate (RuBP) by CO_2 to form two molecules of 3-phosphoglycerate (3PGA). The molecules of 3PGA then enter the reduction phase of the CB cycle whereby 3PGA is phosphorylated consuming ATP and producing 1,3-bisphosphoglycerate and ADP. This is then reduced with NADPH to form glyceraldehyde-3-phosphate (G3P), $NADP^+$ and Pi. G3P can be isomerized into dihydroxyacetone phosphate (DHAP) and collectively they are referred to as the triose phosphate pool. Triose phosphates can reenter the CB cycle, or be withdrawn to be used in a variety of downstream processes; thus, triose phosphates are often thought to be the main product of the CB cycle. However, any intermediate can be siphoned from the CB cycle for further processing, especially in cyanobacteria, since the CB cycle takes place in the cytosol.

The first fixation reaction presents a problem whereby RuBP is consumed and needs to be replenished before further CO_2 fixation is to occur. Therefore, some of the G3P is recycled through several carbon shuffling reactions. The reactions leading to the regeneration of RuBP are energetically costly and generation of a single molecule of G3P requires consumption of 9 ATP and 6 NADPH . Several molecules of G3P must be produced to fuel the CB cycle for regeneration of RuBP, however some G3P molecules can be siphoned off to several metabolic pathways. One fate of G3P is the metabolic conversion to glucose and subsequent storage in glycogen, which is the main carbon storage product of photosynthesis in cyanobacteria.

Carbon concentrating mechanisms

The high photosynthetic efficiency of cyanobacteria comes, in part, from the concentrating mechanism (CCM) (Daley *et al.*, 2012). Rubisco can also participate in an oxygenation reaction whereby O_2 is fixed instead of CO_2, generating one molecule of 3PGA and one molecule of 2-phosphoglycolate (2PG) (Hackenberg *et al.*, 2012). Not only is the oxygenation reaction energetically wasteful, 2PG is toxic to the cells and must be processed through an energy-consuming photorespiration pathway (Hackenberg *et al.*, 2009), resulting in the conversion of 2PG to 3PGA. The CCM is an elaborate system that cyanobacteria utilize to concentrate CO_2 near rubisco, which can both increase substrate availability for rubisco, maximizing catalytic rates while also greatly suppressing photorespiration by outcompeting O_2 from the active site (Rae *et al.*, 2013). The process starts with active transport of bicarbonate and CO_2 from the extracellular space to the cytosol through several integral membrane proteins located in the plasma membrane (Kamennaya *et al.*, 2015). This process concentrates bicarbonate in the cytosol.

Next, the bicarbonate is further concentrated within the carboxysome, a proteinaceous body, housing rubisco, carbonic anhydrase (CA) and structural proteins (Long *et al.*, 2010; Rae *et al.*, 2012, 2013). It is thought the protein shell is impermeable to O_2, but it is unclear how bicarbonate passes through (Marcus, Berry and Pierce, 1992); however, charged metabolite selectivity has been shown in other types of bacterial microcompartments (Chowdhury *et al.*, 2015). Internal carboxysome CA converts transported bicarbonate into CO_2, the substrate for rubsico (Daley *et al.*, 2012). Therefore, the CCM increases the carboxylation ability of rubisco while minimizing the

amount of oxygenation performed, thus limiting the energy wasted through photorespiration.

The structure of the carboxysome is known to respond to changes in the external environment, including light and CO_2 availability, although the regulatory mechanisms controlling this process are still being actively researched (Eisenhut *et al.*, 2007; Sun *et al.*, 2016). For example, it has been shown the number of carboxysomes increases per cell when as the intensity of incident light is increased, but the molecular basis for this adaptation is not known (Sun *et al.*, 2016). Interestingly, research has solely focused on the carboxysome response to external environmental perturbations. Indeed, there has not been any research into the carboxysome response to solely internal metabolic demand, such as when heterologous sink pathways are activated in static environmental conditions. This will be discussed further in Chapter 3.

Overview of cyanobacterial bioproduction strains

Cyanobacteria are rapidly becoming economically viable solar factories for the production of many chemicals or proteins due to their high photosynthetic efficiencies. Some products can be obtained from natural strains such as, plastic-like PHB from *Synechocycstis sp*. PCC 6803 or food-colorant phycobiliproteins from *Phormidium sp* (Tsang, Roberson and Vermaas, 2013; Khazi, Demirel and Dalay, 2018). Indeed, the molecular toolkit and engineering amenability of cyanobacteria is rapidly developing. This has led to an expanding repertoire of compounds not naturally produced in cyanobacteria. Numerous reviews have been written categorizing cyanobacterial production strains therefore only the salient points will be discussed here (Ducat, Way and Silver, 2011; Yu *et al.*, 2013; Lau, Matsui and Abdullah, 2015).

Several model cyanobacterial strains can be readily genetically modified and, in these organisms, targeted gene knock-outs/knock-ins for pathway modification are relatively simple.

As will be discussed, the particular bioproduct of interest will determine the metabolic pathways that should be modified and influence the genetic elements needed to produce a bioproduction strain. However, there are some engineering methods that appear to increase bioproduction of many different target compounds, independent of the particular product of interest, for example by restricting endogenous pathways. An open question remains as to how the cell responds to changes in metabolic sink demand, such as through restriction of endogenous sinks especially when increased metabolic burden has been introduced from heterologous production pathways.

Molecular pathway construction: "Pull" engineering methods

Bioengineers routinely introduce heterologous metabolic pathways into cyanobacteria to create strains capable of producing novel compounds from photosynthetic metabolism, however these pathways must be optimized in order to attain a productivity that is viable for large-scale applications. The introduced pathways most commonly rely on withdrawal of central carbon intermediates that act as building blocks (Ducat, Way and Silver, 2011; Lai and Lan, 2015) and can be conceptualized as "pulling" these intermediates towards the end-product. Sometimes, synthesis of the desired end-product only requires introduction of a single protein that catalyzes a final missing step in a metabolic pathway, examples include: ethylene (Ungerer *et al.*, 2012; Zhu *et al.*, 2015); or isoprene (Lindberg, Park and Melis, 2010). Alternatively, the production of some products require expression of several enzymes or the construction of entire pathways, including those for ethanol (Deng and Coleman, 1999); 1,3-propanediol (Hirokawa *et al.*, 2016); isobutryaldehyde (Atsumi, Higashide and Liao, 2009); or isopropanol (Kusakabe *et al.*, 2013). Successfully expressing the heterologous pathway is often relatively simple

in comparison to the process of improving flux through the pathway and increasing overall end-product yield.

Engineered strains often have limited productivity partly because engineered heterologous pathways compete with metabolites normally used by endogenous pathways. Often, a newly introduced pathway is not an effective competitor for metabolic intermediates compared to endogenous pathways within the cell. Therefore, increasing flux into the desired product pathway is critical. One broad class of strategies for improving flux through a target pathway can be designated as those that act to increase the rate of withdrawal of precursor metabolites, or the rate of "pulling" carbon towards the target end-product. Several engineering approaches have been used to increase carbon flux into the bioproduction pathway by improving enzymatic productivity and by balancing substrate availability within the cell (Angermayr, Paszota and Hellingwerf, 2012). Angermayer et. al. showed expression of a transhydrogenase improved availability of NADH as a substrate for the co-expressed NADH-consuming lactate dehydrogenase and thus increased flux to a lactate production pathway. However, in this case, transhydrogenase expression was toxic to the cell and lead to decreased cellular growth which could only be partially rescued when co-expressed with the lactate dehydrogenase. A similar approach would the modification of the bioproduction protein's binding site, altering the binding specificity of key enzymatic substrates (e.g. modifying the NADH binding site to utilize NADPH; Park and Choi, 2017). Balancing substrates for bioproduction enzymes has therefore been shown to increase bioproduction, however the decrease in cellular fitness caused by such modifications would not be viable in industrial bioproduction strains.

In general, optimization of the expression of heterologous bioproduction transgenes and translation of enzymatic proteins can be improved by increasing expression of the engineered

transgene. One approach is to modify the promoter such that mRNA expression is improved which can improve protein production and a greater amount of protein in the cell can consume excess metabolic intermediates when metabolites are in abundance (Hirokawa, Maki and Hanai, 2017). Similarly, increased isoprene production has been observed by overexpressing isoprene synthase with an N-terminal fusion of the highly expressed *cpc* gene (Chaves *et al.*, 2017). These strains essentially "pull" metabolites into the bioproduction pathway by creating an overabundance of the heterologous enzyme to react with cellular metabolite pools, and this approach can be effective if the enzymes catalyze rate-limiting or irreversible reactions. In these cases, increasing protein production can lead to an overall increase in metabolic flux to the production pathway.

Engineering approaches for "pulling" metabolites into production pathways can be a time-consuming process and can oftentimes only be applied to a single endpoint metabolite or pathway. Strains engineered to produce a bioproduct by overexpressing an enzyme or pathway can be improved upon by addition of another engineering strategy aiding the diversion of metabolites from endogenous sinks to bioproduction pathways to increase productivity.

Endogenous sink restriction: "Push" engineering methods

Several strategies have been employed to limit metabolic flux to endogenous pathways, with the goal of diverting metabolites to heterologous production pathways. These strategies include nutrient limitation which leads to decreased growth and greater partitioning of carbon to alternative sinks (e.g. lipids)(Ajjawi *et al.*, 2017), genetic knockouts of endogenous pathway genes (e.g. glycogen synthase)(Ducat *et al.*, 2012; Davies *et al.*, 2014; Li, Shen and Liao, 2014) and overexpression of proteins that

decrease endogenous sink capacity (see Chapter 4). In these instances, metabolic flux is decreased to the original endogenous pathway and accumulated metabolites "spillover" into other pathways. Many engineered strains show increased productivity of the target end-product when competing endogenous pathways are inhibited. Because the goal is to substantially reroute metabolic resources towards an exogenous pathway, a common strategy is to downregulate or knockout metabolic steps that normally bear a large total flux. For example, limiting flux towards energy storage compounds that account for a large proportion of cellular carbon (e.g. glycogen/starch or lipids) can free up a large proportion of carbon resources for other metabolic activities. When used in combination with ("pull") efforts to then redirect these newly-available resources towards a target metabolite, the total productivity enhancement can be substantial.

In many cyanobacterial strains, increased productivity of multiple heterologous pathways has been achieved by removing the cells' ability to make glycogen, the major carbon storage compound accounting for 10-20% of total fixed carbon (Ducat *et al.*, 2012; Davies *et al.*, 2014; Van der Woude *et al.*, 2014; Hendry *et al.*). The last step in glycogen synthesis is catalyzed by glycogen synthase, encoded by the *glgC* gene, and Δ*glgC* cells cannot store carbon in the form of glycogen. When metabolites cannot flow into this large metabolic sink, metabolic intermediates accumulate increasing metabolic flux into unintended pathways (Gründel *et al.*, 2012). If an engineered pathway is active, then excess carbon and energy can be redirected to the engineered heterologous sink. In support of this, carbon storage knockout strains have greater productivities than strains expressing only the production pathway (Ducat *et al.*, 2012; Davies *et al.*, 2014; Van der Woude *et al.*, 2014; Veetil, Angermayr and Hellingwerf, 2017; Li, Shen and Liao, 2014).

Yet, restriction of pathways that control endogenous carbon sinks such as glycogen, PHB, or lipids can have unintended negative consequences. One possible complication arising

from endogenous sink restriction is illustrated by the increased light sensitivity often observed in Δ*glgC* strains (Jackson *et al.*, 2015). The high light stress phenotype is thought to occur in part because glycogen may represent a large metabolic sink that can buffer the system against excess solar energy induced photodamage, and without these endogenous sinks overaccumulation of metabolite pools decreases photosynthetic processes leading to the generation of toxic ROS (discussed in Chapter 4). Therefore, Δ*glgC* cells often have decreased growth and limited photosynthetic productivity (Holland *et al.*, 2016) even though the proportion of total flux to the desired end product may be improved. On possibility, discussed in greater detail in Chapter 4, is that accumulated photosynthate causing sink limitation can be readily used and partitioned into engineered heterologous pathways relieving the photosynthetic sink limitation observed from endogenous sink restriction.

Limitations to photosynthesis

The availability of light or CO_2 can limit the overall process of photosynthesis, but cells grown with excess light and CO_2 can become photosynthetically limited by the accumulation of photosynthetic end-products. If light is not available, excited electrons cannot be generated by photosystems for NADPH and ATP production, and if CO_2 is not available, the CB cycle cannot function as rubisco is lacking substrate. However, these limitations are less likely when cyanobacterial strains are grown in bioreactor-like conditions under high light intensities and high CO_2 conditions. In plants, it has been shown that the inadequate use of triose phosphates can limit photosynthetic productivity, termed sink limitation (Paul and Foyer, 2001). However, at the outset of this dissertation project, it was unclear if such limitations were also a concern for photosynthetic

efficiency in cyanobacteria, which possess significantly different cellular and biochemical features in comparison to plants. This dissertation explores the hypothesis that sink limitation of photosynthesis limits photosynthetic capacity in cyanobacterial strains.

Sink limitation in plants

Photosynthesizing cells are concurrently performing the light and dark reactions when light and CO_2 are available, but photosynthetic electron flux and carbon fixation can become limited if the fixed carbon is not utilized (Sharkey *et al.*, 1986; Paul and Foyer, 2001; Adams *et al.*, 2013). Sink limitation in plants often occurs when the capacity to utilize photosynthate in non-photosynthesizing tissues (Sink tissues; e.g. roots and fruits) leads to an accumulation of sugars which limits photosynthetic productivity in actively photosynthesizing tissues (Source tissues). Sink limitation in source cells occurs when CB products increase due to decreased cellular carbohydrate demand, imbalanced photosynthetic activity or by experimentally adding carbohydrates (Demmig-Adams, Garab, *et al.*, 2014). When the CB products cannot be used effectively by the cell, sugars accumulate, stromal P_i decreases, and flux through the CB cycle slows, reducing regeneration of ribulose-5-phosphate. Ultimately, this condition can slow the rate of CO_2 fixation and decrease consumption of the energetic products of the light reactions (Adams *et al.*, 2013). Limited energy consumption then lowers electron flux and ATP synthesis clogging the PET chain, and thereby, limiting absorbed light utilization (Paul and Foyer, 2001; Takizawa, Kanazawa and Kramer, 2008).

At the start of this dissertation, sink limitation of photosynthesis had been studied mostly in plants, owing to the plants ability to partition carbon between source and sink tissues. In aggregate, plant studies have clearly demonstrated a link between sink tissue utilization of photosynthate and the efficiency of photosynthesis in source tissues (Paul and Foyer, 2001;

Quereix *et al.*, 2001; Iglesias *et al.*, 2002), yet a deeper understanding of the molecular mechanisms underlying this source/sink connection is impeded by the complexity of plants. These studies often require girdling or wounding the plant to remove either source or sink tissues which activate the wound response hindering interpretations (DaMatta *et al.*, 2008). Alternatively, researchers have shown that photosynthesis can be experimentally sink inhibited by spraying leaves with a sucrose solution (Lobo *et al.*, 2015); however, experiments that expand the exogenous sink capacity of photosynthetic cells are limited. These studies generally observe carbon partitioning between different tissue types and the photosynthetic response to limited carbon flux between tissues. However, understanding the molecular mechanisms and signals within a single source cell and correlating photosynthetic responses with certain carbon pools is difficult in plants. The multiple tissue types and cellular complexity in plants makes studying the molecular mechanisms of photosynthetic sink limitation a daunting task.

Evidence for sink limitation in cyanobacterial production strains

At the start of this dissertation, it was shown that some cyanobacterial production strains could fix more carbon when heterologous engineered pathways were active (Ducat *et al.*, 2012). Likewise, others have observed increased oxygen evolution rates, which suggest increased photosynthetic activity during heterologous pathway production (Oliver *et al.*, 2013). These observations are consistent with the idea that cyanobacterial photosynthesis might be limited by the cells ability to use sugars produced by photosynthesis or sink limitation.

In the last five years, there has been increasing evidence that algal strains are photosynthetically sink limited in bioreactor-like conditions and that heterologous

pathway production can decrease sink limitation resulting in increased photosynthetic capacity. For example, Demmig-Adams et al. 2017 showed *C. euryale* had greater photosynthetic efficiency when they were exporting glycerol (Demmig-Adams, Stewart, *et al.*, 2014; Demmig-Adams *et al.*, 2017). Similar observations suggest relief of sink limitation occurs when a non-carbon NADPH consuming P450 pathway is introduced (Berepiki, Hitchcock, Christopher Mark Moore, *et al.*, 2016) resulting in greater PET rates. Conversely, photosynthetic efficiency and NADPH consumption decrease when endogenous sinks are removed (*e.g.*, Δ*glgC*; Holland *et al.*, 2016). Likewise, endogenous sink restriction leads to an increase in sink limitation which can decrease photosynthetic capacity. In one published example, removal of glycogen as an endogenous sink led to decreased cellular growth, but this growth defect could be partially rescued when metabolites were diverted and consumed by a heterologous sink pathway (Li, Shen and Liao, 2014; Chapter 4).

This body of evidence supports the idea that processes other than light absorption or carbon fixation can limit photosynthetic productivity in engineered strains grown in bioreactor-like conditions. At the start of this dissertation, there was very little research into sink limitation in single celled phototrophic production strains. Here I show, the photosynthetic response to decreased sink limitation by heterologous sucrose export in *S. elongatus.* Specifically, in chapter 2, I show that the quantum yield of PSII increases proportionally to an increase in the rate of sucrose export. I further characterized the light reaction response showing that relative electron transport rates are increased, and sucrose export decreases the acceptor side limitation of PSI while oxidizing the PQ pool. In chapter 3, I present preliminary data that suggest carboxysome size may increase in response to sucrose export, and that induction of this heterologous sucrose sink leads to increased RbcL expression relative to PSII, while, increased RbcS-GFP expression

within the cell is observed which allows us to speculate on a mechanism for regulating carboxysome size through differential translation of CcmM. Chapter 4 then describes studies of sink limitation in growth arrested cells and how carbon can be partitioned from endogenous sinks to heterologous sinks to increase productivity of engineered strains. Finally, in chapter 5, I discuss questions that have arisen from these studies and provide a perspective on future directions that may build off of the increased understanding of the role of sink limitation in unicellular microbes towards a deeper understanding of photosynthetic metabolism.

REFERENCES

REFERENCES

Adams, W. W. et al. (2013) 'May photoinhibition be a consequence, rather than a cause, of limited plant productivity?', Photosynthesis Research, 117(1–3), pp. 31–44. doi: 10.1007/s11120-013-9849-7.

Allahverdiyeva, Y. et al. (2013) 'Flavodiiron proteins Flv1 and Flv3 enable cyanobacterial growth and photosynthesis under fluctuating light.', Proceedings of the National Academy of Sciences of the United States of America, 110(10), pp. 4111–6. doi: 10.1073/pnas.1221194110.

Ajjawi, I. et al. (2017) 'Lipid production in Nannochloropsis gaditana is doubled by decreasing expression of a single transcriptional regulator', Nature Biotechnology. Nature Publishing Group, 35(7), pp. 647–652. doi: 10.1038/nbt.3865.

Angermayr, S. A., Paszota, M. and Hellingwerf, K. J. (2012) 'Engineering a cyanobacterial cell factory for production of lactic acid', Applied and Environmental Microbiology, 78(19), pp. 7098–7106. doi: 10.1128/AEM.01587-12.

Atsumi, S., Higashide, W. and Liao, J. C. (2009) 'Direct photosynthetic recycling of carbon dioxide to isobutyraldehyde.', Nature biotechnology. Nature Publishing Group, 27(12), pp. 1177–80. doi: 10.1038/nbt.1586.

Battchikova, N. et al. (2011) 'Identification of novel Ssl0352 protein (NdhS), essential for efficient operation of cyclic electron transport around photosystem I, in NADPH:plastoquinone oxidoreductase (NDH-1) complexes of Synechocystis sp. PCC 6803.', The Journal of biological chemistry. American Society for Biochemistry and Molecular Biology, 286(42), pp. 36992–7001. doi: 10.1074/jbc.M111.263780.

Berepiki, A. et al. (2016) 'Tapping the unused potential of photosynthesis with a heterologous electron sink', ACS Synthetic Biology, p. acssynbio.6b00100. doi: 10.1021/acssynbio.6b00100.

Cameron, J. (2011) 'Redox Homeostasis in Cyanobacteria', (May 2011).

Campbell, D. and Oquist, G. (1996) 'Predicting light acclimation in cyanobacteria from nonphotochemical quenching of photosystem II fluorescence, which reflects state transitions in these organisms', Plant physiology, pp. 1293–1298.

Chaves, J. E. et al. (2017) 'Engineering Isoprene Synthase Expression and Activity in Cyanobacteria', ACS Synthetic Biology, p. acssynbio.7b00214. doi: 10.1021/acssynbio.7b00214.

Christopher, H., Rensburg, J. Van and Ende, W. Van Den (2018) 'UDP-Glucose : A Potential Signaling Molecule in Plants ?', frontiers in Plant Science, 8(January), pp. 6–11. doi: 10.3389/fpls.2017.02230.

Chukhutsina, V. et al. (2015) 'Cyanobacterial Light-Harvesting Phycobilisomes Uncouple From Photosystem I During Dark-To-Light Transitions', Scientific Reports. Nature Publishing Group, 5(August), p. 14193. doi: 10.1038/srep14193.

Cramer, W. A., Hasan, S. S. and Yamashita, E. (2011) 'The Q cycle of cytochrome bc complexes: A structure perspective', Biochimica et Biophysica Acta (BBA) - Bioenergetics. Elsevier, 1807(7), pp. 788–802. doi: 10.1016/J.BBABIO.2011.02.006.

Daley, S. M. E. et al. (2012) 'Regulation of the cyanobacterial CO2-concentrating mechanism involves internal sensing of NADP+ and a-ketogutarate levels by transcription factor CcmR', PLoS ONE, 7(7), pp. 1–10. doi: 10.1371/journal.pone.0041286.

Davies, F. K. et al. (2014) 'Engineering Limonene and Bisabolene Production in Wild Type and a Glycogen-Deficient Mutant of Synechococcus sp. PCC 7002', Frontiers in Bioengineering and Biotechnology, 2(June), pp. 1–11. doi: 10.3389/fbioe.2014.00021.

Demmig-Adams, B., Stewart, J. J., et al. (2014) 'Insights from Placing Photosynthetic Light Harvesting into Context', The Journal of Physical Chemistry Letters, 5, pp. 2880–2889. doi: 10.1021/jz5010768.

Demmig-Adams, B., Garab, G., et al. (2014) Non-Photochemical Quenching and Energy Dissipation in Plants, Algae and Cyanobacteria. 40th edn. Edited by B. Demmig-Adams et al. Springer (Advances in Photosynthesis and Respiration). doi: 10.1007/978-94-017-9032-1.

Demmig-Adams, B. et al. (2017) 'Algal glycerol accumulation and release as a sink for photosynthetic electron transport', Algal Research. Elsevier B.V., 21, pp. 161–168. doi: 10.1016/j.algal.2016.11.017.

Deng, M. De and Coleman, J. R. (1999) 'Ethanol synthesis by genetic engineering in cyanobacteria', Applied and Environmental Microbiology, 65(2), pp. 523–528.

Ducat, D. C. et al. (2012) 'Rerouting carbon flux to enhance photosynthetic productivity', Applied and Environmental Microbiology, 78, pp. 2660–2668. doi: 10.1128/AEM.07901-11.

Ducat, D. C., Way, J. C. and Silver, P. a. (2011) 'Engineering cyanobacteria to generate high-value products', Trends in Biotechnology, 29(2), pp. 95–103. doi: 10.1016/j.tibtech.2010.12.003.

Eisenhut, M. et al. (2007) 'Long-term response toward inorganic carbon limitation in wild type and glycolate turnover mutants of the cyanobacterium Synechocystis sp. strain PCC 6803', Plant Physiol, 144(4), pp. 1946–1959. doi: 10.1104/pp.107.103341.

Hackenberg, C. et al. (2009) 'Photorespiratory 2-phosphoglycolate metabolism and photoreduction of O2 cooperate in high-light acclimation of Synechocystis sp. strain PCC 6803', Planta, 230(4), pp. 625–637. doi: 10.1007/s00425-009-0972-9.

Hackenberg, C. et al. (2012) 'Low-carbon acclimation in carboxysome-less and photorespiratory mutants of the cyanobacterium synechocystis sp. strain PCC 6803', Microbiology, 158(2), pp. 398–413. doi: 10.1099/mic.0.054544-0.

Hickman, J. W. et al. (2013) 'Glycogen synthesis is a required component of the nitrogen stress response in Synechococcus elongatus PCC 7942', Algal Research. Elsevier B.V., 2(2), pp. 98–106. doi: 10.1016/j.algal.2013.01.008.

Hirokawa, Y. et al. (2016) 'Cyanobacterial production of 1,3-propanediol directly from carbon dioxide using a synthetic metabolic pathway', Metabolic Engineering. Elsevier, pp. 1–7. doi: 10.1016/j.ymben.2015.12.008.

Hirokawa, Y., Maki, Y. and Hanai, T. (2017) 'Improvement of 1,3-propanediol production using an engineered cyanobacterium, Synechococcus elongatus by optimization of the gene expression level of a synthetic metabolic pathway and production conditions', Metabolic Engineering. Elsevier, 39(December 2016), pp. 192–199. doi: 10.1016/j.ymben.2016.12.001.

Holland, S. C. et al. (2016) 'Impacts of genetically engineered alterations in carbon sink pathways on photosynthetic performance', Algal Research. Elsevier B.V., 20, pp. 87–99. doi: 10.1016/j.algal.2016.09.021.

Jackson, S. a. et al. (2015) 'Dynamics of Photosynthesis in the Glycogen-Deficient glgC Mutant of Synechococcus sp. PCC 7002', Applied and Environmental Microbiology, (July), p. AEM.01751-15. doi: 10.1128/AEM.01751-15.

Jiang, Y.-L. et al. (2017) 'Coordinating carbon and nitrogen metabolic signaling through the cyanobacterial global repressor NdhR', Proceedings of the National Academy of Sciences, p. 201716062. doi: 10.1073/pnas.1716062115.

Juergens, M. T. et al. (2015) 'The Regulation of Photosynthetic Structure and Function during Nitrogen Deprivation in Chlamydomonas reinhardtii', Plant Physiology, 167(2), pp. 558–573. doi: 10.1104/pp.114.250530.

Kamennaya, N. A. et al. (2015) 'Installing extra bicarbonate transporters in the cyanobacterium Synechocystis sp. PCC6803 enhances biomass production', Metabolic Engineering, 29, pp. 76–85. doi: 10.1016/j.ymben.2015.03.002.

Khazi, M. I., Demirel, Z. and Dalay, M. C. (2018) 'Evaluation of growth and phycobiliprotein composition of cyanobacteria isolates cultivated in different nitrogen sources'. Journal of Applied Phycology.

Kramer, D. M. and Evans, J. R. (2011) 'The importance of energy balance in improving photosynthetic productivity.', Plant physiology, 155(January), pp. 70–78. doi: 10.1104/pp.110.166652.

Krasikov, V. et al. (2012) 'Time-series resolution of gradual nitrogen starvation and its impact on photosynthesis in the cyanobacterium Synechocystis PCC 6803', Physiologia Plantarum, 145(3), pp. 426–439. doi: 10.1111/j.1399-3054.2012.01585.x.

Kusakabe, T. et al. (2013) 'Engineering a synthetic pathway in cyanobacteria for isopropanol production directly from carbon dioxide and light', Metabolic Engineering. Elsevier, 20, pp. 101–108. doi: 10.1016/j.ymben.2013.09.007.

Lai, M. and Lan, E. (2015) 'Advances in metabolic engineering of cyanobacteria for photosynthetic biochemical production', Metabolites, 5(4), pp. 636–658. doi: 10.3390/metabo5040636.

Lau, N., Matsui, M. and Abdullah, A. A. (2015) 'Cyanobacteria : Photoautotrophic Microbial Factories for the Sustainable Synthesis of Industrial Products', 2015. doi: 10.1155/2015/754934.

Lindberg, P., Park, S. and Melis, A. (2010) 'Engineering a platform for photosynthetic isoprene production in cyanobacteria, using Synechocystis as the model organism', Metabolic Engineering. Elsevier, 12(1), pp. 70–79. doi: 10.1016/j.ymben.2009.10.001.

Long, B. M. et al. (2010) 'Functional Cyanobacterial b-Carboxysomes Have an Absolute Requirement for Both Long and Short Forms of the CcmM Protein', Plant Physiology, 153(1), pp. 285–293. doi: 10.1104/pp.110.154948.

Maarleveld, T. R. et al. (2014) 'A data integration and visualization resource for the metabolic network of Synechocystis sp. PCC 6803.', Plant physiology, 164(3), pp. 1111–21. doi: 10.1104/pp.113.224394.

Mao, H. Bin et al. (2002) 'The redox state of plastoquinone pool regulates state transitions via cytochrome b6f complex in Synechocystis sp. PCC 6803', FEBS Letters, 519(1–3), pp. 82–86. doi: 10.1016/S0014-5793(02)02715-1.

Marcus, Y., Berry, J. A. and Pierce, J. (1992) 'Photosynthesis and photorespiration in a mutant of the cyanobacterium Synechocystis PCC 6803 lacking carboxysomes', Planta, 187(4), pp. 511–516. doi: 10.1007/BF00199970.

Martin, G. J. O. et al. (2014) 'Lipid profile remodeling in response to nitrogen deprivation in the microalgae Chlorella sp. (Trebouxiophyceae) and Nannochloropsis sp. (Eustigmatophyceae)', PLoS ONE, 9(8). doi: 10.1371/journal.pone.0103389.

Messinger, J. et al. (2009) 'Photosystem II', in, pp. 1–15. doi: 10.1002/9780470015902.a0022548.

Michelet, L. et al. (2013) 'Redox regulation of the Calvin-Benson cycle: something old, something new.', Frontiers in plant science, 4(November), p. 470. doi: 10.3389/fpls.2013.00470.

Mullineaux, C. W. (2014a) 'Co-existence of photosynthetic and respiratory activities in cyanobacterial thylakoid membranes', Biochimica et Biophysica Acta - Bioenergetics. Elsevier B.V., 1837(4), pp. 503–511. doi: 10.1016/j.bbabio.2013.11.017.

Mullineaux, C. W. (2014b) 'Electron transport and light-harvesting switches in cyanobacteria.', Frontiers in plant science, 5(January), pp. 1–6. doi: 10.3389/fpls.2014.00007.

Mullineaux, C. W. and Allen, J. F. (1990) 'State 1-State 2 transitions in the cyanobacterium Synechococcus 6301 are controlled by the redox state of electron carriers between Photosystems I and II', Photosynthesis Research, 23, pp. 297–311. doi: 10.1007/BF00034860.

Oliver, J. W. K. et al. (2013) 'Cyanobacterial conversion of carbon dioxide to 2,3-butanediol.', Proceedings of the National Academy of Sciences of the United States of America, 110(4), pp. 1249–54. doi: 10.1073/pnas.1213024110.

Park, J. and Choi, Y. (2017) 'Cofactor engineering in cyanobacteria to overcome imbalance between NADPH and NADH: A mini review', Frontiers of Chemical Science and Engineering, 11(1), pp. 66–71. doi: 10.1007/s11705-016-1591-1.

Paul, M. J. and Foyer, C. H. (2001) 'Sink regulation of photosynthesis.', Journal of experimental botany, 52(360), pp. 1383–1400. doi: 10.1093/jexbot/52.360.1383.

Pospísil, P. (2009) 'Production of reactive oxygen species by photosystem II.', Biochimica et biophysica acta, 1787(10), pp. 1151–1160. doi: 10.1016/j.bbabio.2009.05.005.

Rae, B. D. et al. (2012) 'Structural determinants of the outer shell of b-carboxysomes in Synechococcus elongatus PCC 7942: Roles for CcmK2, K3-K4, CcmO, and CcmL', PLoS ONE, 7(8), pp. 14–19. doi: 10.1371/journal.pone.0043871.

Rae, B. D. et al. (2013) 'Cyanobacterial carboxysomes: Microcompartments that facilitate CO 2 fixation', Journal of Molecular Microbiology and Biotechnology, 23(4–5), pp. 300–307. doi: 10.1159/000351342.

Raszewski, G. et al. (2008) 'Spectroscopic Properties of Reaction Center Pigments in Photosystem II Core Complexes: Revision of the Multimer Model', Biophysical Journal. Cell Press, 95(1), pp. 105–119. doi: 10.1529/BIOPHYSJ.107.123935.

Rohnke, B. A. et al. (2018) 'RcaE-Dependent Regulation of Carboxysome Structural Proteins Has a Central Role in Environmental Determination of Carboxysome Morphology and Abundance in Fremyella diplosiphon', mSphere, 3(1), pp. e00617-17. doi: 10.1128/mSphere.00617-17.

Schuurmans, R. M. et al. (2014) 'The Redox Potential of the Plastoquinone Pool of the Cyanobacterium Synechocystis Species Strain PCC 6803 Is under Strict Homeostatic Control', Plant Physiology, 165(1), pp. 463–475. doi: 10.1104/pp.114.237313.

Sharkey, T. D. et al. (1986) 'Limitation of Photosynthesis by Carbon Metabolism 1', Plant physiology, 81, pp. 1123–1129. doi: 10.1104/pp.81.4.1123.

Sun, Y. et al. (2016) 'Light modulates the biosynthesis and organization of cyanobacterial carbon fixation machinery through photosynthetic electron flow', Plant Physiology, 171(May), p. pp.00107.2016. doi: 10.1104/pp.16.00107.

Takizawa, K., Kanazawa, A. and Kramer, D. M. (2008) 'Depletion of stromal Pi induces high "energy-dependent" antenna exciton quenching (qE) by decreasing proton conductivity at CF O-CF1 ATP synthase', Plant, cell & environment, 31(2), pp. 235–43. doi: 10.1111/j.1365-3040.2007.01753.x.

Tikhonov, A. N. (2014) 'The Cytochrome b 6 f complex at the crossroad of photosynthetic electron transport pathways', Plant Physiology and Biochemistry. Elsevier Masson SAS, 81(December), pp. 1–20. doi: 10.1016/j.plaphy.2013.12.011.

Trost, P. et al. (2006) 'Thioredoxin-dependent regulation of photosynthetic glyceraldehyde-3-phosphate dehydrogenase: Autonomous vs. CP12-dependent mechanisms', Photosynthesis Research, 89, pp. 263–275. doi: 10.1007/s11120-006-9099-z.

Tsai, A. Y.-L. and Gazzarrini, S. (2014) 'Trehalose-6-phosphate and SnRK1 kinases in plant development and signaling: the emerging picture.', Frontiers in plant science, 5(April), p. 119. doi: 10.3389/fpls.2014.00119.

Tsang, T. K., Roberson, R. W. and Vermaas, W. F. J. (2013) 'Polyhydroxybutyrate particles in Synechocystis sp. PCC 6803: facts and fiction', Photosynthesis Research, 118(1–2), pp. 37–49. doi: 10.1007/s11120-013-9923-1.

Tsimilli-Michael, M., Stamatakis, K. and Papageorgiou, G. C. (2009) 'Dark-to-light transition in Synechococcus sp. PCC 7942 cells studied by fluorescence kinetics assesses plastoquinone redox poise in the dark and photosystem II fluorescence component and dynamics during state 2 to state 1 transition', Photosynthesis Research, 99(3), pp. 243–255. doi: 10.1007/s11120-009-9405-7.

Ueno, Y. et al. (2016) 'Energy Transfer in Cyanobacteria and Red Algae: Confirmation of Spillover in Intact Megacomplexes of Phycobilisome and Both Photosystems', The Journal of Physical Chemistry Letters, pp. 3567–3571. doi: 10.1021/acs.jpclett.6b01609.

Ungerer, J. et al. (2012) 'Sustained photosynthetic conversion of CO2 to ethylene in recombinant cyanobacterium Synechocystis 6803', Energy & Environmental Science, 5(10), p. 8998. doi: 10.1039/c2ee22555g.

Wang, W., Liu, X. and Lu, X. (2013) 'Engineering cyanobacteria to improve photosynthetic production of alka(e)nes.', Biotechnology for biofuels. Biotechnology for Biofuels, 6(1), p. 69. doi: 10.1186/1754-6834-6-69.

Van der Woude, A. D. et al. (2014) ‘Carbon sink removal: Increased photosynthetic production of lactic acid by Synechocystis sp. PCC6803 in a glycogen storage mutant’, Journal of Biotechnology. Elsevier B.V., 184, pp. 100–102. doi: 10.1016/j.jbiotec.2014.04.029.

Yu, Y. et al. (2013) ‘Development of synechocystis sp. PCC 6803 as a phototrophic cell factory’, Marine Drugs, 11(8), pp. 2894–2916. doi: 10.3390/md11082894.

Zhou, J. et al. (2014) ‘Production of optically pure d-lactate from CO2 by blocking the PHB and acetate pathways and expressing d-lactate dehydrogenase in cyanobacterium Synechocystis sp. PCC 6803’, Process Biochemistry. Elsevier Ltd, 49(12), pp. 12–21. doi: 10.1016/j.procbio.2014.09.007.

Zhu, T. et al. (2015) ‘Enhancing photosynthetic production of ethylene in genetically engineered Synechocystis sp. PCC 6803’, Green Chem. Royal Society of Chemistry, 17(1), pp. 421–434. doi: 10.1039/C4GC01730G.

CHAPTER 2: INCREASED PHOTOCHEMICAL EFFICIENCY IN CYANOBACTERIA VIA AN ENGINEERED SUCROSE SINK

This Chapter was previously published with permission from Oxford University Press:

Bradley W. Abramson, Benjamin Kachel, David M. Kramer, Daniel C. Ducat; Increased Photochemical Efficiency in Cyanobacteria via an Engineered Sucrose Sink, Plant and Cell Physiology, Volume 57, Issue 12, 1 December 2016, Pages 2451–2460, https://doi.org/10.1093/pcp/pcw169

Abstract:

In plants, a limited capacity to utilize or export the end products of the Calvin Benson cycle (CB) from photosynthetically-active source cells to non-photosynthetic sink cells can result in reduced carbon capture, photosynthetic electron transport (PET) and lowered photochemical efficiency. The downregulation of photosynthesis caused by reduced capacity to utilize photosynthate has been termed "sink limitation". Recently, several cyanobacterial and algal strains engineered to over-produce target metabolites have exhibited increased photochemistry suggesting possible source-sink regulatory mechanisms may be involved. I directly examined photochemical properties following induction of a heterologous sucrose "sink" in the unicellular cyanobacterium *Synechococcus elongatus* PCC 7942. I show that total photochemistry increases proportionally to the experimentally controlled rate of sucrose export. Importantly, the quantum yield of PSII (ΦII) increases in response to sucrose export while the PET chain becomes more oxidized from less PSI acceptor-side limitation, suggesting increased CB activity and a decrease in sink limitation. Enhanced photosynthetic activity and linear electron flow is detectable within hours of induction of the heterologous sink and is

independent of pigmentation alterations or the ionic/osmotic effects of the induction system. These observations provide direct evidence that secretion of heterologous carbon bioproducts can be used as an alternative approach to improve photosynthetic efficiency, presumably by bypassing sink limitation. Our results also suggest that engineered microalgal production strains are valuable alternative models for examining photosynthetic sink limitation because they enable greater control and monitoring of metabolite fluxes relative to plants.

Introduction

A balance between photosynthetic production of sugars by source tissues (mesophyll cells) and sugar consumption by sink tissues (e.g. root cells and fruits) must be maintained for plant health and survival. In plants, sink limitation occurs under conditions where the rate of photosynthesis is limited neither by light nor carbon fixation, but by insufficient withdrawal of products from the Calvin-Benson (CB) cycle (Sharkey et al. 1986; Paul & Foyer 2001; Sawada et al. 1986; Adams et al. 2013). Sink limitation can occur in plants when there is an increase in CB products due to increased photosynthetic activity or by experimental carbohydrate feeding (Demmig-Adams, Garab, et al. 2014; Krapp et al. 1991). Likewise, sink limitation is observed when demand for CB products decreases due to a restriction in flux to intracellular carbon pools (e.g. starch or sucrose) and when intercellular carbon flux is disrupted (i.e. impaired export of sucrose from source tissues), or under nutrient limitation (von Schaewen et al. 1990; Adams et al. 2013). Sink limitation results in an accumulation of soluble sugars, depletion of intracellular free phosphate, lowered ATP synthase activity, and elevated proton motive force (Takizawa et al. 2008). These effects lead to decreased carbon assimilation and lowered photosynthetic efficiency (Yang et al. 2015; Paul & Foyer 2001; Herold 1980; Sawada et al. 1986). To date, photosynthetic sink limitation has been studied almost exclusively in multicellular plants.

In microalgae, it is becoming evident that heterologous metabolic pathway activity can act as a photosynthetic sink, thereby reducing inefficiencies caused by sink limitation (Figure 2.1A). This idea is bolstered by recent observations of microalgal strains that show greater rates of oxygen evolution and carbon fixation when engineered to export metabolites. For example, different strains of cyanobacteria engineered to export significant quantities of sucrose (Ducat et al. 2012), isobuteraldehyde (Li et al. 2014), 2,3–butanediol (Oliver et al. 2013) or ethlyene (Ungerer et al. 2012) all exhibited increased photosynthetic activity as measured by oxygen evolution, biomass formation, and/or carbon fixation rates. Likewise, in single celled algae engineered to export glycerol, increased oxygen evolution and the quantum yield of PSII (ΦII) are observed (Demmig-Adams, Stewart, et al. 2014) Yet, photosynthetic enhancements in these strains are often measured long after activation of the engineered pathway, which complicates interpretation of the direct effects of heterologous sinks on photosynthetic activity. In most of the aforementioned studies, the algae and cyanobacteria reported have been modified to constitutively over-express the introduced pathways, thus the measurements are conducted long after cells have reached a new steady state (Ungerer et al. 2012; Li et al. 2014; Demmig-Adams, Stewart, et al. 2014). In those strains where the heterologous pathway was placed under inducible promoters (Ducat et al. 2012; Oliver et al. 2013; Nozzi & Atsumi 2015), analyses of photosynthetic activity have not directly assayed efficiency and measurements were at least 24h after induction of the pathway. It is therefore difficult to ascribe increased photosynthetic efficiency specifically to sink effects rather than pathway-specific phenotypes or indirect effects, such as transcriptional changes. Finally, some of these results were complicated by experiments exhibiting

conflicting enhancements in only a subset of the measured photosynthetic parameters (Oliver & Atsumi 2015), or by an instance where metabolite over production resulted in increased photoinhibition (Kato et al. 2016).

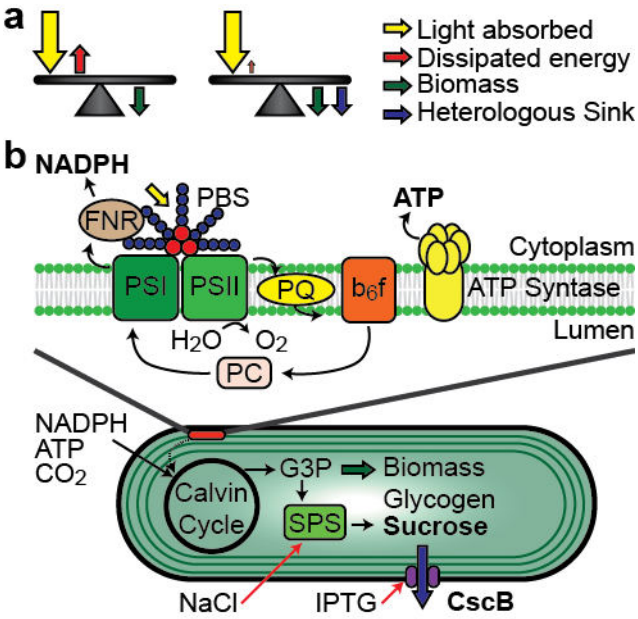

FIGURE 2.1: OVERVIEW OF ENERGY BALANCE IN ENGINEERED *S. ELONGATUS* STRAIN.
Cartoon schematics of source/sink balance in cyanobacteria where: a) Absorbed light energy (yellow arrow) is balanced with the energy requirements of cellular metabolism (green arrow), whereas excess energy is dissipated via non-photochemical quenching (red arrow). Engineered metabolic sinks (blue arrow) increases cellular energy requirements. Energy for sustaining the new sink is partially drawn from photons which would otherwise be dissipated, resulting in greater light use efficiency. b) Cartoon schematic of photosynthetic electron transport chain and heterologous sucrose export pathway. Light energy is absorbed and used to generate NADPH and ATP for carbon fixation by the Calvin Benson Cycle. G3P is a major product of the Calvin cycle that is metabolized to sucrose, with the commitment steps catalyzed by SPS. Sucrose is exported by cscB induction and activation of SPS (by salt addition or by inducible over-expression). PSI: Photosystem I, PSII: Photosystem II, PBS: Phycobilisome, PQ: Plastoquinone, B6f: Cytochrome B6f, PC: Plastocyanin, FNR: Ferredoxin:NADPH oxidoreductase, G3P: Glyceraldehyde-3-phosphate, SPS: Sucrose Phosphate Synthase, CscB: Sucrose permease.

To directly examine the relationship between heterologous metabolite secretion and sink limitation I examined photosynthetic parameters in *Synechococcus elongatus* PCC 7942, hereafter *S. elongatus*, immediately following the induction of a heterologous sucrose-secretion

pathway (Figure 2.1B). *S. elongatus* is a freshwater species that naturally produces sucrose in the cytoplasm as an osmoprotectant when sodium chloride (NaCl) is added to the medium (Hagemann 2011). I have previously shown that this photosynthetically derived pool of sucrose is secreted by heterologous expression of sucrose permease, cscB, or members of the SWEET family of sucrose transporters (Figure 2.1B) (Ducat et al. 2012; Xuan et al. 2013). This system provides a platform whereby a substantial heterologous sink can be experimentally induced by addition of IPTG, thereby allowing examination of photosynthetic parameters during the period of acclimation to a new metabolic sink. Furthermore, the "sink size" can be experimentally controlled by altering the osmolarity of the medium allowing exported sucrose to be tuned from 1% to ~80% of total carbon fixed (Ducat et al. 2012). Our previous results indicated that total photosynthetic activity increased in cultures days after sucrose export was induced, but I could not determine if this was due to an increase in photosynthetic efficiency or a direct effect of decreased sink inhibition.

Here, I measure spectroscopic properties of the photosystems in response to induction of the heterologous sucrose sink. I find evidence that both PSII activity and ΦII increase within hours of induction of sucrose export and the magnitude of the increase in PSII operating efficiency is correlated with the rate of sucrose export. Furthermore, PSI appears more oxidized and the rate-limiting steps within the photosynthetic electron transport (PET) chain are altered following induction of sucrose export. Importantly, photosynthetic enhancements are independent of the method used to induce sucrose export such as salt stress. Together, our results are consistent with an increase in

photochemical efficiency and increased photosynthetic flux following activation of a heterologous secretion pathway in *S. elongatus*.

Results

I first determined the metabolic sink demand in *S. elongatus* bearing an IPTG-inducible cscB construct (Ducat et al. 2012) when induced to export sucrose at different rates. If exported sucrose is acting as a metabolic sink to relieve sink inhibition, any resulting photosynthetic alterations should occur proportionally to the size of the induced heterologous sink. To approximate the size of the heterologous sink I measured the rate of sucrose export from cultures induced for 24 h (Figure 2.2A). Sink size (e.g. sucrose export rate) was altered by acclimating cultures within BG11 media supplemented with 100mM, 150mM or 200 mM NaCl (hereafter BG100, BG150 and BG200, respectively) (Ducat et al. 2012). In non-supplemented media (BG0), no detectable sucrose export was observed, regardless of cscB induction. As expected, higher rates of sucrose and lower cell growth is observed with increasing osmotic pressure (Burnap 2015), therefore I calculated the sucrose secretion rate per cell to estimate the size of the metabolic sink imposed. Cultures exported sucrose at a rate of 0.067, 0.15, 0.28 pg sucrose $cell^{-1}$ h^{-1} in BG100, BG150 or BG200 respectively (Figure 2.2A). Uninduced cultures in higher salt conditions had detectable, albeit minimal, sucrose export rates owing to leaky cscB expression (Figure 2.3).

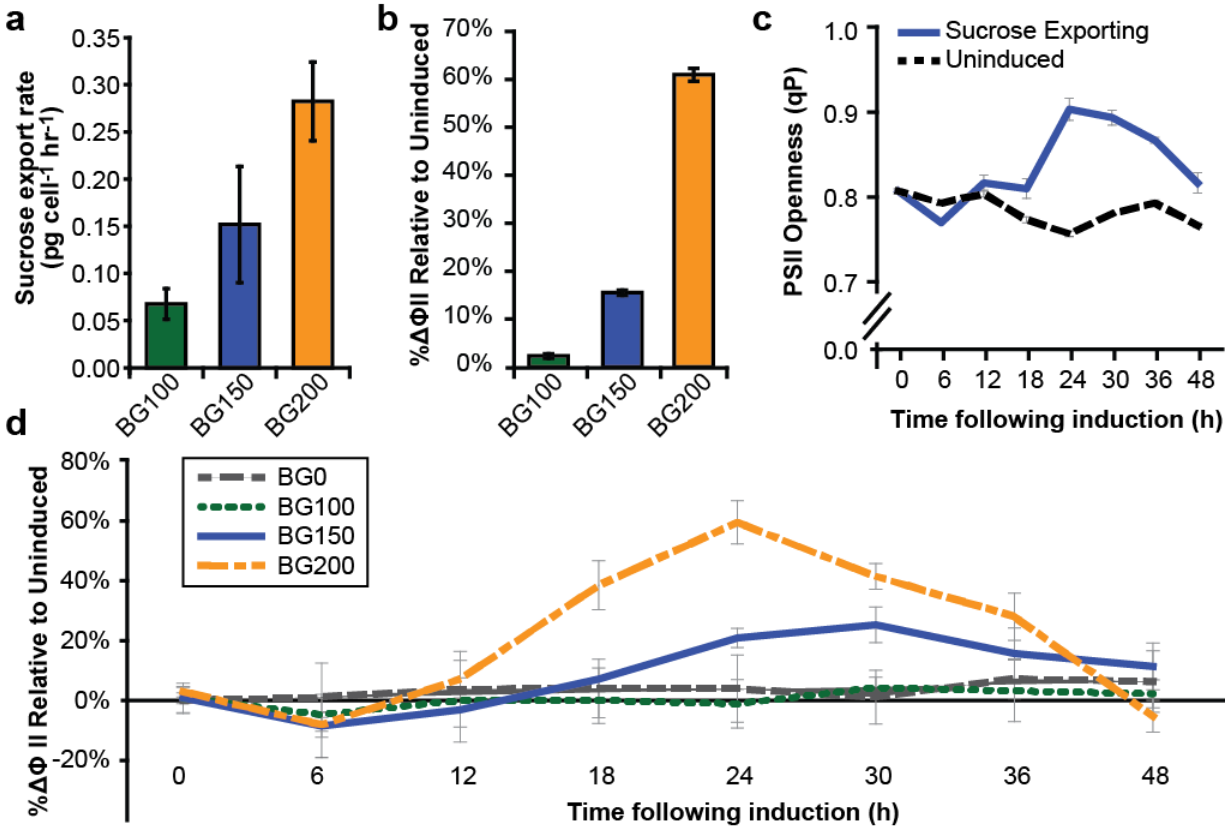

FIGURE 2.2: PHOTOCHEMICAL EFFICIENCY INCREASES FOLLOWING SUCROSE EXPORT AND IS CORRELATED WITH SINK SIZE.

a) Sucrose export rates in different media conditions at 24 hours post induction. **b)** The change in ΦII in different media conditions 24 hours after the induction of sucrose export, relative to uninduced controls in the same media conditions. **c)** Photochemical quenching (qP) of excitation energy in PSII measured over time after induction (blue) and uninduced (black). Cultures were acclimated to BG150 media, 1mM IPTG was added at time 0 for induced cultures. **d)** Change in ΦII over time after induction relative to an uninduced control. BG0, BG100, BG150, BG200 denote BG11 media supplemented with 0, 100, 150 or 200 mM NaCl. All experiments are averages of 3 biological replicates (n=3).

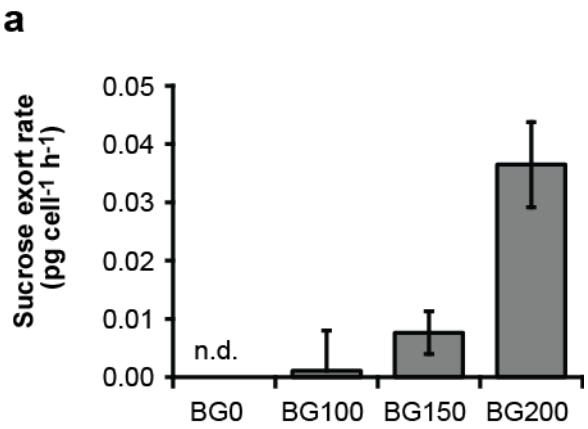

FIGURE 2.3: SUCROSE EXPORT RATE OF UNINDUCED CULTURES.
Sucrose export rate in indicated media without the addition of IPTG. BG0 sucrose export was not detectable (n.d.). Data are averages of replicate samples (n=3).

If sucrose secretion is acting to relieve sink limitation under our culture conditions, one might expect photosynthetic capacity and/or efficiency to increase as sink size increases. One measurement of photosynthetic efficiency is ΦII, which measures the percentage of total absorbed light used for photochemistry by PSII at a given actinic light intensity and can be measured non-invasively by room temperature chlorophyll fluorescence (Maxwell & Johnson 2000; Baker 2008). Chlorophyll fluorescence was measured (Figure 2.42) and ΦII calculated at a light intensity of 100 μmol photons m^{-2} s^{-1} 24 h post induction (Figure 2.2B). ΦII was compared between sucrose exporting cultures and uninduced cultures in similar conditions. 24 hours after induction ΦII increased 2.3, 15.5 or 60.9 % in BG100, BG150 or BG200, respectively (Figure 2.2B). As 1 mM IPTG was added for each culture condition, the increase in ΦII could not be attributed solely to *cscB* expression. Indeed, ΦII increases at 24 hours following sucrose export and the degree of this increase is correlated with the sucrose export rate at 24 hours (Figure 2.2A).

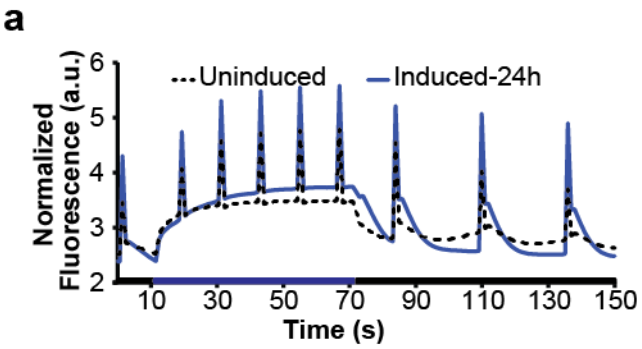

FIGURE 2.4: CHLOROPHYLL FLUORESCENCE TRACE IN BG150 AT 24 HOURS. Chlorophyll a fluorescence measurements were taken with 100 µmol photons m-2 s-1 of blue actinic light and blue measuring beam. The black bar denotes the sample is in the dark and the blue bar denotes when the actinic light was turned on. Spikes are saturation pulses less than one second. Data are averages of replicate samples (n=3).

The increases I observe in ΦII could be a function of a more oxidized plastoquinone (PQ) pool, as the PQ pool oxidation state is one variable influencing PSII efficiency in the light (Hogewoning et al. 2012; Campbell et al. 1998). I therefore calculated qP, a measure of PSII "openness" and PQ oxidation state, as previously described (Oxborough & Baker 1997). A qP=1 represents a photosynthetic system where PSII is completely open and able to trap photonic energy and split water to generate electrons for photochemistry, whereas PSII is totally closed at qP=0 (Campbell et al. 1998). I found qP increases by 16% in sucrose-exporting cultures relative to uninduced controls 24 hours after IPTG induction in BG150 (Figure 2.2C). This increase is not observed in BG0 cultures (Figure 2.5A), but is exacerbated in BG200 cultures exporting sucrose at a higher rate (19% greater qP), where qP also rises more rapidly following induction (Figure 2.5B).

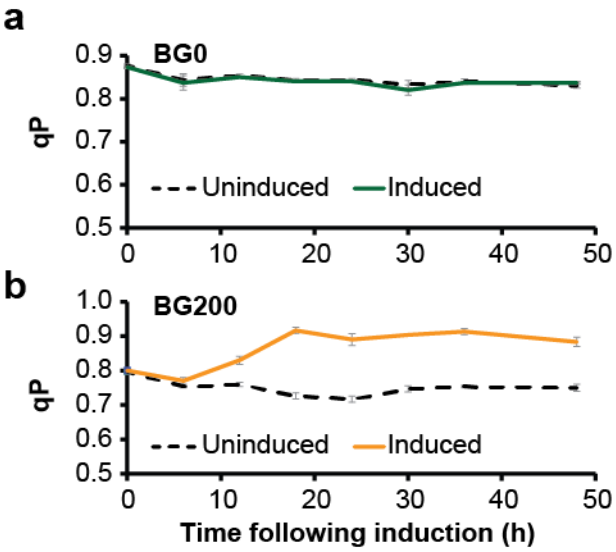

FIGURE 2.5: PHOTOCHEMICAL QUENCHING IN BG0 AND BG200 OVER TIME. a) qP, or 'proportion of open PSII centers' in cscB uninduced and induced cultures in BG0. b) qP as in (a) except with cultivation in BG200. All panels are averages of replicate samples (n=3).

Similarly, I observed that cultures with greater sucrose export rates (larger sink) exhibited both a faster rise of ΦII and an increased total magnitude when measured over time (Figure 2.2D). When measured at an actinic intensity of 100 μmol photons $m^{-2}s^{-1}$, the rise in ΦII was observable between 6 and 18 hours after induction (Figure 2.2D), with the fastest and highest rise in cultures exporting the most sucrose (BG200). Interestingly, ΦII begins to decline back to baseline levels after the first 24-30 hrs, suggesting that there are longer-term sink regulatory effects which may differ from the short-term increases in photosynthetic quantum yield. Our results indicate that ΦII increases within hours of IPTG induction, accompanied by an increasingly oxidized PQ pool, and that the increase is correlated with sucrose export rates.

ΦII values can be effected by changes in total PSII content or by state transitions which alter the absorbance cross-section of PSII without increasing PSII quantum efficiency (Campbell et al. 1998). Therefore, I measured chlorophyll content and the absorbance changes associated with state transitions to determine if ΦII changes were driven by these artifacts. Chlorophyll

concentrations were not significantly affected on a per cell basis between uninduced and induced cultures in BG150 (Figure 2.6A) which implies photosystem content does not significantly change in the first 24 hours. Furthermore, phycobilisome (PBS) concentrations were not significantly affected during the time in which ΦII increases (Figure 2.7). Cyanobacterial PBS can redirect absorbed light energy to PSI (State II) or PSII (State I), and a cell in State I has increased chlorophyll fluorescence and greater ΦII due to the increased light transferred to PSII compared to a cell in State II (Tsimilli-Michael et al. 2009; Kaňa et al. 2012). Flash frozen cells were excited with PBS absorbing light and the fluorescent peaks at 685 nm from PSII and 714 nm from PSI were then used to quantify the excitation transfer from PBS to the photosystems (Clarke et al. 1995) (Figure 2.6B). Comparing uninduced and induced cultures in BG150 showed no significant state transition occurs 24 hours post induction.

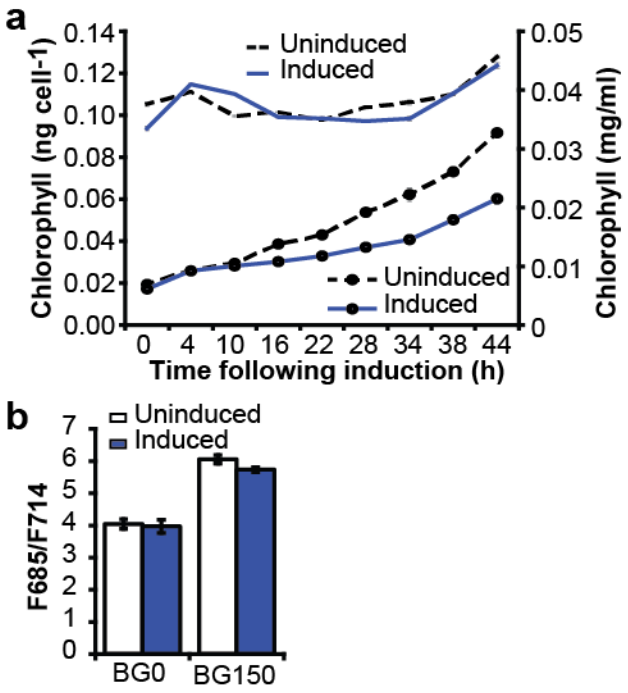

FIGURE 2.6: PHOTOSYNTHETIC EFFICIENCY GAINS ARE INDEPENDENT OF PIGMENT CHANGES.

a) Chlorophyll quantification over time following induction of cscB and sucrose export. Chlorophyll data of BG150 cultures in as chlorophyll per cell (solid lines) and mg/ml (circles and dotted lines). b) Ratio of 77K fluorescence peaks from uninduced and induced cultures in BG0 and BG150 after 24 h induction measured at wavelengths 685 nm (PSII) and 714 nm (PSI). BG0, BG100, BG150, BG200 denote BG11 media supplemented with 0, 100, 150 or 200 mM NaCl. Experiments are averages of 3 biological replicates (n=3).

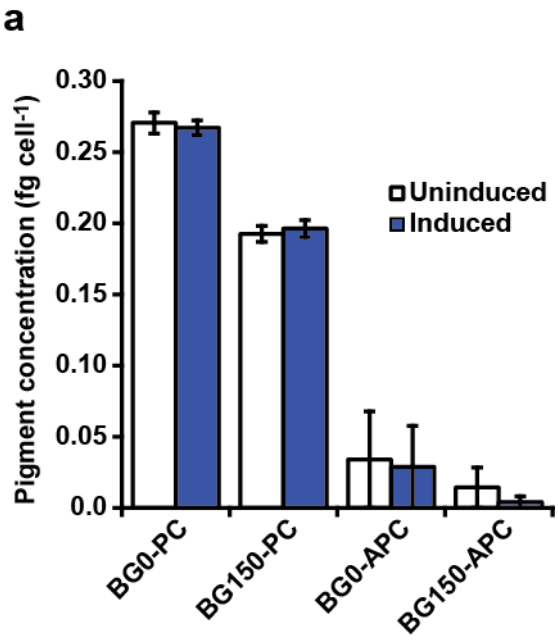

FIGURE 2.7: PHYCOBILIN CONCENTRATION 24 HOURS AFTER INDUCTION. Concentration of phycobilins uninduced or 24 hours after induction from BG0 or BG150 cultures. PC: phycocyanin. APC: Allophycocyanin. Data are averages of 3 replicate samples (n=3).

I observed significant improvements in ΦII and qP 12.18 hours after cscB induction (Figure 2.2C; Figure 2.2D), yet if utilization of CB products and relief of sink limitation are the underlying causes for these effects, ΦII changes should be observable with similar kinetics to sucrose export. I directly measured sucrose export following induction and found detectable sucrose accumulation within 2.4 hours following IPTG addition (Figure 2.8A), earlier than the increase in ΦII I observe at 100 μmol photons m^{-2} s^{-1} (Figure 2.2D). I measured ΦII at multiple actinic light intensities over time to better examine the interplay between source energy and cells with altered sink requirements (Figure 2.8B). At 10 μmol photons m^{-2} s^{-1}, ΦII increases significantly ($p<0.05$) at 6 hours following IPTG induction with an upward trend appearing at 3 hours demonstrating that ΦII is enhanced under low actinic light on a time scale similar to sucrose export. Interestingly, at intensities greater than or equal to the growth light intensity (100 μmol

photons $m^{-2}s^{-1}$) ΦII increases are delayed. This result is surprising given that sink limitation effects should be more pronounced in conditions where light is not limiting. Taken together with the differences in excitation partitioning between uninduced cultures in BG0 and BG150 (Figure 2.8B) and the decrease I observe in the basal ΦII level of uninduced strains at higher salt (Figure 2.9), it is possible NaCl is inhibiting photosynthesis at higher light intensities. Indeed, I find that basal ΦII of uninduced strains decreases with increasing osmotic pressure (Figure 2.9), suggesting that effects of salt at the concentrations used in our experiments could be a confounding variable.

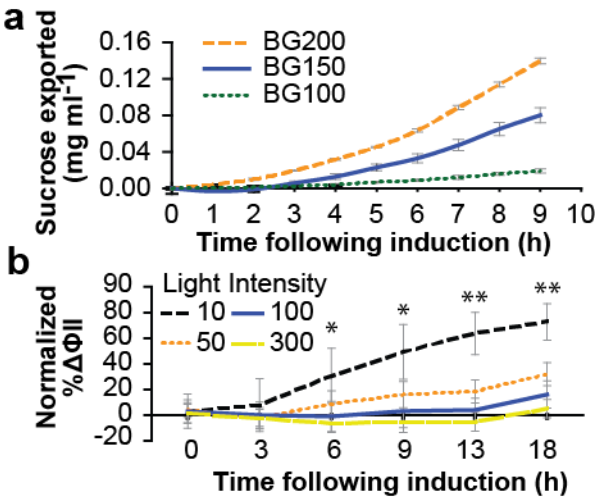

FIGURE 2.8: ΦII INCREASES ON A TIME SCALE COMPARABLE TO SUCROSE EXPORT.

a) Sucrose exported from *S. elongatus* following induction of cscB in BG100, BG150 and BG200. **b)** Normalized percent change in ΦII over time in BG150 when measured with different actinic light intensities. The intensity of the actinic light in this experiment was changed as shown in the figure key. Single asterisks (*) denote $p<0.05$ and double asterisks (**) denote $p<0.01$. BG0, BG100, BG150, BG200 denote BG11 media supplemented with 0, 100, 150 or 200 mM NaCl. All experiments are averages of 3 biological replicates (n=3).

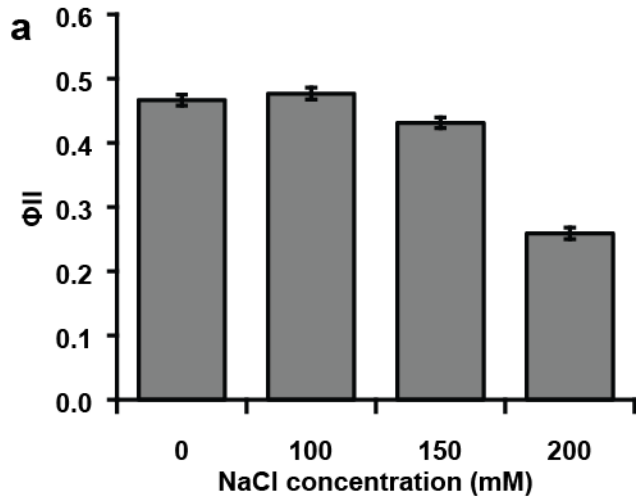

FIGURE 2.9: ΦII VALUE OF UNINDUCED CULTURES WITH RESPECT TO NACL CONCENTRATION.
ΦII of uninduced cultures in the indicated salt-supplemented media. Data are averages of duplicate samples (n=2).

To eliminate the confounding variable of salt stress, I engineered new lines of *S. elongatus* with the goal of creating an inducible sucrose export pathway that did not require increasing the osmolarity of the medium. In *S. elongatus*, a bidomainal protein carries out the final two reactions of sucrose synthesis whereby UDP-glucose and fructose 6-phosphate combine to form sucrose 6-phosphate and the phosphate is removed to yield sucrose (Martínez-Noël et al. 2013) (Figure 2.1B). Salt stress is known to directly increase the activity of sucrose phosphate synthase (SPS) and upregulate *sps* transcription in *S. elongatus* (Hagemann & Marin 1999). Therefore, the *sps* gene from *S. elongatus* (Synpcc7942_0808, SPS-7942) and from the halotolerant *Synechocystis* sp. PCC 6803 (sll0045, SPS-6803) were inducibly overexpressed to create a salt-free, sucrose export system in combination with *cscB* expression. At 24 hours post induction in BG0, cultures expressing only *cscB* had an undetectable amount of sucrose export whereas SPS-7942 and SPS-6803 had rates of 9 & 30 ug ml^{-1} h^{-1}, respectively (Figure 2.10A). Normalized to the cell number, SPS-6803 cultures at 24 hours post induction export sucrose at a rate of

0.028 pg sucrose $cell^{-1}$ h^{-1} which is comparable to cultures induced in BG100 expressing only cscB. Induction in BG0 of SPS-7942 with cscB did not result in significant amounts of sucrose exported compared to the uninduced control because the SPS-7942 enzyme requires a sodium ion to function, whereas SPS-6803 has basal activity without salt addition (Desplats et al. 2005).

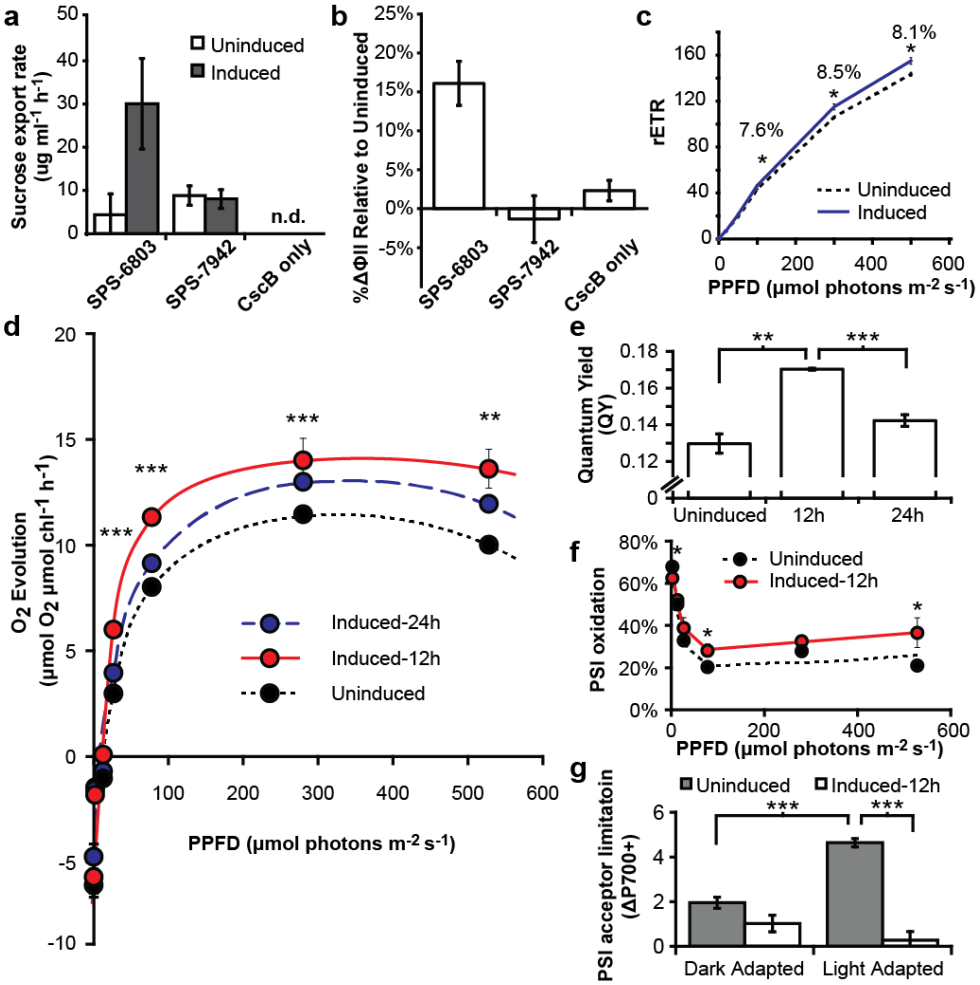

FIGURE 2.10: ENGAGEMENT OF HETEROLOGOUS SUCROSE SINK INCREASES PHOTOSYNTHETIC EFFICIENCY AND PET CHAIN FLUX OF ELECTRONS WITHOUT NACL SUPPLEMENTATION.

a) Sucrose export rate of strains engineered to overexpress sps and cscB in BG0 media 24 hours after induction. Sucrose export in cells expressing only cscB in BG0 was not detectable (n.d.). b) Normalized percent change in ΦII relative to uninduced cultures in BG0 24 hours after induction. c) Relative electron transfer rate (rETR) of SPS-6803 cultures in BG0 at 24 hours after induction and uninduced. Percentages show significant increases in rETR of induced cultures relative to uninduced cultures. d) Oxygen evolution of SPS-6803 cultures at 0, 12, and 24 hours after induction. Asterisk denote significant difference between 12 h and uninduced. e) Quantum yield of photochemistry derived from oxygen evolution data in Figure 2.8d. f) PSI oxidation measured at steady state at multiple light intensities. g) PSI acceptor limitation as observed by the rate of reduction of P700+ during a saturation pulse. Samples are either light acclimated or dark adapted following 12 hours induction in BG0; see Figure 2.12 for representative trace. For all panels asterisk (*) denotes $p<0.05$ whereas (**) denote $p<0.01$ and (***) shows significance at $p<0.001$. BG0 denotes BG11 media supplemented with 0mM NaCl. All experiments are averages of 3 biological replicates (n=3).

SPS-expressing strains exhibit an increase in ΦII consistent with sucrose secretion-mediated relaxation of sink limitation. SPS-6803 cultures without NaCl addition show a 15% increase in ΦII 24 hours after induction relative to uninduced cultures (Figure 2.10B). By contrast, both SPS-7942 and cscB-only strains that do not increase sucrose export upon IPTG induction in BG0, show insignificant changes in ΦII. Furthermore, the relative electron transport rate (rETR) of induced SPS-6803 cultures increased relative to uninduced SPS-6803 cultures in BG0 but only at higher light intensities than 100 µmol photons $m^{-2}s^{-1}$(Figure 2.10C). SPS-6803 cultures 24 hours post induction show a roughly 8% increase in the rETR, calculated as ΦII times PAR (Ralph & Gademann 2005), and which approximates the rate of electrons transported through the PET chain. These results are consistent with sucrose export acting to relieve sink inhibition at high light, and are distinct from the NaCl supplemented cultures expressing only cscB (Figure 2.9B).

Oxygen evolution rates in SPS-6803 cultures in BG0 (Figure 2.10D) were in agreement with the observed increases in rETR and ΦII (Figure 2.10C and Figure 2.9). At 24 hours post induction increased oxygen evolution was seen at light intensities greater than 20 µmol m^{-2} s^{-1} and greater than 10 µmol m^{-2} s^{-1} 12 h after induction ($p<0.05$). The maximum realized quantum efficiency (QY) of oxygen evolution was determined as the slope of the linear light limited region (Skillman et al. 2011) (Figure 2.10E). At 12 hours, QY increased to 0.17 whereas uninduced cultures were 0.13 ($p<0.05$) and had returned to 0.14 at 24 hours post induction. This initial increase in QY followed by a decline towards basal levels is similar to the trend seen in ΦII with NaCl supplemented cultures (Figure 2.2D), further suggesting a long-term sink regulatory acclimation. Increases in QY and ΦII suggest that cells exporting sucrose can utilize more light energy for photochemistry whereby sink limitation has relaxed.

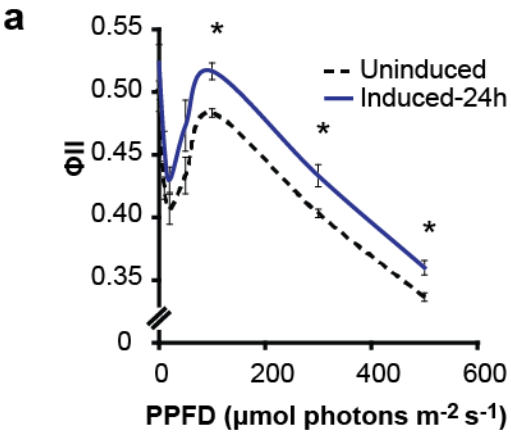

FIGURE 2.11: ΦII VALUES OF SPS-6803 AT MULTIPLE LIGHT INTENSITIES AT 24 HOURS AFTER INDUCTION IN BG0.

a) ΦII data at 24 hours after induction in BG0 media. Data are averages of replicate samples (n=3).

I next examined how increased PSII activity in sucrose-exporting cells could affect PSI and downstream photosynthetic electron transport. To approximate the oxidation state of PSI, the far-red light induced change in absorbance of P700 in PSI was measured (Figure 2.11) (Liu et al. 2012). PSI was more oxidized during illumination at 12 hours following induction compared to an uninduced culture in similar conditions (Figure 2.10F). Greater oxidation at several irradiances suggests either that electron flux from PSII and cytochrome b6f is relatively restricted or that there is increased electron efflux on the acceptor side of PSI. Our previous data shows an increase in ΦII (Figure 2.10B) and oxygen evolution (Figure 2.10D), indicative of increased PSII activity, therefore the increased oxidation of PSI suggests a decrease in PSI acceptor side limitation.

To directly assess donor-side or acceptor-side limitations, PSI oxidation kinetics were evaluated under saturating light conditions. A saturating pulse of light was applied during steady state in order to fully oxidize PSI, and the slope of ΔP700+ was used to approximate the accumulation of reduced P700 over time (Figure 2.11). PSI acceptor-

side limitation and reduction of P700 during saturating light represents electrons unable to be transferred to the acceptor side of PSI and accumulation of donated electrons, whereas relatively stable P700+ levels (i.e. $\Delta P700+ \approx 0$) indicates the carrier pool has sufficient capacity to accept electrons and keep PSI oxidized. Sucrose exporting cultures exhibit decreased acceptor-side limitation as observed by a decrease in the rate of P700+ reduction relative to uninduced cultures when light adapted (Figure 2.10G, 2.11). It is known that enzymes of the CB cycle are inactivated in the dark which decreases consumption of reductant and ATP (Michelet et al. 2013). SPS-6803 cultures were dark adapted and the rate of reduction of P700+ during a saturation pulse was measured (Figure 2.10G). SPS-6803 cultures showed the same amount of reduction of P700+ when dark-adapted, indicating that cscB induction does not alter acceptor-side capacity when the CB is inactive.

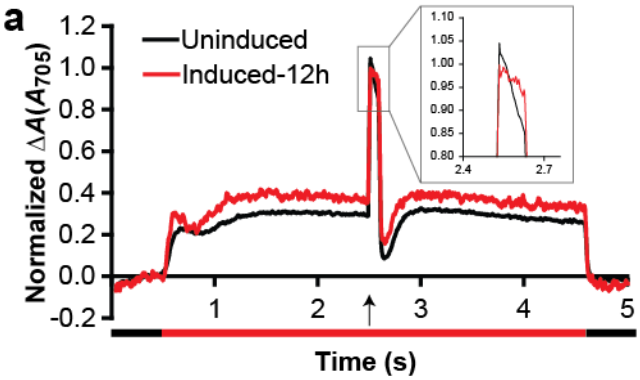

FIGURE 2.12: PSI ABSORBANCE CHANGES.
Representative trace of absorbance changes at 704 nm of an SPS-6803 culture 12h after induction (red) or in the uninduced control. Arrow denotes a 100 ms saturating pulse. Black bars denote samples in the dark and red bar shows where the sample was in actinic light. Data are averages of replicate samples (n=3).

Discussion

Here I use multiple independent methods to assess photosynthetic enhancements in a cyanobacterial strain following activation of a heterologous metabolic sink. I use both a salt-dependent, and an SPS-dependent approach to trigger cytosolic accumulation of sucrose, which

is exported through heterologous sucrose transporters (CscB). Consistent across all of our experiments, I observe increased PSII activity and efficiency shortly after induction of sucrose export (Figs. 2.2, 2.9, 2.10). I show that sucrose export rates can be fine-tuned through addition of increasing NaCl, and observe that enhancements in PSII activity and efficiency are directly correlated with the metabolic burden imposed by the heterologous pathway (Figure 2.2). These enhancements occur within hours of inducing sucrose-export and cannot be solely attributed to artifacts of spectroscopic measurements (Figure 2.6) (Campbell et al. 1998). All of these results are consistent with the hypothesis that the photosynthetic reactions of *S. elongatus* are sink-limited under standard laboratory growth conditions, and that introduction of an additional metabolic sink can relieve this inhibition and enable substantially improved photosynthetic flux and efficiency.

Our data suggest that activation of a heterologous sucrose sink improves multiple photosynthetic parameters. The enhancement of oxygen evolution, qP, QY, rETR and ΦII I observe (Figure 2.2, 2.10) are consistent with increased availability of open PSII centers and a more oxidized PQ pool following initiation of sucrose export. Furthermore I observe that PSI remains more oxidized at steady state (Figure 2.10F), likely a consequence of increased availability of cytosolic electron acceptors (Figure 2.10G). To explain these phenomena, I hypothesize that sucrose synthesis utilizes NADPH and ATP, promoting a relatively oxidized ferredoxin pool that releases sink limitation when the PET chain would otherwise be over-reduced. Consistent with this hypothesis, I observe the greatest enhancement in photosynthesis in SPS-expressing strains exporting sucrose when cultures are analyzed at higher irradiances (Figure 2.10C-F), when the largest sink limitations are expected. In contrast, cells induced to export sucrose by salt stress show

the most pronounced effects at lower light irradiances (Figure 2.9B), which suggests that photosynthetic measurements in salt-treated cells may be convoluted by the direct effects of salt. This is consistent with well-documented photosynthetic inhibition by osmotic shock and direct interference of Na^+ ions with photosystems (Allakhverdiev et al. 2002; Sudhir & Murthy 2004; Hagemann 2011).

While some photosynthetic parameters remain elevated following induction of a sucrose sink, other enhancements are transient. I observe a decrease in ΦII when cells were followed beyond 24 hours after sucrose induction in BG150 (Figure 2.2D). However, sucrose secreting cells continue to exhibit a relatively stable increase in oxygen evolution rates on a per cell basis for multiple days (Ducat et al 2012). Furthermore, chlorophyll content per cell becomes significantly higher 2.3 days following induction of sucrose export, which I hypothesize may be a consequence of long-term acclimation to an increased sink. Similarly, plants show long-term transcriptional changes following experimentally-imposed sink limitation which alter rubisco and PSII content, but these changes were never measured at the onset of sink induction (Lobo et al. 2015). A long-term acclimation to altered sink capacity could be partially driven by transcriptional changes leading to accumulation of photosynthetic proteins. It is known that specific sugars act to signal and regulate carbon balance in plants, both by allosterically modulating enzymatic activities, and modifying gene expression (Jang et al. 1997; Griffiths et al. 2016; Ljung et al. 2015). Whether similar signaling functions are associated with sugars in cyanobacteria remains an open question. Alternatively, or in parallel, an increase in sink capacity could manifest as a more oxidized PQ (Figure 2.2C), which could play a signalling function. The redox state of the PQ pool and cellular redox state has been implicated in many aspects of cyanobacterial metabolism including circadian rhythms, carbon flux through the CB cycle or

respiratory chain as well as the state transition of the cell (Ivleva et al. 2005; Michelet et al. 2013; Mullineaux & Allen 1990). Future studies will be required to identify and to determine the mechanisms leading to short- and long-term responses to increased sink demands.

It is likely similar mechanisms occur in previously reported engineered strains expressing heterologous pathways, suggesting that synthesis and export of carbon products could generally enhance photosynthesis in cultivated microalgae. For example, *S. elongatus* has increased carbon fixation and oxygen evolution rates when exporting isoprene (Gao et al. 2016). Other cyanobacterial species and algae engineered to export ethylene and glycerol, respectively, also exhibit increased oxygen evolution (Ungerer et al. 2012; Zhu et al. 2015; Demmig-Adams et al. 2014), however in these examples only a subset of photosynthetic parameters are observed to improve. Likewise, *S. elongatus* shows increased carbon fixation rates when exporting 2,3-butanediol, but does not exhibit enhanced oxygen evolution (Oliver & Atsumi 2015). It is likely that rerouting carbon towards certain metabolites may result in signaling that influence photosynthetic activities in addition to increasing total sink capacity.

A deeper understanding of the molecular mechanisms used to sense and acclimate to altered sink size may help to engineer systems for greater photochemical efficiencies, thereby increasing the feasibility of many microalgae-based sustainability initiatives (Blankenship et al. 2011). Our data suggest sink engineering is a promising parallel approach to improve microalgal productivity relative to previous efforts, which have largely focused upon improving carbon uptake and fixation rates (Durall & Lindblad 2015; Burnap et al. 2015) or decreasing photosystem antenna size (Melis 2009) to

attenuate excess light absorption. Importantly, I demonstrate that a heterologous sink downstream of carbon fixation can improve photosynthetic efficiency, thereby harnessing energy that might otherwise be dissipated. This is similar to approaches that use photosynthetically produced NADPH to degrade or produce metabolites (Berepiki et al. 2016; Hemschemeier et al. 2008) but distinct in that sucrose synthesis is downstream of the CB cycle and requires ATP and carbon fixation.

Beyond industrial applications, studying engineered sinks in cyanobacteria could provide useful information about molecular regulatory mechanisms of sink limitation that may be transferrable to plants. In plants, sink experiments are often convoluted by complexities in signaling and metabolic flux between multiple tissues or even multiple cell types within a given tissue (Tiessen & Padilla-Chacon 2012). Likewise, sink limitation studies often require environmental or physical stresses to alter the source-sink balance. Many studies of source-sink dynamics require restricting the sink size and observing a decrease in photochemistry (Adams et al. 2013) as opposed to this study where increasing sink size results in paralleled increases in photochemistry. It is possible that further analysis of engineered cyanobacteria similar to the system presented in this study may provide some insight into molecular mechanisms governing sink sensing at the cellular level in plants.

Materials and Methods

Strains and Growth Conditions

Synechococcus elongatus PCC 7942 was grown at constant 32 ˚C temperature and supplemented with 2% CO_2 in a Multitron Infors HT Incubator with ~100 µmol photons m^{-2} s^{-1} of light provided by Sylvania 15 W Gro-Lux fluorescent bulbs. Cultures were shaken at 150 rpm in BG11 supplemented with 1 g/L HEPES to a final pH of 8.3 with NaOH. Cultures were

supplemented with additional NaCl as noted in the text. BG0, BG100, BG150 and BG200 media were supplemented with 0, 100, 150 or 200 mM NaCl, respectively. Cultures were back-diluted to 0.3 OD_{750} every day which acclimated cells to the appropriate medium for at least three days prior to experiments or IPTG induction. Where appropriate, 1 mM IPTG was added to induce cscB, SPS-6803 or SPS7942 expression in liquid cultures. Chloramphenicol was used to select for cscB containing cells in BG0 and selection was removed prior to acclimating cultures to NaCl supplemented medium. Chloramphenicol (25 mg $liter^{-1}$) and Kanamycin (50 mg $liter^{-1}$) were used to maintain cscB and SPS-6803 or SPS-7942 containing cells, respectively.

Strain Construction

S. elongatus with a genomically integrated copy of *cscB* under an IPTG inducible promoter was used as previously described (Ducat et al. 2012). Sucrose phosphate synthase genes were PCR amplified from host genomes (Synpcc7942_0808,SPS-7942) and *Synechocystis* sp. PCC 6803 (sll0045,SPS-6803) and standard Gibson assembly techniques were used to insert these genes into the multiple cloning site of NS2 (pAM1579; Addgene ID 40240) which contains an IPTG inducible promoter driving SPS expression. Plasmids were submitted to Addgene as SPS-6803 (ID #80458) and SPS-7942 (ID #80459). *S. elongatus* strains were confirmed to have complete knock-ins by PCR. Functional sucrose export characterization was determined by sucrose quantification of the supernatant after induction.

Sucrose Quantification

Cultures were grown as described in the text. At indicated timepoints, cells were pelleted in a benchtop centrifuge and the supernatant was sampled for sucrose assays.

Sucrose quantification was determined using the Sucrose/D-Glucose Assay Kit (Megazyme: K-SUCGL). A standard curve of the relationship between cell number and OD_{750} was generated with the use of a BD-Accuri (BD Biosciences) and Genesys 20 photospectrometer (Thermo), respectively. Sucrose export rates were converted into a per cell basis during experiments by measurement of OD750 and calculation of total cell number for a given time point from the resulting standard curve.

Fluorescence Measurements

Preliminary ΦII measurements were performed on a custom-built PAM fluorimeter with a pulsed measuring beam (450-nm peak-emission LED). The sample was then illuminated with 100 μmol photons m^{-2} s^{-1} of photosynthetic photon flux density (450-nm peak-emission LED). Chlorophyll fluorescence was filtered with a long-pass 695 nm filter in front of the detector. ΦII measurements in this publication were performed using an Aquapen AP-C 100 (Photon Systems Instruments, Drasov, Czech Republic) using blue LEDs and protocols LC1 or NPQ1. Two mililiter samples were collected and dark adapted for a minimum of 1 minute where appropriate. All measurements are the average of at least 3 biological replicates ($n \geq 3$) unless noted.

77K Fluorescence

100 μl samples were placed in an optically-clear 96-well plate and acclimated to the growth light for greater than 10 min, 24 h by IPTG addition, or remained uninduced. Samples were flash frozen in liquid nitrogen without shading. PBS were excited with a World Star Tech laser (DPGL-05S) at wavelength 532 nm and the fluorescence of the sample was measured by an Ocean Optics(HR2000s+ES) spectrometer coupled to a fiber-optic cable 1 mm in diameter at a bandwidth of 5 nm. Baseline subtraction was performed using BG0 media without cells as a reference. Spectra were then normalized to the PBS peak at roughly 660 nm and the ratio of

fluorescence intensity at 685 nm and 714 nm was determined. Measurements are the average of 10 technical measurements and 3 biological replicates.

Oxygen Evolution

Oxygen evolution was measured from a 2 ml culture in a cuvette with a temperature-controlled, stirring-enabled cuvette holder (standard 1-cm path length). Cells were maintained in growth media as described in "Samples and Growth Conditions" and samples were measured within minutes of withdrawal from 2% CO_2 incubators - as with other fluorescence based measurements. The sample was then illuminated with a pair of LEDs (Luxeon III LXHL-PD09, Philips) with maximal emission at 620 nm. Light intensity was altered as noted in the text. Oxygen production was measured using an Ocean Optics (NeoFox-GT) and rates were determined as the linear slope once acclimated to a given light intensity, approximately five minutes after acclimation. The oxygen evolution rate was then normalized to the chlorophyll quantity of the sample.

Pigment Quantification

Chlorophyll was extracted as previously described (Zarel et al. 2015) in 90% methanol where the absorbance was measured using a Genysis 20 spectrometer at appropriate wavelengths. Phycobiliproteins were extracted at room temperature in 50 mM Tris-buffered lysozyme (5mg/ml) solution supplemented 10 mM EDTA with silicone dioxide and shaken overnight. Absorbance measurements and calculations were performed as in (Turner 1994).

PSI Absorbance Changes

As described by Juergens et al. 2015 the absorbance changes attributed to P700 redox changes were monitored using a measuring LED (peak emission, 720 nm) filtered

through a 5-nm band pass filter centered at 700 nm, giving an emission peak at approximately 705 nm. A Schott RG695 color glass filter protected the detector from actinic light. The sample was then illuminated at an irradiance described in the text from a pair of LEDs (Luxeon III LXHL-PD09, Philips) with maximal emission at 620 nm, directed toward opposite sides of the cuvette, perpendicular to the measuring beam. Percent P700 oxidation was calculated as $(P_{ox}-P_{ss})/(P_{red}-P_{ox})$, where P_{ox} is the total population of P700 oxidized by a saturating pulse of light, P_{ss} is the steady state level of oxidation and P_{red} is the level of P700 reduced in the dark. PSI traces were normalized to the maximum oxidation state during a saturating pulse (Pox). PSI acceptor limitation was determined from the linear slope of the saturating pulse in light acclimated or 30min dark adapted samples either uninduced or induced.

Funding

This work was supported by the Office of Science of the U.S. Department of Energy DE-FG02.91ER2002.

Disclosures

The authors have no conflicts of interest to declare.

Acknowledgments

The authors would like to acknowledge Dr. Ben Lucker for his insightful comments and guidance in spectroscopic measurements.

REFERENCES

REFERENCES

Adams, W. et al., 2013. May photoinhibition be a consequence, rather than a cause, of limited plant productivity? Photosynthesis Research, 117(1-3), pp.31–44.

Allakhverdiev, S.I. et al., 2002. Salt stress inhibits the repair of photodamaged photosystem II by suppressing the transcription and translation of *psbA* genes in *Synechocystis*. Plant physiology, 130(3), pp.1443–1453.

Baker, N.R., 2008. Chlorophyll fluorescence: a probe of photosynthesis in vivo. Annual review of plant biology, 59, pp.89–113.

Berepiki, A. et al., 2016. Tapping the unused potential of photosynthesis with a heterologous electron sink. ACS Synthetic Biology, p.acssynbio.6b00100.

Blankenship, R.E. et al., 2011. Comparing photosynthetic and photovoltaic efficiencies and recognizing the potential for improvement. Science (New York, N.Y.), 332(6031), pp.805–9.

Burnap, R.L., 2015. Systems and photosystems: cellular limits of autotrophic productivity in cyanobacteria. Frontiers in bioengineering and biotechnology, 3(January).

Burnap, R.L., Hagemann, M. & Kaplan, A., 2015. Regulation of CO2 Concentrating Mechanism in Cyanobacteria. , pp.348–371.

Campbell, D. et al., 1998. Chlorophyll fluorescence analysis of cyanobacterial photosynthesis and acclimation. Microbiology and Molecular Biology Reviews, 62(3), pp.667–683.

Clarke, A.K. et al., 1995. Dynamic responses of photosystem II and phycobilisomes to changing light in the cyanobacterium Synechococcus sp. PCC 7942. Planta, pp.553–562.

Demmig-Adams, B., Stewart, J.J., et al., 2014. Insights from Placing Photosynthetic Light Harvesting into Context. The Journal of Physical Chemistry Letters, 5, pp.2880–2889.

Demmig-Adams, B., Garab, G., et al., 2014. Non-Photochemical Quenching and Energy Dissipation in Plants, Algae and Cyanobacteria 40th ed. B. Demmig-Adams et al., Springer.

Desplats, P., Folco, E. & Salerno, G.L., 2005. Sucrose may play an additional role to that of an osmolyte in Synechocystis sp. PCC 6803 salt-shocked cells. Plant Physiology and Biochemistry, 43, pp.133–138.

Durall, C. & Lindblad, P., 2015. Mechanisms of carbon fixation and engineering for increased carbon fixation in cyanobacteria. Algal Research, 11, pp.263–270.

Ducat, D.C. et al., 2012. Rerouting carbon flux to enhance photosynthetic productivity. Applied and Environmental Microbiology, 78, pp.2660–2668.

Gao, X. et al., 2016. Engineering the methylerythritol phosphate pathway in cyanobacteria for photosynthetic isoprene production from CO2. Energy Environ. Sci., 9, pp.1400–1411.

Hagemann, M., 2011. Molecular biology of cyanobacterial salt acclimation. FEMS Microbiology Reviews, 35(1), pp.87–123.

Hagemann, M. & Marin, K., 1999. Salt-induced Sucrose Accumulation is Mediated by Sucrose-phosphate-synthase in Cyanobacteria. Journal of Plant Physiology, 155(3), pp.424–430.

Hemschemeier, A. et al., 2008. Hydrogen production by Chlamydomonas reinhardtii: An elaborate interplay of electron sources and sinks. Planta, 227(2), pp.397–407.

Herold, A., 1980. Regulation of photosynthesis by sink activity - the missing link. New Phytologist, 86, pp.131–144.

Hogewoning, S.W. et al., 2012. Photosynthetic Quantum Yield Dynamics: From Photosystems to Leaves. The Plant Cell, 24(5), pp.1921–1935.

Griffiths, C.A., Paul, M.J. & Foyer, C.H., 2016. Metabolite transport and associated sugar signalling systems underpinning source/sink interactions. Biochimica et Biophysica Acta (BBA) - Bioenergetics, 1857, pp.1715–1725.

Ivleva, N.B. et al., 2005. LdpA: a component of the circadian clock senses redox state of the cell. The EMBO journal, 24(6), pp.1202–1210.

Jang, J.C. et al., 1997. Sugar sensing and signaling in plants. The Plant cell, 9(1), pp.5–19.

Ljung, K., Nemhauser, J.L. & Perata, P., 2015. New mechanistic links between sugar and hormone signalling networks. Current Opinion in Plant Biology, 25, pp.130–137.

Michelet, L. et al., 2013. Redox regulation of the Calvin-Benson cycle: something old, something new. Frontiers in plant science, 4(November), p.470.

Mullineaux, C.W. & Allen, J.F., 1990. State 1-State 2 transitions in the cyanobacterium Synechococcus 6301 are controlled by the redox state of electron carriers between Photosystems I and II. Photosynthesis Research, 23, pp.297–311.

Jang, J.C. et al., 1997. Sugar sensing and signaling in plants. The Plant cell, 9(1), pp.5–19.

Juergens, M.T. et al., 2015. The Regulation of Photosynthetic Structure and Function during Nitrogen Deprivation in Chlamydomonas reinhardtii. Plant physiology, 167(February), pp.558–573.

Kaňa, R. et al., 2012. The slow S to M fluorescence rise in cyanobacteria is due to a state 2 to state 1 transition. Biochimica et Biophysica Acta (BBA) - Bioenergetics, 1817, pp.1237–1247.

Kato, A. et al., 2016. Modulation of the balance of fatty acid production and secretion is crucial for enhancement of growth and productivity of the engineered mutant of the cyanobacterium Synechococcus elongatus. Biotechnology for Biofuels, 9(1), p.91.

Krapp, A., Quick, W.P. & Stitt, M., 1991. Ribulose-1,5-bisphosphate carboxylase-oxygenase, other Calvin-cycle enzymes, and chlorophyll decrease when glucose is supplied to mature spinach leaves via the transpiration stream. Planta, 186(1), pp.58–69.

Li, X., Shen, C.R. & Liao, J.C., 2014. Isobutanol production as an alternative metabolic sink to rescue the growth deficiency of the glycogen mutant of Synechococcus elongatus PCC 7942. Photosynthesis research, 120(3), pp.301–10.

Liu, Lu-Ning. et al., 2012. Control of electron transport routes through redox-regulated redistribution of respiratory complexes. Proceedings of the National Academy of Sciences, 109(28), pp.11431–11436.

Lobo, A.K.M. et al., 2015. Exogenous sucrose supply changes sugar metabolism and reduces photosynthesis of sugarcane through the down-regulation of Rubisco abundance and activity. Journal of Plant Physiology, 179, pp.113–121.

Martínez-Noël, G.M. a et al., 2013. First evidence of sucrose biosynthesis by single cyanobacterial bimodular proteins. FEBS Letters, 587, pp.1669–1674.

Maxwell, K. & Johnson, G.N., 2000. Chlorophyll fluorescence--a practical guide. Journal of experimental botany, 51(345), pp.659–668.

Melis, A., 2009. Solar energy conversion efficiencies in photosynthesis: Minimizing the chlorophyll antennae to maximize efficiency. Plant Science, 177(4), pp.272–280.

Michelet, L. et al., 2013. Redox regulation of the Calvin-Benson cycle: something old, something new. Frontiers in plant science, 4(November), p.470.

Mullineaux, C.W. & Allen, J.F., 1990. State 1-State 2 transitions in the cyanobacterium Synechococcus 6301 are controlled by the redox state of electron carriers between Photosystems I and II. Photosynthesis Research, 23, pp.297–311.

Nozzi, N.E. & Atsumi, S., 2015. Genome Engineering of the 2,3-Butanediol Biosynthetic Pathway for Tight Regulation in Cyanobacteria. ACS Synthetic Biology, 4(11), pp.1197–1204.

Oliver, J.W.K. et al., 2013. Cyanobacterial conversion of carbon dioxide to 2,3-butanediol. Proceedings of the National Academy of Sciences of the United States of America, 110(4), pp.1249–54.

Oliver, J.W.K. & Atsumi, S., 2015. A carbon sink pathway increases carbon productivity in cyanobacteria. Metabolic Engineering, pp.1–7.

Oxborough, K. & Baker, N.R., 1997. Resolving chlorophyll a fluorescence images of photosynthetic efficiency into photochemical and non-photochemical components - Calculation of qP and Fv'/Fm' without measuring Fo'. Photosynthesis Research, 54(1989), pp.135–142.

Paul, M.J. & Foyer, C.H., 2001. Sink regulation of photosynthesis. Journal of experimental botany, 52(360), pp.1383–1400.

Ralph, P.J. & Gademann, R., 2005. Rapid light curves: A powerful tool to assess photosynthetic activity. Aquatic Botany, 82(3), pp.222–237.

Sawada, S. et al., 1986. Influence of carbohydrates on photosynthesis in single, rooted soybean leaves used as a source-sink model. Plant and Cell Physiology, 27(4), pp.591–600.

von Schaewen, A. et al., 1990. Expression of a yeast-derived invertase in the cell wall of tobacco and Arabidopsis plants leads to accumulation of carbohydrate and inhibition of photosynthesis and strongly influences growth and phenotype of transgenic tobacco plants. The EMBO journal, 9(10), pp.3033–44.

Sharkey, T.D. et al., 1986. Limitation of Photosynthesis by Carbon Metabolism 1. Plant physiology, 81, pp.1123–1129.

Skillman, J. et al., 2011. Photosynthetic Productivity: Can Plants do Better? Thermodynamics - Systems in Equilibrium and Non-Equilibrium, (1992), pp.35–68.

Sudhir, P. & Murthy, S.D.S., 2004. Effects of salt stress on basic processes of photosynthesis. Photosynthetica, 42(4), pp.481–486.

Takizawa, K., Kanazawa, A. & Kramer, D.M., 2008. Depletion of stromal Pi induces high "energy-dependent" antenna exciton quenching (qE) by decreasing proton conductivity at CF O-CF1 ATP synthase. Plant, cell & environment, 31(2), pp.235–43.

Tiessen, A. & Padilla-Chacon, D., 2012. Subcellular compartmentation of sugar signaling: links among carbon cellular status, route of sucrolysis, sink-source allocation, and metabolic partitioning. Frontiers in plant science, 3(January), p.306.

Tsimilli-Michael, M., Stamatakis, K. & Papageorgiou, G.C., 2009. Dark-to-light transition in Synechococcus sp. PCC 7942 cells studied by fluorescence kinetics assesses plastoquinone redox poise in the dark and photosystem II fluorescence component and dynamics during state 2 to state 1 transition. Photosynthesis Research, 99(3), pp.243–255.

Turner, M., 1994. Microalgae — biotechnology and microbiology. Journal of Experimental Marine Biology and Ecology, 183, pp.300–301.

Ungerer, J. et al., 2012. Sustained photosynthetic conversion of CO2 to ethylene in recombinant cyanobacterium Synechocystis 6803. Energy & Environmental Science, 5(10), p.8998.

Xuan, Y.H. et al., 2013. Functional role of oligomerization for bacterial and plant SWEET sugar transporter family. Proceedings of the National Academy of Sciences of the United States of America, 110(39), pp.E3685–94.

Yang, J.T. et al., 2015. Triose phosphate use limitation of photosynthesis: short-term and long-term effects. Planta.

Zarel, T., Sinetova, M.A. & Cerveny, J., 2015. Measurement of Chlorophyll a and carotenoids Concentration in Cyanobacteria. Bio-protocol, 9(May).

Zhu, T. et al., 2015. Enhancing photosynthetic production of ethylene in genetically engineered Synechocystis sp. PCC 6803. Green Chem., 17(1), pp.421–434.

CHAPTER 3: CARBOXYSOME COMPOSITION IS DYNAMICALLY ALTERED IN RESPONSE TO INCREASED SINK DEMAND IN SYNECHOCOCCUS ELONGATUS PCC7942

Introduction

Cyanobacteria have elaborate mechanisms to concentrate CO_2 near the carbon fixing enzyme rubisco. The first stage in the carbon concentrating mechanism (CCM) requires concentrating bicarbonate in the cytoplasm by actively transporting inorganic carbon (Ci) into the cell through expression of Ci transporters (Eisenhut *et al.*, 2007). Ci is further concentrated in the proteinaceous bacterial micro-compartment, the carboxysome. The carboxysome consists of an external layer of shell proteins thought to act as a diffusive barrier for large and/or apolar compounds, and a luminal space that is highly concentrated with rubisco. Rubisco is organized into a paracrystalline array through interactions with the CcmM protein (Long *et al.*, 2010; Cameron *et al.*, 2013). In addition, carboxysomes also encapsulate proteins with carbonic anhydrase (CA) activity, which catalyzes the conversion of bicarbonate to CO_2, therefore CA creates a high CO_2 concentration near rubisco, while the shell proteins limit CO_2 escape and oxygen penetration (Cameron *et al.*, 2013). Altogether, the carboxysome greatly increases rubisco's caboxylase activity, and intact carboxysomes are required for cyanobacterial growth under ambient CO_2 conditions (Long *et al.*, 2007). Additionally, assembly of carboxysomes requires coordination of a number of different proteins, collectively requires a significant portion of cellular resources, and therefore requires careful regulation in response to environmental changes.

Cyanobacteria regulate both number of carboxysomes within the cell and the carboxysome morphology in response to dynamic environmental conditions (Whitehead *et al.*, 2014; Sun *et al.*, 2016), presumably to optimize carbon capture under different growth regimes. For example, it was shown that cells grown under high light have an increased density of carboxysomes compared to low-light grown cells, and that the carbon fixation rate correlates

positively with the number of carboxysomes per cell (Whitehead *et al.*, 2014; Sun *et al.*, 2016). Likewise, it has been shown that low carbon availability increases transcript abundance for many of the carboxysome structural proteins and rubisco subunits (Woodger, Badger and Price, 2003). A two-component regulator (RcaE) that responds to light quality and intensity was shown to play a critical role in regulation of carboxysome morphology and transcript abundance of many CCM genes in addition to altering CcmM protein accumulation (Rohnke *et al.*, 2018). Interestingly, the CcmM protein helps to organize the core of the carboxysome through three rubisco small-subunit-like-domains (SSLD) which interact with RbcL to nucleate it within the carboxysome. In addition, CcmM is translated into a short (M35) and long (M58) isoform and both are essential for functional carboxysomes while an increase in the ratio of M35 to M58 was shown to increase the carboxysome size (Long *et al.*, 2010, 2011). How carboxysome biogenesis and features are regulated remain an open question, but one emerging hypothesis is that carboxysome size may be regulated in part through control over the amount of RbcL that is nucleated in the lumen; where an increased proportion of M35 may nucleate a larger rubisco core and M58 levels may increase the recruitment of shell proteins, thus favoring a lower carboxysome volume:surface area. It is clear that carboxysome abundance and morphology are regulated by changes in environmental factors (i.e. light and CO_2) but little is known about the regulation of carboxysome morphology in response to internal metabolic sink limitation.

To date, most research has focused on the analysis of carboxysome responses to changing environmental conditions as opposed to internal metabolic demands. Without changes to environmental conditions, internal metabolic sink demands can occur from genetic knockouts that restrict metabolite consumption or through engineered integration of bioproduction pathways that increase metabolic sink demand. Within a natural context, differences in gene

expression or metabolite pools between neighboring cells could be expected to influence the perceived metabolic load even if the cells share an identical environmental condition. For example, in a population of cyanobacteria with a heterogeneous distribution of glycogen reserves, the perceived demand for assimilation of new carbon substrates can be different between cells even if all cells share the same environment. Because bioproduction strains have been modified with exogenous pathways that often require extra energy and carbon, especially if the target product is exported, these strains could provide an alternative approach to modulate metabolic demand (Savakis, Angermayr and Hellingwerf, 2013).

I previously presented data to demonstrate that cyanobacteria engineered with an expanded heterologous sink have increased photosynthetic efficiency and photosynthetic electron flux (Abramson et al. 2016; Chapter 2). This presents a novel background to disentangle carboxysome regulatory mechanisms in response to increased metabolic sink demand versus perturbations in environmental conditions, such as light or CO_2. Many cyanobacterial production strains show greater carbon uptake and fixation when heterologous pathways are active but carboxysome morphological features are not observed (Ducat *et al.*, 2012; Ungerer *et al.*, 2012; Oliver and Atsumi, 2015). One possibility for the increase in photosynthetic activity is the relief of sink inhibition when carbon compounds are exported (Chapter 1; Abramson et al., 2016). Sink limitation of photosynthesis occurs when cells are photosynthetically limited by the cellular capacity to use reduced sugars when ample light and CO_2 are available (Paul and Foyer, 2001; Yang *et al.*, 2015). It remains unclear if any changes to the carboxysome composition or localization will respond in strains that are exporting photosynthetically derived carbon and energy and if the mechanisms of sensing a heterologous sink are similar to mechanisms involved in environmental sensing.

In this chapter, preliminary data is presented which might suggest that a change in carboxysome components occurs in response to experimentally-induced sucrose export. To this end, I constructed a carboxysome reporter strain by genomically integrating an *rbcS-GFP* fusion gene expressed from the *rbcS* promoter to study the response of the carboxysome to heterologous sucrose export; analogously to prior reporter strains with fluorophore-labeled RbcL subunits (Sun *et al.*, 2016; Savage *et al.*, 2010). I observe when cells are exporting sucrose, the number of carboxysomes does not change but the fluorescence intensity derived from RbcS-GFP increases within the cell, suggesting greater RbcS-GFP protein production within the cell. This is accompanied by an increase in the ratio of RbcL:PsbA (PSII subunit) suggesting RbcL protein production within the cell is increased. Finally, preliminary data may show that the ratio of CcmM35:M58 increases which might suggest a mechanism for increasing rubisco localization within the carboxysome and a morphological response to heterologous sinks.

Results

Carboxysome reporter construction and confirmation of function in an engineered cyanobacterium

To non-destructively visualize carboxysome dynamics, I constructed a C-terminal fusion of the small subunit of rubisco (RbcS) with GFP controlled by the *rbcS* promoter (Figure 3.1a). This construct was integrated into a neutral site of the genome within a previously engineered sucrose exporting (Suc-Ex) strain containing sucrose phosphate synthase and sucrose permease (Abramson *et al.*, 2016, and Chapter 2). This allows the visualization of the regulation of RbcS-GFP, and consequently carboxysome regulation, in response to induction of a heterologous carbon sink.

To confirm that insertion of RbcS-GFP did not disrupt carboxysome function and formation, I exposed the carboxysome reporter strain (CBR) to environmental conditions known to influence regulation of the carboxysome (Figure 3.1). First, RbcS-GFP localized to aggregates that are distributed along the length of the cell similar to a previously characterized RbcL-GFP fusion known to localize to the carboxysomes in high carbon (HC; 2% CO_2) conditions (Sun *et al.*, 2016) and therefore I conclude RbcS-GFP is mostly localized within the carboxysome. Likewise, these cells grow in atmospheric carbon (LC; 0.04% CO_2) conditions, suggesting the carboxysome is intact and functioning since cells with aberrant carboxysome assembly require HC growth conditions (Price *et al.*, 2008, Cameron *et al.*, 2013). It is established that the expression of carboxysome genes is responsive to the availability of CO_2 (Eisenhut *et al.*, 2007; Long *et al.*, 2010) and therefore I determined the RbcS-GFP localization within cells grown in HC and LC conditions (Figure 3.1 b and c). I visually observed there were larger and greater numbers of RbcS-GFP puncta within the cell when cells were grown in LC conditions compared to HC conditions (Figure 3.1a and b). This suggests that the RbcS-GFP promoter is responsive to changing CO_2 concentrations and the genetic elements are functional.

Finally, I quantified representative protein subunit abundance for several photosynthetic complexes (RbcL in rubisco, PsbA in PSII and PsaC in PSI; Figure 3.1d) by Western blot and did not observe any differences compared to the Suc-Ex strain that does not contain the *rbcS-GFP* gene cassette when cells were grown in HC (Figure 3.1e). Therefore, I conclude expression of RbcS-GFP does not interfere with the stoichiometry of photosynthetic complexes nor does RbcS-GFP localization within the carboxysomes interfere with the cell's ability to produce functional carboxysomes when cells are not exporting sucrose.

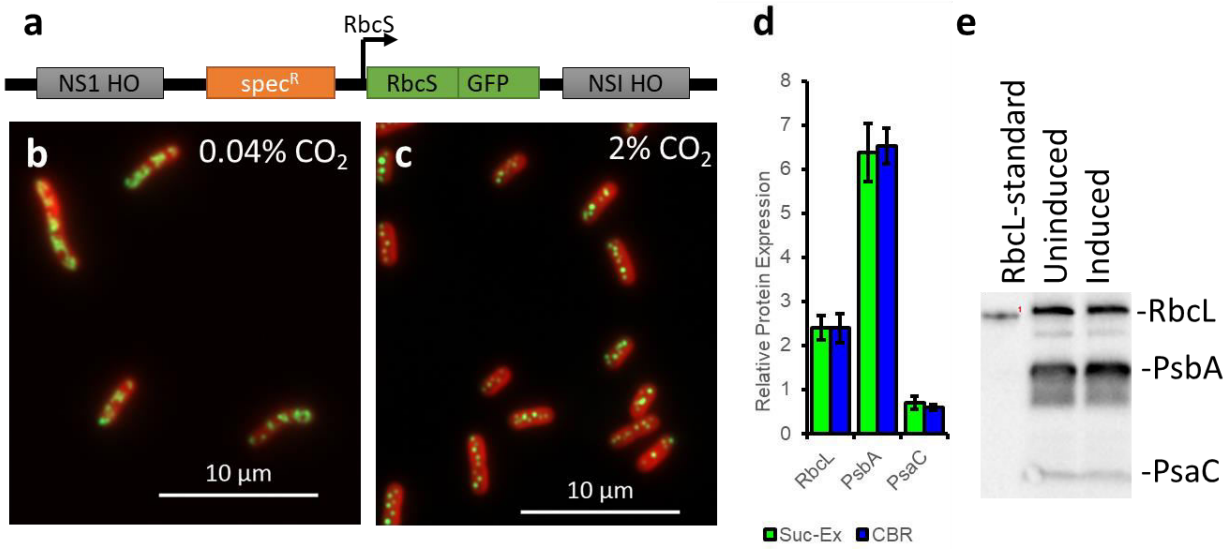

FIGURE 3.1: RUBISCO SMALL SUBUNIT TAGGED WITH GFP FOR CARBOXYSOME LOCALIZATION AND CHARACTERIZATION.
a) Cartoon of the genetic element inserted into the sucrose exporting (Suc-Ex) strain to visualize carboxysomes containing RbcS-GFP (CBR). **b)** Atmospheric carbon conditions visually show larger and a greater number of carboxysomes compared to **c)** high carbon (HC) grown cells. **d)** In HC grown cells, relative protein expression for photosynthetic complexes is not affected by RbcS-GFP, shows the RbcS-GFP fusion does not alter complex stoichiometry. RbcL, PsbA in PSII and PsaC in PSI. **e)** Representative Western blot of the photosynthetic complexes RbcL, PsbA in PSII and PsaC in PSI showing the genetic integration of *rbcS-GFP* does not affect protein expression.Total protein was extracted and equal amounts of protein were loaded for each sample..

Carboxysome numbers and cell morphology are affected by sucrose export

A direct correlation has been reported between carbon fixation rates and the number of carboxysomes per cell (Sun *et al.*, 2016), and sucrose-exporting cells display a ~20% increase in CO_2 fixation rates relative to uninduced controls (Ducat *et al.*, 2012), therefore, I measured the number of carboxysomes within the cell in response to sucrose export (Figure 3.2). To examine if increased CO_2 fixation rates in sucrose-exporting strains can be partially attributed to increased carboxysome number, I induced sucrose export at 0h and monitored carboxysome numbers relative to an uninduced control. All cultures were routinely back diluted to keep them maintained at a low density where light

limitation caused by self-shading would not contribute to the observed phenotypes. I used MicrobeJ as a high-throughput gating and quantification program to assess the number, size, and intensity of carboxysomes within each cell (Ducret, Quardokus and Brun, 2016). The outline of the cells was determined by the chlorophyll auto fluorescence boundary and foci (i.e. carboxysomes) were determined by GFP foci within the cell boundary (see materials and methods for MicrobeJ parameterization). Cells induced to export sucrose showed a greater number of carboxysomes per cell (Figure 3.2a) but the cells also increased in length following induction (Figure3.2b). Since there is a strong linear correlation between the number of carboxysomes per cell and the cell length (Figure 3.2c), I therefore accounted for the increase in cell length and observed no difference in the number of carboxysomes per unit cell length whether cells were induced or remained uninduced (Figure 3.2c).

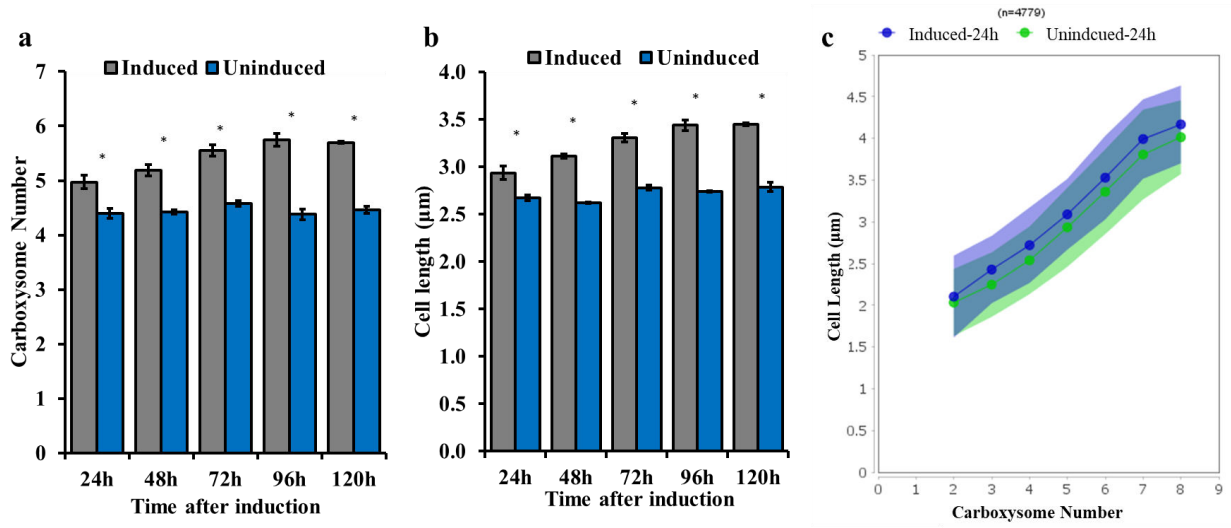

FIGURE 3.2: CARBOXYSOME NUMBER PER CELL IS UNAFFECTED WHEN NORMALIZED TO CELL LENGTH

a) Carboxysome number increases following induction of sucrose export. **b)** Cell length increases significantly following sucrose export. **c)** A linear response between cell length and carboxysome number is observed and sucrose export does not increase the number of carboxysomes normalized to cell length. Graphs are means ±standard error from 3 replicates of n>100 cells and asterisk (*) denote t-test significance at p-value < 0.05.

An induced heterologous sink increases RbcS-GFP intensity within cells

Carboxysomes can change size in response to outside environmental perturbations but little is known about carboxysome morphological changes imposed by increased carbon sink demand. I hypothesized that while the carboxysome density within cells was unaltered, composition and/or morphology of carboxysomes could be impacted in the face of increased metabolic demand following sucrose export. I first measured RbcS-GFP signal in sucrose-secreting cells in comparison to uninduced controls, using the mean intensity of chlorophyll fluorescence as a reference to normalize fluorescence data (Figure 3.3a and b). Although some changes in chlorophyll fluorescence were observed between days, there was no significant change in mean chlorophyll fluorescence intensity between uninduced and induced cultures (Figure 3.3a). To account for an increase in the cell length of sucrose exporting cells, the mean cellular GFP pixel intensity was measured

within the entire cell boundary (Figure 3.3b). The mean cellular GFP pixel intensity takes the average intensity of all the pixels within the cell and therefore is normalized for the number of pixels within the cell's gated area. The mean GFP intensity increased significantly following induction of sucrose export suggesting there is increased expression from the *rbcS* promoter driving RbcS-GFP expression. It is unclear from this measurement if RbcS-GFP is localized within the carboxysome or diffuse in the cytoplasm, therefore, a closer investigation into the partitioning of RbcS-GFP within the cells was called for.

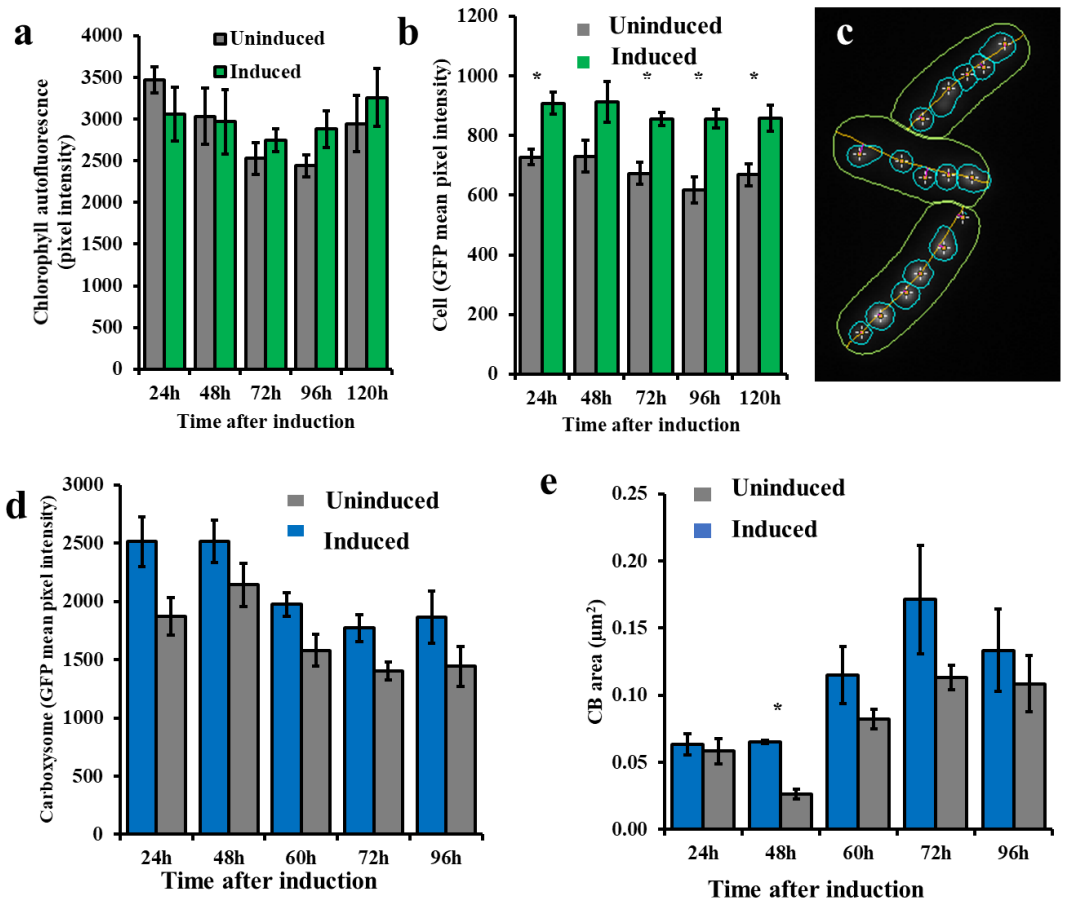

FIGURE 3.3: SUCROSE EXPORT LEADS TO GREATER RBCS-GFP PRODUCTION **a)** Chlorophyll fluorescence is shown as an exposure control and there is no change between uninduced and induced cultures throughout the course of these experiments **b)** RbcS-GFP mean cellular fluorescence intensity increases suggesting greater RbcS-GFP production within the cell gate. **c)** Representative cells showing MicrobeJ gating for cells and carboxysomes. The cell outline is yellow while the RbcS-GFP foci with the cells are outlined in blue. **d)** The mean intensity of RbcS-GFP localized within the carboxysomes increases in cultures induced to export sucrose. **e)** The size of the carboxysomes increases in response to sucrose export. Graphs are means±stdev from 3 replicates of n>100 cells and asterisk (*) denote t-test significance at p-value < 0.05.

RbcS-GFP localized within the carboxysome was approximated by determining the RbcS-GFP fluorescence intensity within carboxysome puncta. The carboxysome area was calculated by MicrobeJ (Figure 3.3c) (See materials and methods) using identical algorithm parameters for uninduced and induced cultures. The mean GFP pixel intensity within the carboxysome region increased in cells induced to export sucrose compared to

uninduced cells (Figure 3.3d), albeit not significantly (p-value > 0.05). The average size of the carboxysomes also appears to increase in response to sucrose export after 48h (Figure 3.3e), although limitations in the resolution of fluorescence microscopy preclude determination of the exact magnitude of this response. Therefore, I conclude that RbcS-GFP production increases in response to induction of a heterologous sucrose sink however it is difficult to determine if all of this RbcS-GFP is localized to the carboxysome lumen or if some portion remains in the cytosol.

Sink demand increases RbcL expression.

Cells exporting sucrose increase the production of RbcS-GFP within the cell (Figure 3.3) suggesting there might be changes in RbcL since the small and large subunits oligomerize forming functional rubisco complexes. Since, RbcS expression is known to increase linearly with RbcL (Long *et al.*, 2011), I measured the amount of RbcL in relation to the other photosynthetic complexes to understand how sink demand might alter photosynthetic complex stoichiometry. The ratio of subunits of the photosynthetic complexes, RbcL:PsbA (subunit of PSII) (Figure 3.4a) and RbcL:PsaC (subunit of PSI) (Figure 3.4b), were measured. Interestingly, I found that the amount of RbcL increased relative to PsbA after 48h and 96h following sucrose induction, however, there is no measurable difference in the ratio of RbcL:PsaC (Figure 3.4). Additionally, CcmM is known to nucleate RbcL within the carboxysome and a slight increase in the ratio of the short form of CcmM35 and M58 is observed 24h after activation of a heterologous sink, although not significantly (p-value > 0.05) (Figure 3.4d). These data suggest that sucrose export leads to an increase in the relative abundance of RbcL:PsbA but not RbcL:PsaC.

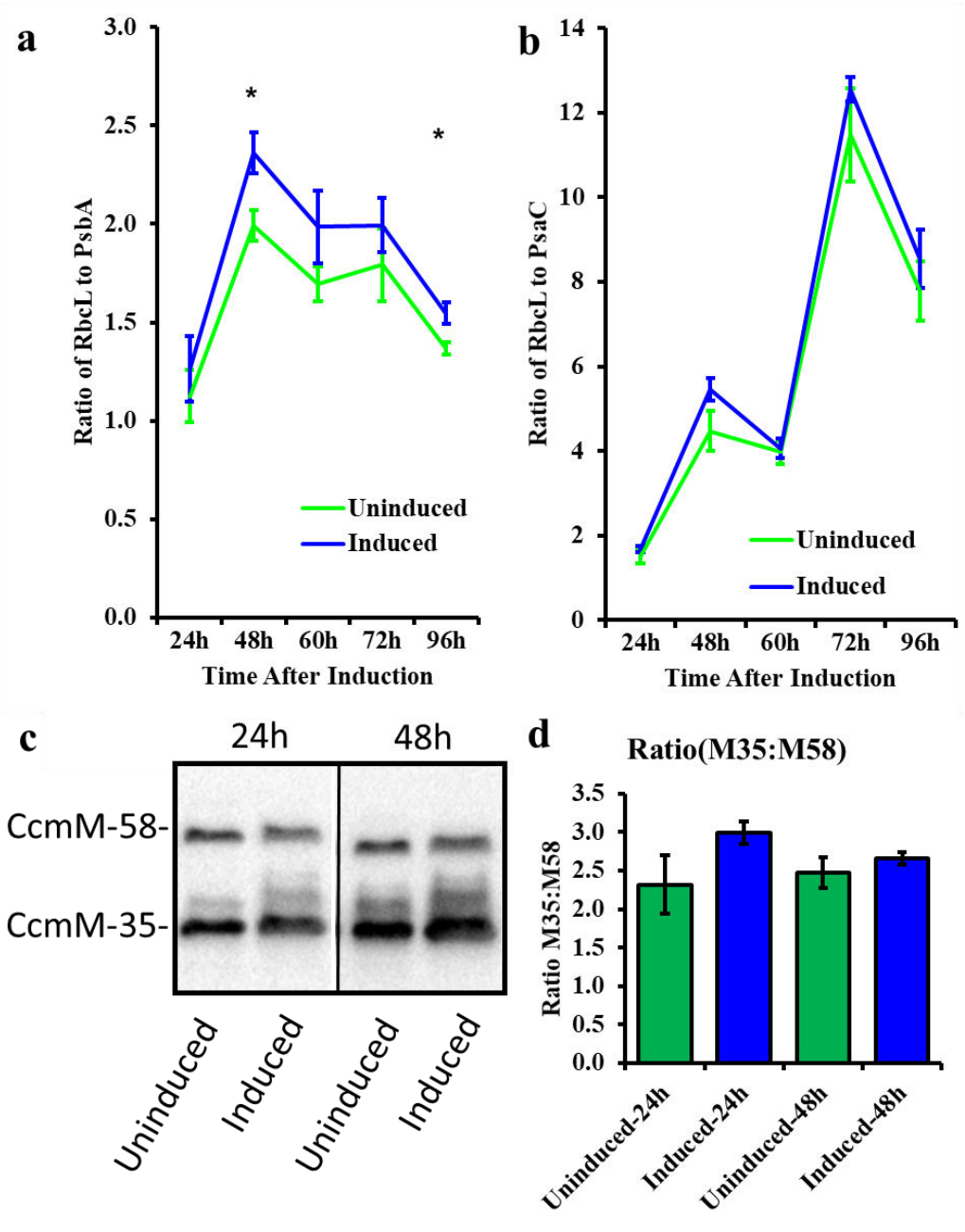

FIGURE 3.4: WESTERNQUANTIFICATION OF PHOTOSYNTHETIC COMPLEXES. **a)** The ratio of RbcL and PsbA (subunit of PSII) increases 48h and 96h after sucrose export is induced. **b)** The ratio of RbcL to PsaC (subunit of PSI) remains unaltered in response to sucrose export. **c)** Representative Western blots for CcmM. Westerns were quantified and plotted in **d)** The ratio of the short (CcmM-35) and long (CcmM-58) form of the rubisco scaffolding protein was measured. Graphs are mean ± stdev from 3 replicates and Asterisk (*) denote t-test significance at p-value < 0.05.

Discussion

This preliminary data chapter focuses on changes to the proteinaceous carbon fixation fixation organelle, the carboxysome, in response to an expanded heterologous carbon sink sink (sucrose export). Overall, these data show sucrose export can elicit a cellular response which significantly increases production of RbcS-GFP, as well as increasing the ratio of untagged RbcL to a subunit of PSII (PsbA). Currently, it is less clear if there is an increase in the expression of the endogenous form of RbcS, and further research will be required to definitively show that rubisco subunits are correctly targeted to the carboxysome. An increase in carboxysome size, as measured by fluorescence microscopy, would be consistent with increased loading of rubisco cargo within the carboxysome lumen, however additional experiments may be required to evaluate the statistical significance and higher-resolution imaging approaches could greatly increase confidence in this interpretation.

Fluorescent reporters target to the carboxysome can be used to visualize carboxysomes and allows for high-throughput quantification of carboxysome properties across many cells. However, there are uncertainties introduced in the interpretation of these fluorescent carboxysome reporters. It is advantageous to use fluorescent protein tags to visualize carboxysomes because they can be observed in live cells relatively easily over time allowing one to observe the dynamic processes within a cell. However, carboxysomes can range in size and measuring minor changes in cell structures can be difficult with fluorescent microscopy. These fluorescent observations could be bolstered and confirmed with ultramicroscopy techniques with increased resolution. Ultramicroscopy techniques are often used to visualize carboxysomes in fixed cells (Long *et al.*, 2010; Rohnke *et al.*, 2018) but lack the throughput for convenient

visualization of dynamic process such as how cellular components might respond to rapid changes in metabolic sink demand.

It was previously shown that sucrose export can relieve sink limitation of photosynthesis leading to increased photochemical efficiency and a decrease in PSI acceptor side limitation (Chapter 2 and Abramson et, al. 2016). A decreased PSI acceptor limitation could occur if the CB cycle is consuming more energy for carbon fixation, which is supported by increased rates of CO2 fixation in sucrose-secreting cells (Ducat *et al.*, 2012). In further support of the idea that sucrose export leads to greater CB cycle activity, I observed increased production of RbcS-GFP (Figure 3.3) as well an increase in the ratio of RbcL to a subunit of PSII (PsbA) (Figure3.4). Rubisco is known to have a slow catalytic rate and therefore greater rubisco quantities within the cell might suggest greater carbon fixation rates.

While a handful of studies have looked at how the carboxysome is regulated in response to environmental cues (Price *et al.*, 2008; Sun *et al.*, 2016), and some regulators involved in this process have been described (Long *et al.*, 2011; Rohnke *et al.*, 2018), the overall molecular mechanisms of carboxysome regulation remain unclear. Complicating our understanding of this regulation, the environmental cues known to lead to increased carboxysome number (i.e., high light and low inorganic carbon availability; Eisenhut *et al.*, 2007; Sun *et al.*, 2016) impact many signaling and metabolic pathways in cyanobacteria simultaneously. For example, the phytochrome RcaE has been implicated in directly sensing changes in the external light intensity to transduce a signal for the regulation of carboxysomes (Ronhke *et al.*, 2018; Li *et. al.*, 2011), changes in light intensity and quality also alter photosynthetic activity and can therefore radically change internal signals and metabolite pools. Disentangling the RcaE-controlled transcriptional

network from other pathways that are affected by changes in light quality could be assisted by alternative approaches to alter the metabolic network while environmental conditions remain constant. In this chapter, I observed how the carboxysome responds not to perturbed environmental conditions, but to internal carbon sink demand in a strain that exports sucrose. When these results are corroborated, they could provide some of the first evidence that carboxysomes are regulated in response to internal metabolic demands independently of changes to environmental conditions. This sink limitation regulatory sensing mechanism could be determined through cellular metabolomics and proteomics (See Chapter 5 for discussion).

The regulation and protein stoichiometry leading to complete carboxysome assembly remains unclear; however, many of the structural protein constituents are known along with their interacting partners (Long *et al.*, 2010; Cameron *et al.*, 2013). Interestingly, CcmM contains three rubisco-small-subunit-like-domains (SSLD), thought to bind and nucleate the RbcL core within the carboxysome (Long *et al.*, 2010; Kerfeld and Melnicki, 2016). Due to an internal ribosome binding site, CcmM can be translated into as a short form (M35) containing three SSLDs or long form (M58) containing an N-terminal domain that interacts with CcmN as well as the three SSLDs. M35 overexpression alone alters the size and shape of the carboxysomes and is able to nucleate rubisco to form puncta, whereas, M58 interacts with CcmN to recruit the outer shell of the carboxysome creating smaller carboxysomes (Long *et al.*, 2010). An alteration in the ratio of M35:M58 has the potential to regulate carboxysome morphology. Since M35 nucleates RbcL within the cell, a greater amount of M35 could increase the amount of protein packaged within the carboxysome increasing the size of the carboxysome. Whereas a decreased ratio of M35:M58 might recruit shell proteins more readily to enclose the nucleated rubisco. An increase in the ratio of M35:M58 could therefore fine tune the ratio of nucleated RbcL compared to

encapsulated RbcL resulting in larger carboxysomes. I measured the intensity of RbcS-GFP nucleated to the carboxysomes along with the M35:M58 ratio. I hypothesize from these data that future studies will show a statistically greater amounts of rubisco packaging within the carboxysome in response to sucrose export. It is clear that induction of a sucrose export system leads to cellular elongation (Figure3.2b) and induction of SPS can account for substantial protein levels within the cell (Figure 4.1.2e), therefore normalization to a protein with a constant quantity within the cell is needed as an accurate control for protein quantification (See Chapter 5 for more discussion).

This chapter establishes a connection between internal metabolic demands and the carbon fixation machinery. These results clearly demonstrate a cellular response to sucrose export that leads to an increase in rubisco content within the cell (Figure 3.3 and 3.4). Although the direct signals of an expanded carbon sink are not known the cell clearly responds by increasing rubisco quantities within the cell. Future research into the localization and activity of rubisco will need to be performed, however, preliminary data shown here might suggest a mechanism for how greater amounts of rubisco can be localized to the carboxysome through CcmM interactions.

Materials and methods

Cell culture and growth conditions and construct design

Cultures of *S. elongatus* PCC7942 were grown in an Infors Multitron with 100 µmol m^{-2} s^{-1} compact fluorescent lighting supplemented with 2% CO_2 in BG-11 medium (pH 8.3) buffered with 1g/L HEPES and at 30 degrees Celsius. Low carbon (0.04%) cells grown in a culture room with compact fluorescent lighting set to 30 degrees Celsius in

BG-11 medium as previously described. Cultures were back-diluted daily unless otherwise noted. 1mM IPTG was added to cultures when induced.

The Suc-Ex strain was constructed as previously describe by Abramson et, al. 2016 and RbcS-GFP was synthesized by IDT gblock and cloned into the Neutral Site 1. *S. elongatus* was transformed by incubating DNA with cells overnight. Selection was carried out with BG11 plates with spectinomycin (100mg/L).

Microscopy and MicrobeJ

Imaging was carried out on a Zeiss Axio Observer D1 microscope (100x1.3NA) with an Axiocam 503 (mono color) camera. MicrobeJ (v5.12d) as previously described (Ducret, Quardokus and Brun, 2016) was used to outline cells based on chlorophyll autofluorescence and carboxysome foci were based on GFP fluorescence. The main attributes for cell gating by medial axis are as follows (Length: 1-5; Width:0.6-1.5; Area: 1-max; Angularity: 0-0.5) and smoothed maxima foci (carboxysome) determination by (Tolerance: 300; z-score:25; Length: 0-2; Width: 0-2; Intensity: (500-max).

Protein quantification

Total protein was exacted from cells resuspended in 1x Lamellie buffer and boiled for 10 minutes. Protein quantification was performed with a Thermo Scientific Pierce Protein Assay Kit following manufacture directions. SDS-PAGE was performed and protein blotting for westerns were performed with BioRad Trans-Blot® Turbo™ Transfer System. Proteins were detected with Agrisera Photosynthesis Tool Kit (AS04-051) and primary antibodies were used at a dilution of RbcL-1:5000; PsbA-1:10000; PsaC-1:2000 and detected with Thermo Scientific West Femto HRP secondary reagent. Antibody for CcmM detection was graciously provided by Dr. Kerfeld's laboratory and used at 1:5000. Imaging and western quantification was performed on

BioRad gel imager using Image Lab software. Chlorophyll content was measured from equal sample volumes used to extract total protein for later normalization.

REFERENCES

REFERENCES

Abramson, B. W. et al. (2016) 'Increased photochemical efficiency in cyanobacteria via an engineered sucrose sink', Plant and Cell Physiology, 0(October), pp. 1–10. doi: 10.1093/pcp/pcw169.

Cameron, J. C. et al. (2013) 'Biogenesis of a bacterial organelle: The carboxysome assembly pathway', Cell. Elsevier Inc., 155(5), pp. 1131–1140. doi: 10.1016/j.cell.2013.10.044.

Cot, S. S. W., So, A. K. C. and Espie, G. S. (2008) 'A multiprotein bicarbonate dehydration complex essential to carboxysome function in cyanobacteria', Journal of Bacteriology, 190(3), pp. 936–945. doi: 10.1128/JB.01283-07.

Ducat, D. C. et al. (2012) 'Rerouting carbon flux to enhance photosynthetic productivity', Applied and Environmental Microbiology, 78, pp. 2660–2668. doi: 10.1128/AEM.07901-11.

Ducret, A., Quardokus, E. M. and Brun, Y. V. (2016) 'MicrobeJ, a tool for high throughput bacterial cell detection and quantitative analysis', Nature Microbiology. Nature Publishing Group, 1(7), p. 16077. doi: 10.1038/nmicrobiol.2016.77.

Eisenhut, M. et al. (2007) 'Long-term response toward inorganic carbon limitation in wild type and glycolate turnover mutants of the cyanobacterium *Synechocystis* sp. strain PCC 6803', Plant Physiology, 144(4), pp. 1946–1959. doi: 10.1104/pp.107.103341.

Kerfeld, C. A. and Melnicki, M. R. (2016) 'Assembly, function and evolution of cyanobacterial carboxysomes', Current Opinion in Plant Biology. Elsevier Ltd, 31, pp. 66–75. doi: 10.1016/j.pbi.2016.03.009.

Li, J., Li, G., Wang, H., & Wang Deng, X. (2011). Phytochrome Signaling Mechanisms. The Arabidopsis Book / American Society of Plant Biologists, 9, e0148. http://doi.org/10.1199/tab.0148

Long, B. M. et al. (2007) 'Analysis of carboxysomes from *Synechococcus* PCC7942 reveals multiple rubisco complexes with carboxysomal proteins CcmM and CcaA', Journal of Biological Chemistry, 282(40), pp. 29323–29335. doi: 10.1074/jbc.M703896200.

Long, B. M. et al. (2010) 'Functional cyanobacterial b-carboxysomes have an absolute requirement for both long and short forms of the CcmM protein', Plant Physiology, 153(1), pp. 285–293. doi: 10.1104/pp.110.154948.

Long, B. M. et al. (2011) 'Over-expression of the b-carboxysomal CcmM protein in Synechococcus PCC7942 reveals a tight co-regulation of carboxysomal carbonic anhydrase (CcaA) and M58 content', Photosynthesis Research, 109(1–3), pp. 33–45. doi: 10.1007/s11120-011-9659-8.

Oliver, J. W. K. and Atsumi, S. (2015) ‘A carbon sink pathway increases carbon productivity in cyanobacteria’, Metabolic Engineering. Elsevier, pp. 1–7. doi: 10.1016/j.ymben.2015.03.006.

Paul, M. J. and Foyer, C. H. (2001) ‘Sink regulation of photosynthesis.’, Journal of experimental botany, 52(360), pp. 1383–1400. doi: 10.1093/jexbot/52.360.1383.

Peña, K. L. et al. (2010) ‘Structural basis of the oxidative activation of the carboxysomal gamma-carbonic anhydrase, CcmM.’, Proceedings of the National Academy of Sciences of the United States of America, 107(6), pp. 2455–60. doi: 10.1073/pnas.0910866107.

Rohnke, B. A. et al. (2018) ‘RcaE-dependent regulation of carboxysome structural proteins has a central role in environmental determination of carboxysome morphology and abundance in Fremyella diplosiphon’, mSphere, 3(1), pp. e00617-17. doi: 10.1128/mSphere.00617-17.

Savage, D. F. et al. (2010) ‘Spatially ordered dynamics of the bacterial carbon fixation machinery’, Science. American Association for the Advancement of Science, 327(5970), pp. 1258–1261. doi: 10.1126/science.1186090.

Sun, Y. et al. (2016) ‘Light modulates the biosynthesis and organization of cyanobacterial carbon fixation machinery through photosynthetic electron flow’, Plant Physiology, 171(May), p. pp.00107.2016. doi: 10.1104/pp.16.00107.

Ungerer, J. et al. (2012) ‘Sustained photosynthetic conversion of CO2 to ethylene in recombinant cyanobacterium Synechocystis 6803’, Energy & Environmental Science, 5(10), p. 8998. doi: 10.1039/c2ee22555g.

Whitehead, L. et al. (2014) ‘Comparing the in vivo function of a-carboxysomes and b-carboxysomes in two model cyanobacteria’, Plant Physiology, 165(1), pp. 398–411. doi: 10.1104/pp.114.237941.

Woodger, F. J., Badger, M. R. and Price, G. D. (2003) ‘Inorganic Carbon Limitation Induces Transcripts Encoding Components of the CO2 -Concentrating Mechanism in Synechococcus sp . PCC7942 through a Redox-Independent Pathway’, Society, 133(December), pp. 2069–2080. doi: 10.1104/pp.103.029728.coccus.

Yang, J. T. et al. (2015) ‘Triose phosphate use limitation of photosynthesis: short-term and long-term effects’, Planta. Springer Berlin Heidelberg. doi: 10.1007/s00425-015-2436-8.

CHAPTER 4.1: REDIRECTING CARBON TO BIOPRODUCTION VIA A GROWTH ARREST SWITCH IN A SUCROSE-SECRETING CYANOBACTERIUM

This chapter was previously published in Algal Research by Elsevier. For the most up to date version please visit the journal website at www.sciencedirect.com/journal/algal-research.

Authors: Bradley W. Abramson, Josh Lensmire, Yang-Tsung Lin, Emily Jennings, Daniel C. Ducat

Abstract

Cyanobacteria are microbes with high photosynthetic efficiencies, making them a promising target for the production of sustainable bioproducts directly from solar energy and carbon dioxide. The most common efforts to increase cyanobacterial bioproduction involve diverting cellular resources away from cellular biomass and towards a heterologous pathway, for example through nutrient starvation or knockout of genes in competing metabolic pathways. Here I show that an inducible cell growth arrest switch can be used to increase the partitioning of carbon to an engineered sucrose sink. Specifically, I show that overexpression of Regulator of Phycobilisome-Associated B (RpaB), an essential response regulator in *Synechococcus elongatus* PCC 7942, allows for inducible arrest of cell growth and is associated with a >2-fold higher specific productivity of a heterologous sucrose secretion pathway. Finally, I show that sucrose export can partially relieve photosynthetic feedback inhibition imposed by the RpaB dependent growth arrest, allowing sucrose-secreting strains to maintain higher photosynthetic efficiencies. This work provides a new strategy for improving photosynthetic productivity and cyanobacterial bioproduction.

Introduction:

Cyanobacteria are photosynthetic organisms with promising potential for sustainable high-value bioproduct production. The obligate phototrophic, freshwater cyanobacteria, *Synechococcus elongatus* PCC *7942* (hereafter *S. elongatus*), captures solar energy and utilizes it to fix carbon dioxide. In comparison to plants and algae, cyanobacteria have higher photosynthetic efficiencies and are genetically tractable, making them excellent candidates for engineering strains that generate high-value products directly from solar energy and CO_2 (Lai and Lan, 2015). Cyanobacteria have already been modified allowing for the production of a large range of valuable compounds (Nielsen *et al.*, 2016).

Two general strategies are routinely used to reroute cellular resources towards a target metabolic pathway in photosynthetic microbes: 1) increasing the withdrawal of core carbon intermediates by improving pathway stoichiometry and balancing the rate limiting enzymes, or; 2) by restricting the flux of carbon to native metabolic pathways that compete for cellular resources. The first strategy requires tailored engineering of enzyme activities and expression that is specific to a given pathway. By contrast, the latter approach can be applied to improve production of many end products in production strains. For example, the main carbon storage product, glycogen, often accounts for 10-20% of total fixed carbon in growing cyanobacteria (Hendry *et al.*, 2017); therefore, suppression of flux to this product can lead to redirection of these cellular resources to alternative natural or engineered metabolic sinks. Indeed, genetic knockouts of glucose-1 phosphate adenylyl transferase (*glgC*) creates glycogen deficient strains which have been shown to have improved production of numerous products (e.g. sucrose (Ducat *et al.*,

2012), isobutanol (Li, Shen and Liao, 2014), limonene (Davies *et al.*, 2014) and lactate (Van der Woude *et al.*, 2014)).

Aside from genetic mutation, another common strategy for restricting flux to endogenous carbon sinks is through the use of a culture medium that is limited for key nutrients required for cell growth (Antal and Lindblad, 2005; Panda and Mallick, 2007; Klähn and Hagemann, 2011; Martin *et al.*, 2014). In both cyanobacteria and algae, perhaps the best studied example of this is cultivation under nitrogen-limited conditions, which restricts cellular capacity to form key metabolites needed for protein synthesis and cell growth. This leads to global changes in the transcriptome and proteome, changes in carbon partitioning, slows cellular growth rates, and encourages overall accumulation of products with a higher C:N ratio (Herrero, Muro-Pastor and Flores, 2001). Such an approach has been routinely used to increase the accumulation of many products, including lipids, polyhydroxyalkanoates, alcohols, and hydrogen gas (Mata, Martins and Caetano, 2010; Sharma, Schuhmann and Schenk, 2012; Hickman *et al.*, 2013; Osanai *et al.*, 2013; Anfelt *et al.*, 2015).

Yet, inhibiting metabolic sinks through pathway deletion or nutrient deprivation can create new problems that may limit their application at scale. For example, Δ*glgC* cells exhibit sensitivity to stress, including high light sensitivity, that is presumed to be partially due to their inability to store excess light energy (source) in glycogen reserves (sink) (Carrieri *et al.*, 2012; Gründel *et al.*, 2012). Similarly, exposure to nutrient limitation can lead to a gradual decline in photosynthetic activity, efficiency, and cell viability (Sauer *et al.*, 2001; Choi *et al.*, 2016). Thus, this approach requires nutrient cycling to maintain the productivity of cultures for long-term culturing. Since liquid handling costs for typical continuous culture of cyanobacteria and algae are a significant barrier to commercialization (Aflalo *et al.*, 2007; Markou and Nerantzis, 2013),

a requirement for additional media cycling might further exacerbate such concerns of scaled cyanobacterial cultivation.

Recently, overexpression of the sensor histidine protein kinase, Regulator of Phycobilisome-Associated B (RpaB), was shown to lead to growth arrest and/or lethality (Moronta-Barrios, Espinosa and Contreras, 2013). RpaB is an essential two component response regulator that is phosphorylated through interactions with the environmentally-responsive sensor kinase, NblS. RpaB then transduces the signal in part by binding the promoter regions of downstream genes (Hanaoka and Tanaka, 2008). While many aspects of RpaB's signaling network remain to be elucidated, it is thought that NblS-RpaB activate an adaptive response in cyanobacteria under a variety of stress conditions, including high-light, salt-stress, and cold shock (Hsiao *et al.*, 2004; Tu *et al.*, 2004; Piechura, Amarnath and O'Shea, 2017). In *S. elongatus*, overexpression of RpaB arrests cell growth, decreases the cell length to width ratio (Moronta-Barrios, Espinosa and Contreras, 2013) and suppresses the circadian rhythm (Espinosa *et al.*, 2015). Consistent with canonical response regulators, RpaB has a highly conserved residue (D56) in its receiver domain that can accept a phosphate group to regulate its function. Mutants mimicking a constitutively phosphorylated (D56E) or non-phosphorylatable (D56A) form of RpaB have been previously characterized (López-Redondo *et al.*, 2010; Espinosa *et al.*, 2015). Mutations to this residue in the endogenous copy of RpaB are lethal, while over-expression of RpaB-D56A or RpaB-D56E in a background containing a wildtype copy have also been shown to result in growth arrest (López-Redondo *et al.*, 2010; Moronta-Barrios, Espinosa and Contreras, 2012; Espinosa *et al.*, 2015).

I explored the utility of RpaB as a genetic switch that could suppress cell growth and thereby promote partitioning of carbon to heterologous production pathways. I characterized the effects of RpaB-dependent cell growth arrest in a production strain of *S. elongatus*, specifically assessing the effect on photosynthetic activity and sucrose export. I show that modulation of RpaB activity not only allows for growth arrest in *S. elongatus*, but also increases carbon partitioning to an engineered metabolic sink (i.e. secreted sucrose). Finally, I observed that growth arrest after several days decreases the quantum yield of photosystem II (PSII), but that photosynthetic efficiency is partially rescued by relief of feedback inhibition when sucrose is exported.

Materials and Methods:

Strain Construction

Engineered *S. elongatus*$_{sps}$ was constructed and grown as described previously (Abramson *et al.*, 2016). The theophylline riboswitch, Ptrc and Δ*lacO* were generated from IDT-geneblock. The *lacO* site was rationally mutated to abolish LacI's ability to bind and repress the riboswitch thus allowing independent control of both cassettes. Plasmids were cloned into Neutral Site 1 (NS1) backbones (Clerico, Ditty and Golden, 2001) and plasmids are available at Addgene, RpaB-Ox (Addgene #106932), RpaB-D56E (Addgene #106934) or RpaB-D56A (Addgene #106933) for homologous recombination into the NS1 genomic site.

Strain Growth Conditions

Synechococcus elongatus PCC 7942 was grown in a Multitron Infors HT Incubator with ~100 μmol photons m^{-2} s^{-1} of light at 32˚C and supplemented with 2% CO_2. Lights were Sylvania 15 W Gro-Lux fluorescent bulbs. Cultures of 50ml in 125ml baffled flasks shook at 150 rpm in BG11+1 g/L HEPES at pH8.3 adjusted with NaOH. Cultures were routinely back-diluted to 0.3

OD_{750} unless otherwise noted in the text. Where appropriate, 1 mM IPTG or 500 uM theophylline was added to induce *cscB* and *sps* expression or RpaB translation, respectively. Chloramphenicol (25 mg L^{-1}) was used to select for *cscB* cells and selection was removed prior to experiments. Kanamycin (50 mg L^{-1}) was used to maintain *sps* containing cells. The theophylline dependent riboswitch containing *rpaB* was selected by spectinomycin (50 mg L^{-1}).

Sucrose Quantification

Sucrose export was induced with 1mM IPTG. Cells were collected and pelleted (17,000g) and the supernatant was sampled for sucrose. Sucrose was determined using the Sucrose/D-Glucose Assay Kit (Megazyme: K-SUCGL). Cell numbers were quantified by flow cytometry, BD-Accuri (BD Biosciences) or by OD_{750}nm on a Genesys 20 photospectrometer (Thermo).

Protein Quantification

Samples were collected at times described in the text by centrifugation at 13,000rpm on a benchtop centrifuge to collect the cell pellet. Total protein was extracted in Laemmli buffer by boiling for 20 minutes. Protein quantification was performed with Coomassie Plus Protein Assay Reagent (No. 23236) according to the manual and equal protein concentrations were loaded for SPS-PAGE. Gels were stained with Coomassie stain and imaged. Quantification was performed with the Gel Analyzer plugin from ImageJ.

Fluorescence Measurements

ΦII and qP measurements and calculations were performed using an Aquapen AP-C 100 (Photon Systems Instruments, Drasov, Czech Republic) using blue LEDs and

the NPQ1 protocol. 2ml of dark adapted samples were used for the measurement. All measurements are the average of at least 3 biological replicates (n≥3) unless noted.

Results:

Orthogonal Control Over Growth Arrest and Sucrose Export

I first constructed a strain containing both an inducible sucrose export system (*cscB* and *sps*; IPTG controlled) and the riboswitch-regulated *rpaB* (Figure 4.1.1BC; hereafter *S. elongatus*$_{\text{cscB-rpaB}}$), and tested the capacity to independently control the two heterologous pathways (Nakahira *et al.*, 2013; Ma, Schmidt and Golden, 2014; Nozzi *et al.*, 2017). I first examined the effects of activation of RpaB translation on the growth rates of *S. elongatus* to see if I observed inhibition of cell growth and division as has been previously reported for RpaB-overexpressing strains (RpaB-Ox)(Moronta-Barrios, Espinosa and Contreras, 2013). I observed that the addition of 500uM theophylline greatly reduced the growth rate of *S. elongatus*$_{\text{cscB-rpaB}}$ (Figure 4.1.2A). This growth arrest was not a function of theophylline toxicity, as I did not observe a significant effect of theophylline on wildtype cultures (Figure 4.1.3), nor in reference lines bearing only the *cscB* and *sps* cassettes (*S. elongatus*$_{\text{sps}}$; Figure 4.1.2A). I then examined cell lines where RpaB is mutated in a key phosphorylated residue to mimic constitutively phosphorylated (RpaB-D56E), or unphosphorylated (RpaB-D56A), protein. Activation of RpaB-D56E or RpaB-D56A also slowed cell growth, albeit not as effectively as overexpression of the unmodified RpaB (Figure 4.1.2A).

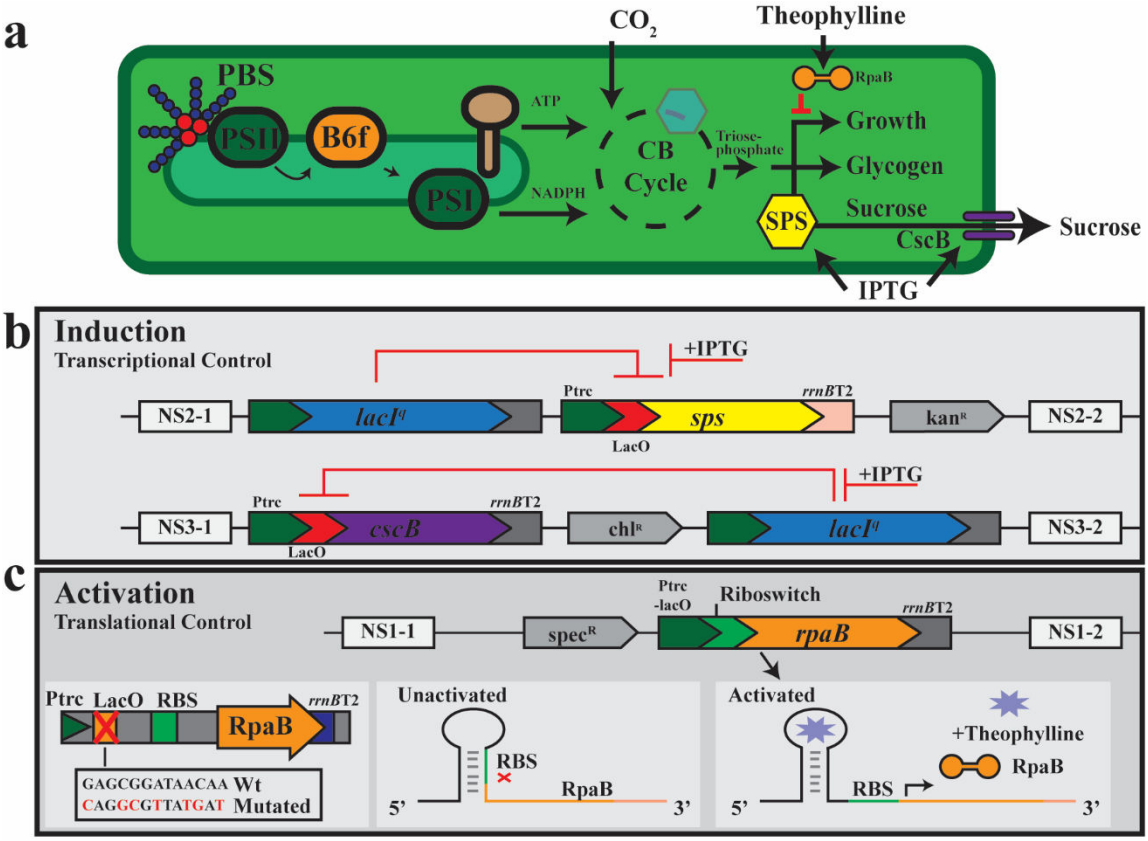

FIGURE 4.1.1: SCHEMATIC OF ENGINEERED SUCROSE EXPORTING STRAIN AND MOLECULAR SWITCHES THEREIN.

a) *S. elongatus* was engineered with two molecular switches for RpaB dependent growth arrest and sucrose production. **b)** *S. elongatus*$_{sps}$ contains two genetic insertions for IPTG induction of *cscB* and *sps* leading to inducible sucrose export **c)** The *S. elongatus*$_{cscB\text{-}rpaB}$ strain contains a theophylline switch allowing translational expression of RpaB which inhibits cell division.

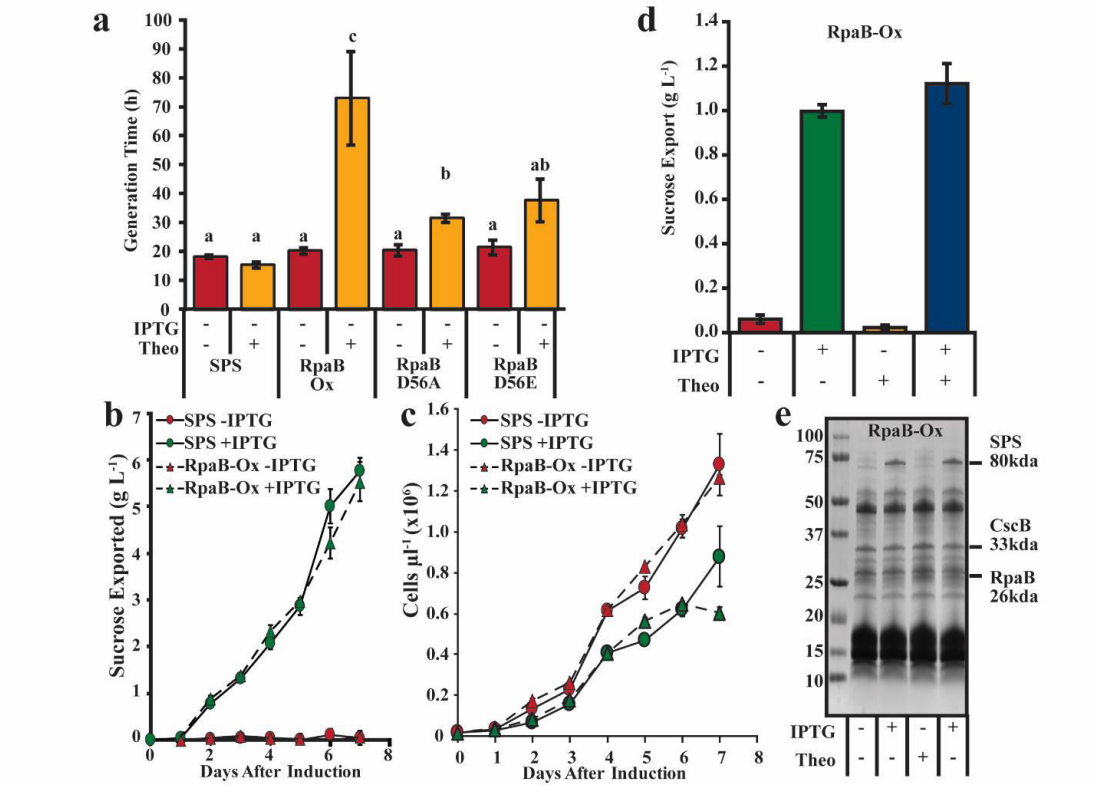

FIGURE 4.1.2: TWO MOLECULAR SWITCHES INDEPENDENTLY ALLOW SUCROSE EXPORT AND CELL GROWTH ARREST.

a) Generation time of RpaB-Ox, RpaB-D56A and RpaB-D56E strains after translational activation with theophylline (Theo). SPS (*S. elongatus*$_{sps}$) is a control line, lacking an RpaB cassette. Un-activated (-Theo) cultures have similar generation times whereas activated RpaB strains show increased generation times 24h after activation. **b)** Cells export sucrose when 1mM IPTG is added to the culture. The addition of an un-activated copy of RpaB does not affect the sucrose export rate. **c)** Carbon is partitioned toward sucrose export (+IPTG), resulting in slower cell growth in both control, SPS, and un-activated RpaB strains **d)** Sucrose export is observed only when IPTG is added to the medium of RpaB strain and theophylline does not affect sucrose export. **e)** Coomassie stained SDS-PAGE showing SPS accounts for 4.8±0.5% of the total protein. All experiments are n=3 and significance is by ttest with $p<0.05$.

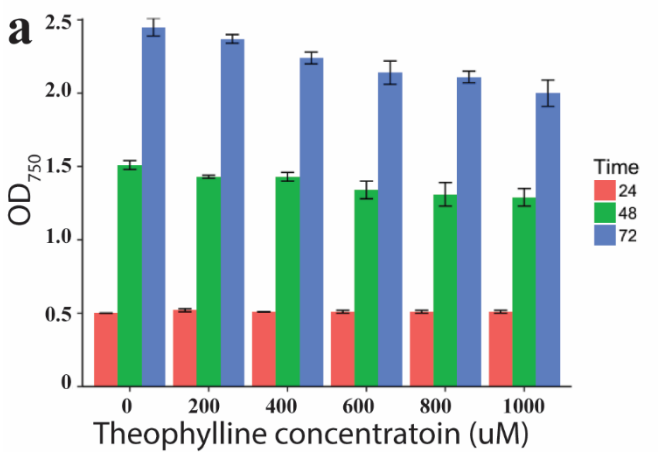

FIGURE 4.1.3: DETERMINATE OF NON-INHIBITORY THEOPHYLLINE CONCENTRATION
Wildtype *S. elongatus* was inoculated in fresh BG11 media at an OD_{750} ~ 0.015 and exposed to several concentrations of theophylline to examine the independent effects of this chemical on growth rates. At the highest concentrations of theophylline tested (1000 µM), a slight negative impact on growth was detectable at time points ≥72 hours.

I next verified that integration of the riboswitch RpaB cassette did not alter cells' capacity to induce sucrose export. *S. elongatus*$_{cscB\text{-}rpaB}$ or *S. elongatus*$_{sps}$ strains were grown for 7 days with or without 1mM IPTG induction and exported sucrose was measured (Figure 4.1.2B). When induced with IPTG, the total amount of sucrose exported by both *S. elongatus*$_{cscB\text{-}rpaB}$ and *S. elongatus*$_{sps}$ was comparable, while uninduced cultures did not show appreciable levels of exported sucrose (Figure 4.1.2B). No significant change in the growth rates between the two lines were observed, although induction of sucrose export did slow growth (Figure 4.1.2C), likely due to the reallocation of cellular carbon as has been reported previously in sucrose-exporting lines (Ducat *et al.*, 2012; Abramson *et al.*, 2016; Hays *et al.*, 2017).

Finally, I examined whether sucrose export could be maintained concurrently with the activation of RpaB. Utilizing the *S. elongatus*$_{cscB\text{-}rpaB}$ strain, I examined sucrose export 24 hours following the addition of IPTG and/or theophylline in comparison to a

control strain grown in the absence of either chemical inducer (Figure 4.1.2D). In all cultures with induced *cscB/sps* (i.e. IPTG added), appreciable levels of sucrose were measured regardless of the addition of theophylline. Addition of theophylline alone did not result in exported sucrose. I verified increased protein levels of SPS under the appropriate conditions via SDS-PAGE (Figure 2E). Interestingly, the SPS band migrated to a size roughly 10kDa less than anticipated and therefore was confirmed by gel extraction and mass spectrometry (SPS was enriched 20-fold over the next identified protein). Analyzed by ImageJ, the SPS band accounted for 4.8±0.5% of the total cellular protein when induced. This is a greater level of induction than is typically observed in *S. elongatus*. Protein bands for CscB or for RpaB could not be identified when induced or activated, respectively (Figure 4.1.2E), however the functional phenotypes for sucrose export (Figure 4.1.2D) and growth inhibition (Figure 4.1.2A) could be readily observed. Altogether, these results indicate that the heterologous sucrose export cassette and growth arrest cassette can function orthogonally and operate independently as designed.

RpaB-Induced Growth Inhibition Increases Sucrose Productivity

I next examined if the growth inhibition caused by activation of RpaB could divert cellular resources to sucrose export similar to knockouts of competing metabolic pathways or nutrient-limited cultivation (Ducat *et al.*, 2012; Li, Shen and Liao, 2014; Jackson *et al.*, 2015). I have previously shown that induction of sucrose export in *S. elongatus* causes short-term enhancements in photosynthetic efficiency and activity, but that the cells acclimate to a new steady-state within 48 hours after induction (Abramson *et al.*, 2016). Therefore, I first induced sucrose export in *S. elongatus*$_{\text{cscB-rpaB}}$ with the addition of IPTG and allowed the cells to acclimate for 48h, then examined the impact of the activation of RpaB, or the RpaB phosphomimicks 24 hours after activation (Figure 4.1.4A). I found higher specific rates of

sucrose production relative to paired controls in all three strains (Figure 4.1.4AB). In comparison to either of the mutants, activation of RpaB-Ox led to the highest rate of sucrose export, 9.12±0.83 pg $cell^{-1}$ d^{-1}.

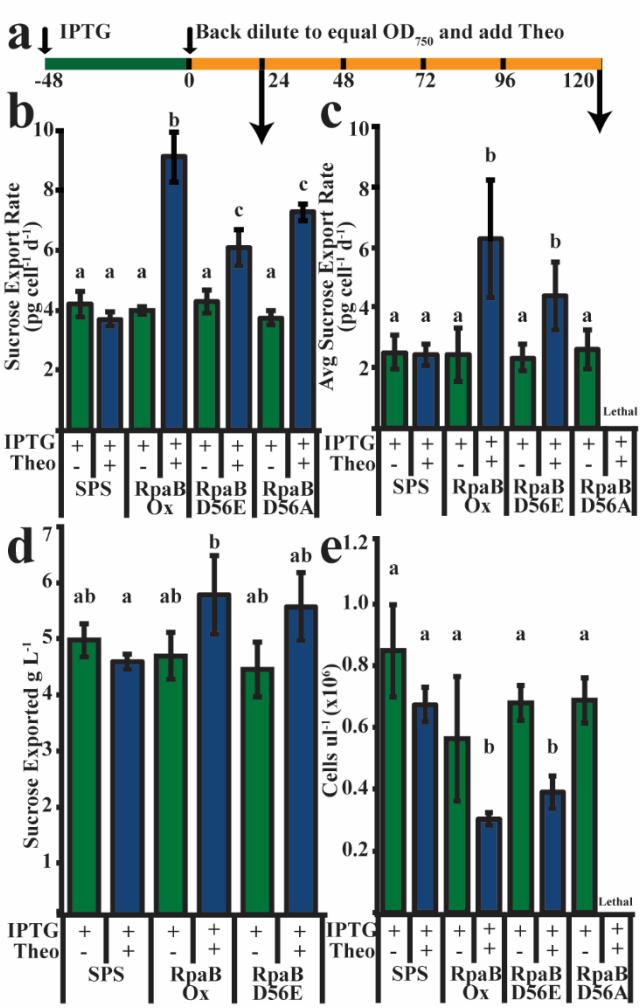

FIGURE 4.1.4: GROWTH ARRESTED CELLS HAVE INCREASED PRODUCTIVITY AND TOTAL SUCROSE OUTPUT.
a) Schematic of experiment. Cells were induced by IPTG to export sucrose 48h prior to back-dilution and addition of theophylline (Theo) at time = 0h. **b)** Sucrose export rate 24h after growth arrest by theophylline addition. All RpaB strains, growth arrested with theophylline, showed increased sucrose export rates per cell **c)** Sucrose export rate averaged over the course of 120h after activation. RpaB-Ox and RpaB-D56E exhibit an increase in productivity when theophylline is added, while RpaB-D56A was lethal after 48h of activation. **d)** Total amount of sucrose exported at 120h after theophylline addition. RpaB-Ox produces significantly more sucrose compared to an activated control strain (SPS). **e)** Final cell densities 120h after activation. RpaB-Ox and RpaB-D56E show significantly less cell growth following theophylline addition whereas RpaB-D65A was dead after 48h of activation. All experiments are n=3 and significance is by t-test with $p<0.05$.

As some prior reports have suggested that overexpression of RpaB can decrease cell viability (Moronta-Barrios, Espinosa and Contreras, 2012), I next sought to determine if the

higher specific productivity caused by RpaB activation could be maintained over longer time frames. After 5 days of activation of either RpaB-Ox or the RpaB-D56E phospho-mimic, significantly higher specific productivities were maintained (Figure 4.1.4C). Interestingly, activation of the non-phosphosphorylatable RpaB-D56A led to cell chlorosis and greatly reduced sucrose productivity after 2 days, accompanied by a steady decline in OD_{750} (Figure 4.1.5), that could be indicative of cell death and lysis. By contrast, overexpression of the wildtype form of RpaB led to the greatest specific productivity of sucrose (Figure 4.1.4C), and the highest total sucrose accumulation over 5d (Figure 4.1.4D). Perhaps not coincidentally, the wildtype RpaB was also the most effective at inhibiting cell growth (Figures 4.1.4E and 4.1.2A).

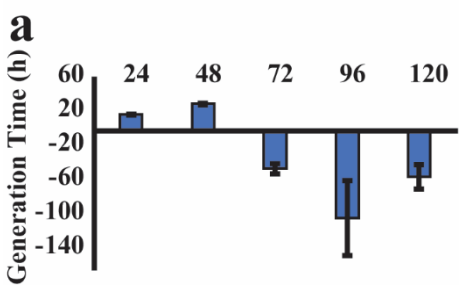

FIGURE 4.1.5: GROWTH RATE OF RPAB-D56A OVER TIME.
RpaB-D56A is lethal after 2 days of activation with 500uM Theophylline. Generation times are calculated by the change in OD_{750} over the time periods indicated.

Sucrose Export Relieves Photosynthetic Sink Limitation Caused by Growth Arrest

In all photosynthetic organisms, an imbalance between the rates of "source" energy generated by the light reactions and utilization of that energy by metabolic "sinks" can lead to decreased photosynthetic efficiency, generation of harmful reactive oxygen species, and gradual damage/downregulation of photosynthetic machinery (Latifi, Ruiz and Zhang, 2009; Demmig-Adams *et al.*, 2014). For example, nutrient limitation restricts flux through many metabolic pathways, and the subsequent downregulation of

photosystems and light-harvesting machinery under these conditions has been well documented in many organisms (Hagemann, 2011; Salomon *et al.*, 2013). I therefore examined chlorophyll a fluorescence to determine the quantum yield of photosystem II (ΦII) in cells that were growth inhibited by overexpression of RpaB. As might be anticipated, 5 days after activation of RpaB, ΦII was diminished relative to control cultures lacking the riboswitch-RpaB cassette (Figure 4.1.6A).

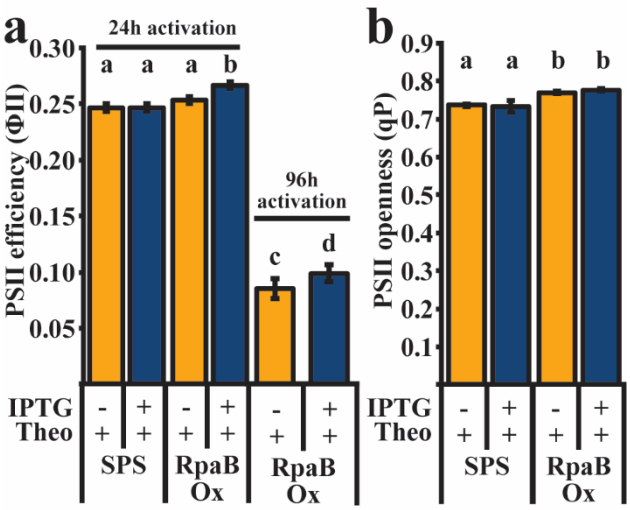

FIGURE 4.1.6: PHOTOSYNTHETIC ENHANCEMENTS OCCUR WHEN GROWTH ARRESTED CELLS ARE EXPORTING SUCROSE.
a) ΦII, a measure of PSII operating efficiency, increases in RpaB-Ox when growth arrested by addition of theophylline (Theo) and exporting sucrose (ITPG). Growth arrest causes ΦII to decrease 96h after expression of RpaB, however the sucrose sink alleviates some of the photosynthetic feedback inhibition **b)** After 48h of activation by theophylline, qP, a measure of PSII openness is increased in RpaB-Ox compared to SPS. All experiments are n=3 and significance is by ttest with $p<0.05$.

I have previously shown that sucrose export can increase photosynthetic efficiency and activity by relieving sink-inhibition of photosynthesis under normal growth conditions (Abramson *et al.*, 2016), suggesting that sucrose export may act as an alternative sink for excess ATP and/or NADPH. In agreement with this interpretation, I observed higher ΦII in growth-inhibited cells that were also induced to export sucrose at both 24h and 5 days after growth

inhibition by RpaB activation (Figure 4.1.4A). Similarly, I observed higher values of, qP, a measure of plastoquinone oxidation of the photosynthetic electron transport chain (Campbell *et al.*, 1998) in sucrose-exporting strains (Figure 4.1.6B). Roughly, qP equates to the "openness" of PSII, where qP=1 means PSII will transfer electrons with 100% efficiency to plastoquinone and qP=0 means plastoquinone is unable to accept electrons from PSII (Oxborough and Baker, 1997). Interestingly, qP was 4.5±2% and 5.9±0.6 higher at 48h after activation of *S. elongatus*$_{\text{cscB-rpaB}}$ cells whether the cells were exporting sucrose or uninduced, respectively (Figure 4.1.6C).

Discussion:

Here I show that carbon can be diverted from cellular growth to a heterologous production pathway through a novel genetic growth inhibition switch by overexpressing the response regulator RpaB. I observe nearly 3-fold higher rates of sucrose secretion in *S. elongatus*$_{cscB\text{-}rpaB}$ strains that are chemically activated to overexpress RpaB (Figure 4.1.4C). Towards this goal, I adapted a tunable theophylline dependent riboswitch previously reported for *S. elongatus* so that it can be used in tandem with other IPTG inducible promoters allowing for separate control of two cassettes (Figures 4.1.1 and 4.1.2). Finally, I show that sucrose export could partially relieve photosynthetic feedback inhibition of PSII imposed by RpaB dependent growth inhibition (Figure 4.1.6). These data provide a new engineering approach for increasing culture productivities by limiting cellular biomass accumulation leading to greater carbon partitioning into a heterologous engineered sink.

The use of a genetic switch for controlled suppression of growth and division offers certain advantages relative to standard methods for improving the product titer

from cyanobacteria engineered to produce valuable metabolites from sunlight and CO_2. As previously discussed, knockouts of endogenous metabolic sinks (such as glycogen) or cultivation under nutrient-limited conditions can improve productivity of a target metabolite by rerouting flux of cellular carbon to a product of interest. However, these approaches can lead to undesirable consequences that complicate the use of these methods at large scales and lead to instabilities in engineered strains. By contrast, an inducible mechanism for cell growth arrest can bypass unwanted genetic instabilities common to constitutive systems (Yang, Sleight and Sauro, 2013). As the molecular toolkit for cyanobacteria continues to improve (Hagemann and Hess, 2018), genetic switches offer the promise of user-programmed pathway activation with inexpensive inducers or under desired conditions (e.g. high cell density), in contrast to potentially expensive liquid handling required for nutrient cycling. Since RpaB is a response regulator that controls the activation of many genes under stress conditions (Kato *et al.*, 2011; Moronta-Barrios, Espinosa and Contreras, 2012), changes in its activity might also be expected to have numerous unintentional impacts on the cell physiology beyond growth arrest. However, if the molecular mechanisms related to RpaB-mediated growth arrest can be elucidated, a genetic switch that specifically induces genes necessary for growth arrest could be used, resulting in fewer pleotropic effects.

Indeed, the mechanisms whereby RpaB induces growth and division arrest remain unclear. While RpaB overexpression has previously been shown to cause a growth arrest phenotype (Moronta-Barrios, Espinosa and Contreras, 2013), I observed slower growth rates for the wildtype RpaB as well as both RpaB-D56E (phosphomimic) and RpaB-D56A (non-phosphorylatable form). This was somewhat unexpected, as the different phospho-forms of RpaB might be expected to have different physiological outputs. Indeed, this aspartate residue of

RpaB is part of a receiver domain that is phosphorylated under certain conditions (e.g. light stress; (Moronta-Barrios, Espinosa and Contreras, 2012)) and is thought to control the output of RpaB (López-Redondo *et al.*, 2010). For example, it is known that RpaB is closely coordinated with RpaA, another key transcriptional regulator of circadian cycles in *S. elongatus* (Hanaoka *et al.*, 2012). Recent ChIP-Seq analysis (Piechura, Amarnath and O'Shea, 2017) has begun to show that RpaB becomes increasingly phosphorylated with decreased light in the diel cycle, promoting expression of a subset of "dusk" genes. Recently, it has been shown that targets of RpaB include other transcription factors, thus the web of genes downstream of RpaB is complex (Piechura, Amarnath and O'Shea, 2017). Further study is necessary to understand the interactions between RpaB and its partners that lead to growth arrest.

Beyond its implications for improving bioproduction by redirecting carbon, our data may be of interest for other fundamental and applied cyanobacterial fields. One surprising observation was that induction of *sps* from a standard IPTG-responsive promoter led to an accumulation of 4.8±0.5% of the total protein as SPS (Figure 2E). While high levels of protein expression are routinely observed in bacteria such as *E. coli*, to our knowledge most inducible promoters in *S. elongatus* or other cyanobacteria do not result in such a strong accumulation of protein. A few other proteins, including the GUS enzyme can accumulate to >10% of soluble protein with the use of a constitutive *psbA1* promoter according to ThermoFisher Scientific (cat. A24230), however this system lacks inducibility and would not work for potentially lethal protein expression, such as RpaB-D56A. Additionally, a recent report showed very high isoprene synthase (IspS) accumulation from a fusion of the *cpcB* promoter and *cpcB* leader peptide but the fusion

had limited IspS enzymatic activity (Chaves *et al.*, 2017). Therefore, it may be that certain sequence determinants in the 5' portion of *sps* gene might promote higher expression and/or stability of the protein product that could be useful for high-expression systems in cyanobacteria, though more details will need to be elucidated.

Finally, I observe that the activity of a heterologous sucrose export pathway may be beneficial to cyanobacteria under conditions where endogenous metabolism is otherwise restricted (Figure 4.1.6). Specifically, I find that the engineered sucrose export pathway allows *S. elongatus* to maintain a higher photosynthetic efficiency (ΦII; Figure 4.1.6A) and a more oxidized plastoquinone pool (qP; Figure 4B) when natural metabolic sinks are restricted by overexpression of RpaB. An abundance of source energy (absorbed light) relative to utilization of that energy (sinks) can be problematic in photosynthetic organisms because these conditions can lead to photoinhibition and photodamage caused by overreduction of the electron transport chain (Paul and Foyer, 2001). For example, prolonged nutrient limitation leads to downregulation of photosynthetic activity in part because of source/sink imbalances and inefficient repair of damaged photosystems (Salomon *et al.*, 2013). Our data is consistent with recent reports that suggest that heterologous pathways that lead to secretion of bioproducts into the medium may be an additional way to utilize excess source energies in cyanobacteria, potentially buffering cells against conditions of excess source energies (Davies *et al.*, 2014; Li, Shen and Liao, 2014; Abramson *et al.*, 2016). Interestingly, I also find that overexpression of RpaB alone improves measurements of the openness of PSII (qP), although the mechanism for this is unclear. Given that RpaB was previously shown to affect phycobilisome state transitions (Ashby, 1999), which are governed by the redox state of the cell (Mao *et al.*, 2002), it is possible that alterations to the light harvesting machinery could account for this phenotype. Regardless,

one implication of this work is that even though heterologous bioproduction pathways typically incur a fitness cost due to the diversion of cellular resources away from growth and reproduction, there may be conditions under which secretion of valuable metabolites could improve the viability of engineered cyanobacteria.

REFERENCES

REFERENCES

Abramson, B. W. *et al.* (2016) 'Increased Photochemical Efficiency in Cyanobacteria via an Engineered Sucrose Sink', *Plant and Cell Physiology*, 0(October), pp. 1–10. doi: 10.1093/pcp/pcw169.

Aflalo, C. *et al.* (2007) 'On the relative efficiency of two- vs. one-stage production of astaxanthin by the green algaHaematococcus pluvialis', *Biotechnology and Bioengineering*. Wiley Subscription Services, Inc., A Wiley Company, 98(1), pp. 300–305. doi: 10.1002/bit.21391.

Anfelt, J. *et al.* (2015) 'Genetic and nutrient modulation of acetyl-CoA levels in Synechocystis for n-butanol production', *Microbial Cell Factories*. BioMed Central, 14(1), p. 167. doi: 10.1186/s12934-015-0355-9.

Antal, T. K. and Lindblad, P. (2005) 'Production of H2 by sulphur-deprived cells of the unicellular cyanobacteria Gloeocapsa alpicola and Synechocystis sp. PCC 6803 during dark incubation with methane or at various extracellular pH', *Journal of Applied Microbiology*, 98(1), pp. 114–120. doi: 10.1111/j.1365-2672.2004.02431.x.

Ashby, M. (1999) 'Cyanobacterial ycf27 gene products regulate energy transfer from phycobilisomes to photosystems I and II', *FEMS Microbiology Letters*, 181(2), pp. 253–260. doi: 10.1016/S0378-1097(99)00547-9.

Campbell, D. *et al.* (1998) 'Chlorophyll fluorescence analysis of cyanobacterial photosynthesis and acclimation', *Microbiology and Molecular Biology Reviews*, 62(3), pp. 667–683. Available at: http://mmbr.asm.org/content/62/3/667.short (Accessed: 8 January 2015).

Carrieri, D. *et al.* (2012) 'Photo-catalytic conversion of carbon dioxide to organic acids by a recombinant cyanobacterium incapable of glycogen storage', *Energy & Environmental Science*, 5(11), pp. 9457–9461. doi: 10.1039/C2EE23181F.

Chaves, J. E. *et al.* (2017) 'Engineering Isoprene Synthase Expression and Activity in Cyanobacteria', *ACS Synthetic Biology*, p. acssynbio.7b00214. doi: 10.1021/acssynbio.7b00214.

Choi, S. Y. *et al.* (2016) 'Transcriptome landscape of Synechococcus elongatus PCC 7942 for nitrogen starvation responses using RNA-seq', *Scientific Reports*. Nature Publishing Group, 6(April), p. 30584. doi: 10.1038/srep30584.

Clerico, E. M., Ditty, J. L. and Golden, S. S. (2001) 'Specialized Techniques for Site-Directed Mutagenesis in Cyanobacteria', *Channels*, pp. 153–172.

Davies, F. K. *et al.* (2014) 'Engineering Limonene and Bisabolene Production in Wild Type and a Glycogen-Deficient Mutant of Synechococcus sp. PCC 7002', *Frontiers in Bioengineering and Biotechnology*, 2(June), pp. 1–11. doi: 10.3389/fbioe.2014.00021.

Demmig-Adams, B. *et al.* (2014) 'Insights from Placing Photosynthetic Light Harvesting into Context', *The Journal of Physical Chemistry Letters*, 5, pp. 2880–2889. doi: 10.1021/jz5010768.

Ducat, D. C. *et al.* (2012) 'Rerouting carbon flux to enhance photosynthetic productivity', *Applied and Environmental Microbiology*, 78, pp. 2660–2668. doi: 10.1128/AEM.07901-11.

Espinosa, J. *et al.* (2015) 'Cross-talk and regulatory interactions between the essential response regulator RpaB and cyanobacterial circadian clock output', *Proceedings of the National Academy of Sciences*, p. 201424632. doi: 10.1073/pnas.1424632112.

Gründel, M. *et al.* (2012) 'Impaired glycogen synthesis causes metabolic overflow reactions and affects stress responses in the cyanobacterium Synechocystis sp. PCC 6803', *Microbiology (United Kingdom)*, 158(12), pp. 3032–3043. doi: 10.1099/mic.0.062950-0.

Hagemann, M. (2011) 'Molecular biology of cyanobacterial salt acclimation', *FEMS Microbiology Reviews*, 35(1), pp. 87–123. doi: 10.1111/j.1574-6976.2010.00234.x.

Hagemann, M. and Hess, W. R. (2018) 'Systems and synthetic biology for the biotechnological application of cyanobacteria', *Current Opinion in Biotechnology*. Elsevier Ltd, 49, pp. 94–99. doi: 10.1016/j.copbio.2017.07.008.

Hanaoka, M. *et al.* (2012) 'RpaB, another response regulator operating circadian clock-dependent transcriptional regulation in Synechococcus elongatus PCC 7942', *Journal of Biological Chemistry*, 287(31), pp. 26321–26327. doi: 10.1074/jbc.M111.338251.

Hanaoka, M. and Tanaka, K. (2008) 'Dynamics of RpaB-promoter interaction during high light stress, revealed by chromatin immunoprecipitation (ChIP) analysis in Synechococcus elongatus PCC 7942', *Plant Journal*, 56(2), pp. 327–335. doi: 10.1111/j.1365-313X.2008.03600.x.

Hays, S. G. *et al.* (2017) 'Synthetic photosynthetic consortia define interactions leading to robustness and photoproduction', *Journal of Biological Engineering*. Journal of Biological Engineering, 11(1), p. 4. doi: 10.1186/s13036-017-0048-5.

Hendry, J. I. *et al.* (2017) 'Rerouting of carbon flux in a glycogen mutant of cyanobacteria assessed via isotopically non-stationary 13C metabolic flux analysis', *Biotechnology and Bioengineering*, 114(10), pp. 2298–2308. doi: 10.1002/bit.26350.

Herrero, A., Muro-Pastor, A. M. and Flores, E. (2001) 'Nitrogen control in cyanobacteria', *Journal of Bacteriology*. American Society for Microbiology, pp. 411–425. doi: 10.1128/JB.183.2.411-425.2001.

Hickman, J. W. *et al.* (2013) 'Glycogen synthesis is a required component of the nitrogen stress response in Synechococcus elongatus PCC 7942', *Algal Research*. Elsevier B.V., 2(2), pp. 98–106. doi: 10.1016/j.algal.2013.01.008.

Hsiao, H. Y. *et al.* (2004) 'Control of photosynthetic and high-light-responsive genes by the histidine kinase DspA: Negative and positive regulation and interactions between signal transduction pathways', *Journal of Bacteriology*. American Society for Microbiology (ASM), 186(12), pp. 3882–3888. doi: 10.1128/JB.186.12.3882-3888.2004.

Jackson, S. A. *et al.* (2015) 'Dynamics of photosynthesis in a glycogen-deficient glgC mutant of Synechococcus sp. strain PCC 7002', *Applied and Environmental Microbiology*, 81(18), pp. 6210–6222. doi: 10.1128/AEM.01751-15.

Kato, H. *et al.* (2011) 'Interactions between histidine kinase NblS and the response regulators RpaB and SrrA are involved in the bleaching process of the cyanobacterium synechococcus elongatus PCC 7942', *Plant and Cell Physiology*, 52(12), pp. 2115–2122. doi: 10.1093/pcp/pcr140.

Klähn, S. and Hagemann, M. (2011) 'Compatible solute biosynthesis in cyanobacteria', *Environmental Microbiology*, 13(3), pp. 551–562. doi: 10.1111/j.1462-2920.2010.02366.x.

Lai, M. and Lan, E. (2015) 'Advances in metabolic engineering of cyanobacteria for photosynthetic biochemical production', *Metabolites*, 5(4), pp. 636–658. doi: 10.3390/metabo5040636.

Latifi, A., Ruiz, M. and Zhang, C. C. (2009) 'Oxidative stress in cyanobacteria', *FEMS Microbiology Reviews*, 33(2), pp. 258–278. doi: 10.1111/j.1574-6976.2008.00134.x.

Li, X., Shen, C. R. and Liao, J. C. (2014) 'Isobutanol production as an alternative metabolic sink to rescue the growth deficiency of the glycogen mutant of Synechococcus elongatus PCC 7942.', *Photosynthesis research*, 120(3), pp. 301–10. doi: 10.1007/s11120-014-9987-6.

López-Redondo, M. L. *et al.* (2010) 'Environmental control of phosphorylation pathways in a branched two-component system', *Molecular Microbiology*, 78(2), pp. 475–489. doi: 10.1111/j.1365-2958.2010.07348.x.

Ma, A. T., Schmidt, C. M. and Golden, J. W. (2014) 'Regulation of gene expression in diverse cyanobacterial species by using theophylline-responsive riboswitches', *Applied and Environmental Microbiology*, 80(21), pp. 6704–6713. doi: 10.1128/AEM.01697-14.

Mao, H. Bin *et al.* (2002) 'The redox state of plastoquinone pool regulates state transitions via cytochrome b6f complex in Synechocystis sp. PCC 6803', *FEBS Letters*, 519(1–3), pp. 82–86. doi: 10.1016/S0014-5793(02)02715-1.

Markou, G. and Nerantzis, E. (2013) 'Microalgae for high-value compounds and biofuels production: A review with focus on cultivation under stress conditions', *Biotechnology Advances*. Elsevier, 31(8), pp. 1532–1542. doi: 10.1016/J.BIOTECHADV.2013.07.011.

Martin, G. J. O. *et al.* (2014) 'Lipid profile remodeling in response to nitrogen deprivation in the microalgae Chlorella sp. (Trebouxiophyceae) and Nannochloropsis sp. (Eustigmatophyceae)', *PLoS ONE*, 9(8). doi: 10.1371/journal.pone.0103389.

Mata, T. M., Martins, A. A. and Caetano, N. S. (2010) 'Microalgae for biodiesel production and other applications: A review', *Renewable and Sustainable Energy Reviews*. Pergamon, 14(1), pp. 217–232. doi: 10.1016/J.RSER.2009.07.020.

Moronta-Barrios, F., Espinosa, J. and Contreras, A. (2012) 'In vivo features of signal transduction by the essential response regulator RpaB from Synechococcus elongatus PCC 7942', *Microbiology*, 158(Pt_5), pp. 1229–1237. doi: 10.1099/mic.0.057679-0.

Moronta-Barrios, F., Espinosa, J. and Contreras, A. (2013) 'Negative control of cell size in the cyanobacterium Synechococcus elongatus PCC 7942 by the essential response regulator RpaB', *FEBS Letters*, 587(5), pp. 504–509. doi: 10.1016/j.febslet.2013.01.023.

Nakahira, Y. *et al.* (2013) 'Theophylline-dependent riboswitch as a novel genetic tool for strict regulation of protein expression in cyanobacterium synechococcus elongatus PCC 7942', *Plant and Cell Physiology*, 54(10), pp. 1724–1735. doi: 10.1093/pcp/pct115.

Nielsen, A. Z. *et al.* (2016) 'Extending the biosynthetic repertoires of cyanobacteria and chloroplasts', *The Plant Journal*, 87(1), pp. 87–102. doi: 10.1111/tpj.13173.

Nozzi, N. E. *et al.* (2017) 'Systematic approaches to efficiently produce 2,3-butanediol in a marine cyanobacterium', *ACS Synthetic Biology*, p. acssynbio.7b00157. doi: 10.1021/acssynbio.7b00157.

Osanai, T. *et al.* (2013) 'Increased bioplastic production with an RNA polymerase sigma factor SigE during nitrogen starvation in Synechocystis sp. PCC 6803.', *DNA research : an international journal for rapid publication of reports on genes and genomes*. Oxford University Press, 20(6), pp. 525–35. doi: 10.1093/dnares/dst028.

Oxborough, K. and Baker, N. R. (1997) 'Resolving chlorophyll a fluorescence images of photosynthetic efficiency into photochemical and non-photochemical components - Calculation of qP and Fv'/Fm' without measuring Fo'', *Photosynthesis Research*, 54(1989), pp. 135–142. doi: 10.1023/A:1005936823310.

Panda, B. and Mallick, N. (2007) 'Enhanced poly-β-hydroxybutyrate accumulation in a unicellular cyanobacterium, Synechocystis sp. PCC 6803', *Letters in Applied Microbiology*, 44(2), pp. 194–198. doi: 10.1111/j.1472-765X.2006.02048.x.

Paul, M. J. and Foyer, C. H. (2001) 'Sink regulation of photosynthesis.', *Journal of experimental botany*, 52(360), pp. 1383–1400. doi: 10.1093/jexbot/52.360.1383.

Piechura, J. R., Amarnath, K. and O'Shea, E. K. (2017) 'Natural changes in light interact with circadian regulation at promoters to control gene expression in cyanobacteria', *eLife*. eLife Sciences Publications Limited, 6, pp. 1–37. doi: 10.1101/193557.

Salomon, E. *et al.* (2013) 'Balancing photosynthetic electron flow is critical for cyanobacterial acclimation to nitrogen limitation', *Biochimica et Biophysica Acta - Bioenergetics*. Elsevier, 1827(3), pp. 340–347. doi: 10.1016/j.bbabio.2012.11.010.

Sauer, J. *et al.* (2001) 'Nitrogen starvation-induced chlorosis in Synechococcus PCC 7942. Low-level photosynthesis as a mechanism of long-term survival.', *Plant physiology*, 126(May), pp. 233–243. doi: 10.1104/pp.126.1.233.

Sharma, K. K., Schuhmann, H. and Schenk, P. M. (2012) 'High Lipid Induction in Microalgae for Biodiesel Production', *Energies*. Molecular Diversity Preservation International, 5(12), pp. 1532–1553. doi: 10.3390/en5051532.

Tu, C. J. *et al.* (2004) 'Consequences of a deletion in dspA on transcript accumulation in Synechocystis sp. strain PCC6803', *Journal of Bacteriology*. American Society for Microbiology, 186(12), pp. 3889–3902. doi: 10.1128/JB.186.12.3889-3902.2004.

Van der Woude, A. D. *et al.* (2014) 'Carbon sink removal: Increased photosynthetic production of lactic acid by Synechocystis sp. PCC6803 in a glycogen storage mutant', *Journal of Biotechnology*. Elsevier B.V., 184, pp. 100–102. doi: 10.1016/j.jbiotec.2014.04.029.

Yang, S., Sleight, S. C. and Sauro, H. M. (2013) 'Rationally designed bidirectional promoter improves the evolutionary stability of synthetic genetic circuits.', *Nucleic acids research*. Oxford University Press, 41(1), p. e33. doi: 10.1093/nar/gks972.

CHAPTER 4.2: REDIRECTING CARBON TO BIOPRODUCTION DURING NITROGEN STARVATION

Introduction

Photosynthetically derived carbon can be partitioned to many pathways regulated by environmental conditions or endogenous molecular mechanisms. In chapter 4.1, I showed that carbon can be diverted from growth to sucrose production by activation of a genetic switch that decreased the growth rate of *S. elongatus*. Though the over-expression of RpaB is likely to lead to a complex cellular phenotype, one way to interpret my results with this inducible growth arrest switch is that reducing growth and division also decreased endogenous sink capacity. Namely, metabolic fluxes that would normally support the production of amino acids, nucleotides, lipids, cell wall and other cellular biomass components would be reduced relative to *S. elongatus* cultures growing normally. I was then able to show that the photosynthetic sink limitations imposed by the growth arrest switch could partially be alleviated when carbon was partitioned to a heterologous sucrose sink. Similar in concept to chapter 4.1, here I use depletion of nitrogen from the medium to decrease cellular growth which limits cellular sink capacity leading to a decrease in photosynthetic efficiency. The decrease in photosynthesis is partially rescued by increasing the sink capacity through induction of a heterologous sucrose export pathway.

This chapter presents preliminary data supporting the hypothesis that endogenous sink restriction (e.g. glycogen knockouts or through nitrogen starvation) increases photosynthetic sink limitation which can be partially alleviated by diversion of carbon to a heterologous sink (e.g. secreted sucrose). Glycogen represents the main carbon storage product in *S. elongatus* and knockouts of glycogen synthase (Δ*glgC*) cannot produce glycogen and Δ*glgC* cells have been shown to accumulate NADPH (Holland *et al.*,

2016) while having decreased growth rates relative to wild-type strains (Jackson *et al.*, 2015). Liao *et al.* 2014 showed that Δ*glgC* cells had decreased cellular growth rates but expression of a heterologous isobutanol production pathway led to partial growth recovery, increased carbon fixation rates, and increased carbon partitioned from cell biomass to production pathway metabolites. The authors hypothesized that the metabolic sink provided by isobutanol production could alleviate the photosynthetic sink limitation (Liao *et al.* 2014), and proposed that isobutanol production partially consumed metabolites that were in excess (*e.g.*, NADPH) thereby balancing cellular NADPH:$NADP^+$ pools (Liao *et al.* 2014). Unfortunately, the researchers did not observe how the photosynthetic electron transport chain responds to restriction of an endogenous sink and/or introduction of an engineered pathway that expands the sink capacity.

Glycogen has been shown to be a large carbon sink, and similarly, the accessibility of nitrogen sources also significantly influences metabolic sink capacity. Not only do nitrite and nitrate require the consumption of reducing equivalents to be converted to ammonia (Cano *et al.*, 2018; Osanai *et al.*, 2013; Anfelt *et al.*, 2015), but in the absence of sufficient nitrogen, a number of critical biomolecules cannot be produced (e.g., amino acids). The resulting bottlenecks in a variety metabolic fluxes can lead to photosynthetic limitations. Overall, growth in nitrogen-limited conditions effects many cellular pathways, reviewed elsewhere (Ohashi *et al.*, 2011; Choi *et al.*, 2016), including decrease amino acid synthesis, protein synthesis, limited cellular growth, and hyperaccumulation of compounds with a high C:N ratio (i.e. lipids or glycogen; Hickman *et al.*, 2013). In part because of the large reorganization of cellular metabolism induced by nitrogen starvation, reducing bioavailable nitrogen in the growth media has been extensively studied as a method to divert carbon and energy from growth to other pathways for the production and accumulation of certain carbon metabolites, such as lipids, hydrogen and polyhydroxyalkanoates

(Raleiras *et al.*, 2013; Martin *et al.*, 2014; Löwe *et al.*, 2017). The diversion of energy and carbon from nitrogen assimilation pathways to other metabolic sinks is one possible way that cells balance energy metabolite pools (e.g. NADPH:$NADP^+$), whereby excess photosynthetically derived NADPH can be consumed by the new pathway to produce compounds with a high C:N ratio thus releasing $NADP^+$ for future reductions. Although there is a substantial research observing the photosynthetic limitations imposed by nitrogen starvation, there is very little research focused on how or if carbon diversion to engineered heterologous sinks can relieve the photosynthetic sink limitation imposed by restriction of nitrogen assimilation pathways.

Under certain contexts where carbon and energy cannot be stored in carbon storage compounds, mechanisms occur leading to the export of high energy carbon metabolites, sometimes termed "metabolic overflow". In *S. elongatus* glycogen-deficient strains have been shown to export organic acids into the medium as an extracellular sink in response to nitrogen starvation (Gründel *et al.*, 2012; Carrieri *et al.*, 2015; Benson *et al.*, 2016). Although the mechanisms for metabolite excretion are not known, it is thought that exporting energy-rich metabolites might act as a protective mechanism for dissipating excess energy when excess metabolites cannot be utilized and sink restriction occurs (i.e. removal of nitrogen assimilation pathways and glycogen storage). The accumulation of certain metabolites (e.g. NADPH and ATP) within the cell can limit photosynthetic productivity and therefore excretion of high energy organic acids might be one cellular mechanism to consume energy metabolites and decrease their accumulation in the cell. It is possible that heterologous metabolic sinks (e.g., secreted sucrose), could

act in an analogous manner to metabolic overflow products to protect cyanobacteria under conditions of severe sink limitation, although this has not been shown before.

Here I set out to study if a sucrose sink can relieve sink limitations imposed by blocking endogenous sinks such as glycogen production and through nitrogen assimilation sinks. As expected, I show glycogen-deficient cultures resuspended in nitrogen free medium demonstrate rapid reductions in photosynthetic efficiency. I hypothesized cells exporting sucrose in nitrogen depleted conditions would allow the engineered sucrose sink to consume over-accumulated energy metabolites to relieve the photosynthetic sink limitation imposed by restricting endogenous sinks. I observed that sucrose-exporting cells still showed a decreased photosynthetic capacity during nitrogen starvation but sucrose export lead to a partial recovery of the quantum yield of PSII (ΦII) and a more oxidized plastoquinone pool which altered the photosynthetic complex stoichiometry. These observations bolster observations in Chapter 4.1 where a molecular growth switch was used to restrict endogenous sinks leading to decreased photosynthetic efficiency and the expanded sink capacity from sucrose export was able to partially alleviate the photosynthetic sink limitation.

Results

Nitrogen limitation decreases growth and increases sucrose specific productivity

It has been shown that nitrogen-starved Δ*glgC* cells are capable of exporting organic acids therefore I hypothesized synthesis and export of sucrose might still occur following nitrogen starvation, but confirmation was required. I first evaluated rates of sucrose secretion from cyanobacterial cells under nitrogen-limited conditions which can arrest cellular growth, as previously shown (Hickman *et al.*, 2013). Indeed, growth arrest has also been observed in Δ*glgC* strains and restricting endogenous sink capacity through both nitrogen starvation and knockouts

of glycogen synthase might yield greater partitioning of carbon to sucrose export thus exacerbating the photosynthetic phenotypes observed later in this study. Sucrose export was induced three days prior to nitrogen starvation to allow the cells to express CscB and SPS: this induction was based upon my prior results which indicate that rates of sucrose export gradually increase in the hours following induction of *cscB* and *sps* and that a number of physiological changes are observed in the first 1-2 days before indicators stabilize (Chapter 2). To minimize any complications due to these changing cell parameters during the first 48 hours after induction, cells were induced to export sucrose three days prior to nitrogen starvation (Chapter 2 and Abramson *et al.*, 2016).

As expected, nitrogen starvation greatly diminished chlorophyll accumulation within the cultures, while nitrogen-replete conditions promoted substantial chlorophyll biomass accumulation. Cells were back diluted to equal chlorophyll concentrations in nitrogen containing medium (replete) or nitrogen free medium (deplete) at a timepoint denoted as 0h. Cultures were allowed to grow for 48h in the respective medium and chlorophyll concentrations were measured (Figure 4.2.1b). In replete culture conditions there is almost a 10-fold increase in the amount of chlorophyll per unit volume after 48h. However, in nitrogen-depleted conditions no significant accumulation of chlorophyll is observed at 24h or 48h (Figure 4.2.1b). Others have shown that nitrogen starvation inhibits cell growth (Hickman *et al.*, 2013; Jackson *et al.*, 2015), and here, a lack of chlorophyll accumulation in deplete conditions might be indicative of decreased cellular growth (see discussion for interpretations of this data).

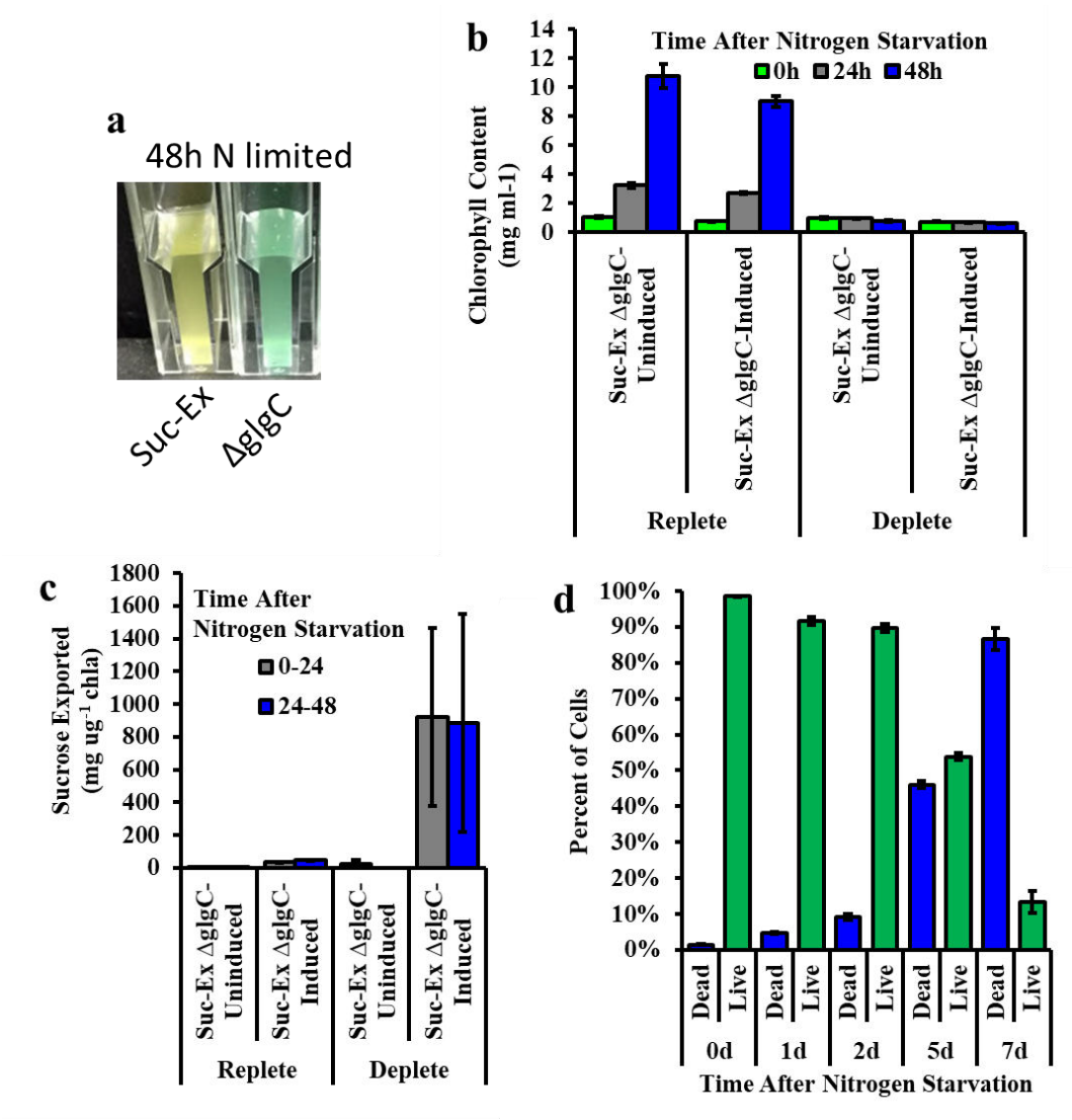

FIGURE 4.2.1: CELLULAR RESPONSE TO NITROGEN STARVATION.
a) Glycogen deficient strains retain phycobilisomes and resist nitrogen starvation induced chlorosis. b) Cells become growth arrested when resuspended in a medium without nitrogen as measured by chlorophyll concentration. Growth arrest is independent of induced sucrose export two days prior to nitrogen starvation. c) Sucrose export rates increase when cells are induced, and nitrogen starved for 24h or 48h relative to induced cultures in replete conditions. d) Greater than 90% of Δ*glgC* cells are alive after 48h nitrogen starvation however suggesting sucrose measured is not due to cell lysis.

Next, I sought to determine if sucrose export was occurring following nitrogen starvation. The amount of sucrose was measured in the supernatant after 24h or 48h of nitrogen starvation or

from cultures that remained in replete conditions and the amount of sucrose exported was normalized to the amount of chlorophyll extracted in equal culture volumes (Figure 4.2.1c). The amount of sucrose exported per µg chlorophyll in the culture increases substantially in deplete conditions compared to replete conditions (Figure 4.2.1c). Uninduced cultures in both replete and deplete conditions did not show appreciable levels of sucrose export and were at the limit of detection for the sucrose assay used here. In replete conditions the maximum rate of sucrose export was observed from induced cultures at a rate of 47.6±1.6 mg sucrose μg^{-1} chlα whereas induced, nitrogen-starved cultures had a rate of 882.9±665.0 mg sucrose μg^{-1} chlα. These observations show that nitrogen starvation does not inhibit sucrose exported to the extracellular space and therefore sucrose export might be able to act as an expanded carbon sink following nitrogen starvation. We also directly assayed cell viability through the use of a vital dye and found greater than 90% of the cell population remained viable (Figure 4.2.1d), suggesting that sucrose measured in the medium is not the result of lysed cells at 48h and is produced photosynthetically and exported.

Sucrose export partially alleviates photosynthetic sink limitation

Previously in chapter 4.1, I showed a molecular switch for growth arrest increased sucrose export and cells exporting sucrose were able to alleviate some of the phenotypes of photosynthetic sink limitation imposed by decreased growth and restricted energetic demands. Similarly, I showed that growth arrested cells due to nitrogen starvation are capable of exporting sucrose and therefore hypothesized that sucrose export could act as an expanded metabolic sink to decrease photosynthetic sink limitations imposed by both nitrogen starvation and glycogen synthesis. Chlorophyll *a* fluorescence was measured

and the photosynthetic efficiency of PSII (ΦII) was calculated following resuspension of cells in nitrogen replete or deplete medium (Figure 4.2.2a). Irrespective of induction status, nitrogen depletion caused a drastic decrease in ΦII (Figure 4.2.2a; dark symbols); however, induced cultures showed an increase in ΦII relative to uninduced cultures (Figure 4.2.2a; open vs. closed symbols). Interestingly, the fast drop in photosynthetic efficiency following nitrogen starvation (<18h) could not be alleviated by sucrose export and sucrose export only increased photosynthetic efficiency, relative to uninduced cultures, greater than 18h after nitrogen starvation.

The increase in ΦII could be the result of a partial rescue of qP, or the oxidation state of the plastoquinone pool, which is observed in sucrose exporting cells in nitrogen depleted conditions (Figure 4.2.2b) (Campbell and Oquist, 1996; Abramson *et al.*, 2016). Both ΦII and qP increase in cells exporting sucrose relative to uninduced controls reaching a maximum of 330% and 95% 48h after nitrogen starvation, respectively (Figure 4.2.2c). However, these increases do not return the photosynthetic phenotypes to maximums observed at 0h (ΦII=0.18 and qP=0.74) after nitrogen starvation. Interestingly, the increases in qP and ΦII do not mitigate the initial decrease in photosynthetic efficiency or decrease in aP due to nitrogen starvation (<18 hours) but increase notably only after 24h.

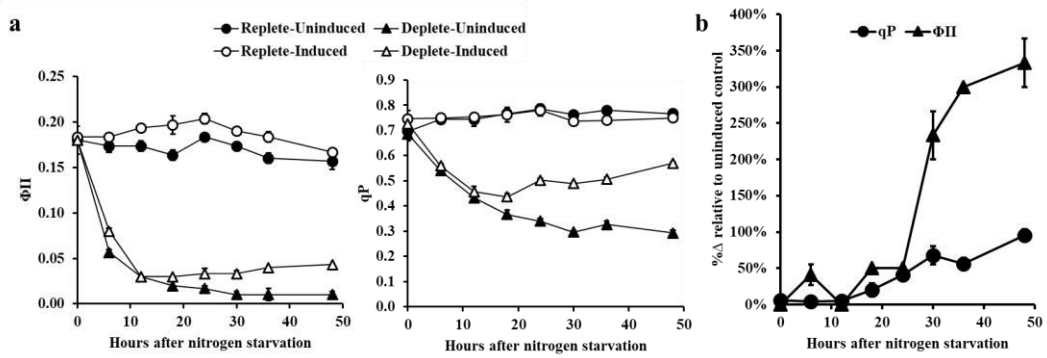

FIGURE 4.2.2: SUCROSE EXPORT PATHWAY MITIGATES PHOTOSYNTHETIC SINK INHIBITION UNDER NITROGEN LIMITED CONDITIONS.
a) ΦII is monitored in cultures under replete or depleted nitrogen conditions and where sucrose export is either induced or uninduced. **b)** qP, a measure of the oxidation sate of the plastoquinone pool and "openness" of PSII increases when sucrose is exported in nitrogen starved cells. **c)** Percent change in ΦII and qP in cultures exporting sucrose relative to uninduced controls during nitrogen starvation. Data are averages (n=3) with standard error.

Photosynthetic complex stoichiometry is altered in response to sucrose export

To assess how a heterologous sink fects photosynthetic complexes, Western blots were performed to compare the protein levels between uninduced and sucrose exporting cultures following nitrogen starvation. Since the chlorophyll content in nitrogen depleted conditions during the time course was unchanged between induced and uninduced cultures (Figure 4.2.1B), total protein was extracted from equal chlorophyll quantities and loaded for SDS-PAGE and Western blotting. As before, induced cultures were allowed to acclimate for three days prior to cell collection and resuspension in a new medium (0h) with or without nitrogen while additional IPTG was added to induced cultures. Western blots for each time point were performed on a single membrane with three primary antibodies for RbcL (subunit of rubisco; 52kDa), PsbA (subunit of PSII; 42kDa) and PsaC (subunit of PSII; 12kDa) on a single membrane.

The accumulation of protein subunits (RbcL, PsbA and PsaC) within each sample was determined and the ratio between induced cultures or uninduced cultures for each

subunit were plotted at timepoints following nitrogen depletion (Figure 4.2.3). At 0h quantification of RbcL and PsbA showed that levels had decreased in induced samples compared to uninduced controls (ratio less than one; Figure 4.2.3). Following nitrogen starvation, a steady increase in the amount of RbcL in sucrose exporting strains relative to uninduced controls is observed. Likewise, following nitrogen starvation, sucrose exporting cultures contain a greater quantity of PsbA. Interestingly, PsaC appears to decrease after 48h of nitrogen starvation. The alterations to these photosynthetic complexes suggests that the addition of a sucrose sink has effects on the cellular environment leading to changes of photosynthetic subunit and possibly complex stoichiometry.

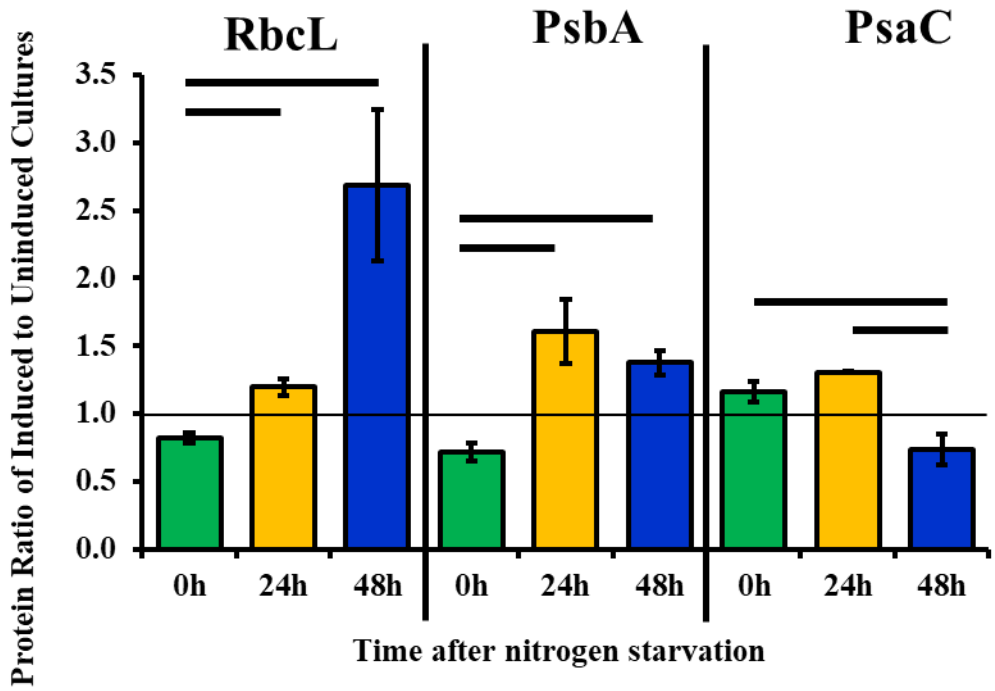

FIGURE 4.2.3: PHOTOSYNTHETIC COMPLEX STOICHIOMETRY IS ALTERED IN RESPONSE TO SUCROSE EXPORT AND NITROGEN LIMITATION.
Cells were induced or remained uninduced three days prior to nitrogen starvation (0h) and Western blots were performed on whole cell lysate for each protein subunit (RbcL, PsbA and PsaC. The ratio between induced and uninduced cultures for each subunit are plotted at 0h, 24h and 48h after resuspension in nitrogen free medium. At 0h, induced cultures showed less RbcL and PsbA expression compared to uninduced cultures. After 48h nitrogen starvation the response to sucrose export results in an increase in RbcL, PsbA content compared to a decrease in PsaC content. Samples are averages (n=3) with standard error and black bars denote significant differences between samples (p-value < 0.05).

Discussion

In this chapter (4.2), I show preliminary evidence suggesting that heterologous sucrose export allows for a partial rescue of photosynthetic sink limitations imposed by endogenous sink restriction through nitrogen starvation alongside glycogen synthase deletion (Δ*glgC*). Restriction of these two sinks has been shown to increase carbon partitioning to endogenous metabolites with a large C:N ratio or to extracellular heterologous engineered sinks, respectively (see 4.2 Introduction). Nitrogen starvation decreased endogenous sink capacity and increased photosynthetic sink limitation

allowing me to measure the alterations to photosynthetic phenotypes in response to induced sucrose export. The heterologous sucrose export sink partially rescued the sink limitation imposed by nitrogen starvation (Figure 4.2.2). In response to relief of sink limitation during nitrogen starvation, cells showed increased ΦII and a more oxidized plastoquinone pool (greater qP) but sucrose export could not rescue the declines in photosynthetic performance observed immediately following the transfer to nitrogen-depleted media (*i.e.*, <18h after transfer). Interestingly, there was an increase in RbcL and PsbA content in cells exporting sucrose relative to uninduced controls following 48h nitrogen starvation. These data support the idea that an engineered sucrose sink can relieve some of the sink limitations imposed by nitrogen starvation and a knockout of glycogen synthesis.

Nitrogen depleted cultures have higher sucrose export rates per chlorophyll quantity compared to nitrogen replete conditions. This could be due to several reasons, first, in replete conditions, cells continue growing to high densities and the resultant cell shading may limit light penetration, limiting sucrose synthesis. Second, the sucrose export rate was determined by normalization to chlorophyll concentrations within the cell and perhaps the quantity of chlorophyll per cell is decreased in response to nitrogen starvation giving rise to an apparent increase in sucrose export rates. Third, glycogen deficient cells in nitrogen limiting conditions have been shown to accumulate excess reductant to the point that so-called "overflow metabolism" occurs and cells export energy-dense organic acids (Carrieri *et al.*, 2015; Benson *et al.*, 2016). Overflow metabolism has been observed in nitrogen starved Δ*glgC* cells when carbon and energy fated for glycogen storage or other cellular processes accumulates in the cell and overflows to organic acid synthesis and excretion to the extracellular space. Increased concentrations of energy metabolites in a sucrose exporting strain could be readily diverted to

sucrose synthesis and to the sucrose export pathway leading to observed increases in sucrose export rates. The accumulation of energy and carbon metabolites and increased metabolic flux to sucrose export during nitrogen starvation in Δ*glgC* cells could be similar to the increased sucrose export observed when growth is arrested by over expression of RpaB (Chapter 4.1). This evidence supports the idea that carbon can be diverted from endogenous sinks to heterologous sinks increasing metabolic flux into the engineered pathway and productivity of the engineered heterologous sink, in this case sucrose export.

Interestingly, the expanded sink capacity by sucrose export during nitrogen starvation was able to relieve some of the photosynthetic sink limitations imposed by nitrogen starvation but not the initial photosynthetic limitations (<18h; Figure 4.2.2). This is surprising since sucrose export was activated three days prior to nitrogen starvation and this suggests a photosynthetic sink limitation mechanism that is independent of a sucrose sink. The initial response to nitrogen starvation is a large accumulation of reductant and an increase in 2-OG levels that cannot not be consumed through nitrogen assimilation pathways and growth (Jiang *et al.*, 2017). The accumulation of large amounts of reductant initially following nitrogen starvation could reduce photosynthetic electron flux and decrease photosynthetic efficiency (Hauf *et al.*, 2013; Hickman *et al.*, 2013) similar to the observations here (Figure 4.2.2). Since sucrose export did not alleviate the fast decrease in photosynthetic efficiency it might suggest that the sucrose synthesis and secretion pathway is not an effective consumer of NADPH relative to the overall NADPH consumption through nitrogen assimilation and growth pathways. Measurements of NADPH:$NADP^+$ pools during nitrogen starvation are needed to

determine how much NADPH might accumulate following nitrogen starvation. In addition, I hypothesize cultures induced to export sucrose might show greater consumption of NADPH leading to a partial relief of sink limitation phenotypes but only at time points greater than 18h following nitrogen starvation.

Likewise, the 2-OG level within the cell is known to affect transcription factors involved in nitrogen assimilation (Ohashi *et al.*, 2011) and an accumulation of 2-OG within the cell is known to regulate many cellular processes both directly and indirectly (Huergo and Dixon, 2015). For example, 2-OG is an allosteric regulator of some enzymes and also controls the activity of a master transcriptional regulator, NtcA. Therefore, it is possible that pathways directly involved in the detection of nitrogen availability (such as those regulated by 2-OG) would be activated following a transition to nitrogen-limited media regardless of the total metabolic sink capacity of the cell. Further studies observing metabolite pool changes in response to sucrose are needed and one might be able to disentangle the key metabolites involved in sensing a sucrose sink compared to a nitrogen sink or other heterologous sinks (See Chapter 5).

Moreover, sucrose export might not occur immediately after nitrogen starvation. The resolution of this dataset for sucrose export is lacking in this context and future studies will need to measure sucrose export in the initial hours following nitrogen starvation (<18h) to determine if sucrose export is occurring. If sucrose export is dampened or abolished immediately following nitrogen depletion, then it would explain why photosynthetic sink limitation is not rescued at the earliest timepoints. Previously it had been shown that Δ*glgC* cells have delayed activation of the CB cycle from dark to light conditions (Holland *et al.*, 2016). To resuspend cells in new medium, cells were centrifuged in the dark for several minutes potentially inactivating the CB cycle and

potentially sucrose production and export. Similarly, future studies need to consider the environmental perturbations imposed by cell handling that might cause inactivation of the CB cycle.

To better understand the molecular response to a heterologous sink I measured accumulation of photosynthetic complex subunits relative to uninduced controls during nitrogen starvation (Figure 4.2.3). Before nitrogen starvation (0h) there is a decrease in RbcL and PsbA presumably stemming from the long-term acclimation response to sucrose export (greater than 48h after induction; See Chapter 2). Sucrose exporting cells have been shown to have greater carbon fixation (Ducat *et al.*, 2012; Chapter 3) and therefore it is surprising that RbcL decreases relative to an uninduced control. However, the photosynthetic response to sucrose export has never been observed in a Δ*glgC* strain which is incapable of producing glycogen and it is unclear what the interplay between sucrose export, glycogen depletion and regulation of photosynthetic complexes might be. Therefore, more studies of the mechanisms of sink limitation in the context of a glycogen deficient strain are needed.

Photosynthetic complex stoichiometry is altered in response to increased sink capacity and might be signaled by an oxidized plastoquinone pool in sucrose-exporting, nitrogen-starved cells which suggests a unique acclimation response to heterologous sink expression. Sucrose export results in greater qP which suggests a more oxidized plastoquinone pool (Figure 4.2.2b, Chapter 2). An oxidized plastoquinone pool results in a state transition whereby phycobilisomes partition more excitation energy to PSII (State I) and less excitation to PSI which can alter the rate of flux of electrons through plastoquinone pool, the membrane soluble PSII interacting electron acceptor. When the

plastoquinone pool becomes oxidized phycobilisomes increase excitation energy to PSII to increase the activity of water oxidation and electron transfer to the plastoquinone pool thereby leading to a more reduced plastoquinone pool (Cameron, 2011; Schuurmans *et al.*, 2014). However, in Δ*glgC* cells, the state transition is inhibited as shown through a slow increase in chlorophyll fluorescence during actinic illumination (Holland *et al.*, 2016). Therefore, to maintain redox homeostasis cells may apply new mechanisms to maintain redox homeostasis allowing cells to increase the rate of electrons input into the PQ pool by increasing expression of PSII (increased PsbA in PSII; Figure 4.2.3). The shift in photosynthetic complex stoichiometry might be a long-term acclimation response to an oxidized plastoquinone pool when cells are incapable of state transitions. This data set suggests that an exogenous sink can relieve some of the sink limitation imposed by nitrogen starvation or by a genetic knockout of glycogen and may suggest a new strategy for balancing energy flux to the plastoquinone pool when the cells cannot perform state transitions.

Materials and Methods

Growth conditions and construct design

Cells were grown as previously described by Abramson et. al., 2016. Sucrose induction was carried out by addition of 1mM IPTG 2 days prior to any nitrogen depletion studies. Cells were collected and resuspended to an equal OD in pH buffered BG-11 with (replete; +N) or without (deplete, -N) $NaNO_3$.

Chlorophyll and sucrose quantification

Sucrose was quantified with Megazyme kit (K-SUCGL) as per manufacture protocols and as previously described in Chapter 2. Chlorophyll content was quantified by resuspending cell pellets in 90% methanol and reading the absorbance on a Genesys 20 spectrometer at A665.

Live/dead staining and quantification

Cells were stained with Alexa Fluor™ 488 NHS Ester (Succinimidyl Ester)(Thermo) and flow cytometry (BD Accuri6) was used to gate cell populations (live vs dead). Cells boiled for 1 minute were used as a positive control for cell membrane permeability and gating of dead cells.

Spectroscopy

Photosynthetic measurements were performed as previously described by Abramson el. al., 2016, on an AquaPen AP-C 100 (see also, chapter 2 and chapter 3 methods).

Protein quantification and Western Blot

Total protein was exacted from cells resuspended in 1x Lamellie buffer and boiled for 10 minutes. Protein quantification was performed with a Thermo Scientific Pierce Protein Assay Kit following manufacture directions. SDS-PAGE was performed and protein blotting for westerns were performed with BioRad Trans-Blot® Turbo™ Transfer System. Proteins were detected with Agrisera Photosynthesis Tool Kit (AS04-051) and primary antibodies were used at a dilution of RbcL-1:5000; PsbA-1:10000; PsaC-1:2000 and detected with Thermo Scientific West Femto HRP secondary reagent. Imaging and western quantification was performed on BioRad gel imager using Image Lab software. Chlorophyll content was measured from equal sample volumes used to extract total protein for later normalization.

REFERENCES

REFERENCES

Abramson, B. W. et al. (2016) 'Increased Photochemical Efficiency in Cyanobacteria via an Engineered Sucrose Sink', Plant and Cell Physiology, 0(October), pp. 1–10. doi: 10.1093/pcp/pcw169.

Benson, P. J. et al. (2016) 'Factors Altering Pyruvate Excretion in a Glycogen Storage Mutant of the Cyanobacterium, Synechococcus PCC7942', Frontiers in Microbiology, 7(April), pp. 1–11. doi: 10.3389/fmicb.2016.00475.

Cameron, J. (2011) 'Redox Homeostasis in Cyanobacteria', (May 2011).

Campbell, D. and Oquist, G. (1996) 'Predicting light acclimation in cyanobacteria from nonphotochemical quenching of photosystem II fluorescence, which reflects state transitions in these organisms', Plant physiology, pp. 1293–1298.

Carrieri, D. et al. (2015) 'Enhancing photo-catalytic production of organic acids in the cyanobacterium Synechocystis sp. PCC 6803 Δ glgC, a strain incapable of glycogen storage', Microbial Biotechnology, 8(2), pp. 275–280. doi: 10.1111/1751-7915.12243.

Davies, F. K. et al. (2014) 'Engineering Limonene and Bisabolene Production in Wild Type and a Glycogen-Deficient Mutant of Synechococcus sp. PCC 7002', Frontiers in Bioengineering and Biotechnology, 2(June), pp. 1–11. doi: 10.3389/fbioe.2014.00021.

Ducat, D. C. et al. (2012) 'Rerouting carbon flux to enhance photosynthetic productivity', Applied and Environmental Microbiology, 78, pp. 2660–2668. doi: 10.1128/AEM.07901-11.

Hickman, J. W. et al. (2013a) 'Glycogen synthesis is a required component of the nitrogen stress response in Synechococcus elongatus PCC 7942', Algal Research. Elsevier B.V., 2(2), pp. 98–106. doi: 10.1016/j.algal.2013.01.008.

Hickman, J. W. et al. (2013b) 'Glycogen synthesis is a required component of the nitrogen stress response in Synechococcus elongatus PCC 7942', Algal Research. Elsevier B.V., 2(2), pp. 98–106. doi: 10.1016/j.algal.2013.01.008.

Holland, S. C. et al. (2016) 'Impacts of genetically engineered alterations in carbon sink pathways on photosynthetic performance', Algal Research. Elsevier B.V., 20, pp. 87–99. doi: 10.1016/j.algal.2016.09.021.

Klotz, A. et al. (2015) 'Nitrogen Starvation Acclimation in Synechococcus elongatus: Redox-Control and the Role of Nitrate Reduction as an Electron Sink', Life, 5, pp. 888–904. doi: 10.3390/life5010888.

Schuurmans, R. M. et al. (2014) ‘The Redox Potential of the Plastoquinone Pool of the Cyanobacterium Synechocystis Species Strain PCC 6803 Is under Strict Homeostatic Control’, Plant Physiology, 165(1), pp. 463–475. doi: 10.1104/pp.114.237313.

CHAPTER 5: CONCLUSIONS

Overview

In this dissertation, *S. elongatus* was engineered to export sucrose which relieved sink limitation resulting in increased photosynthetic efficiency. In chapter 2, it was shown sucrose export increases photosynthetic light use efficiency by PSII (ΦII) and leads to a decrease in PSI acceptor side limitation and greater relative electron transport rates (Abramson et al., 2016). Greater photosynthetic electron flux could be a product of increased rubisco expression and potentially localization within the carbon fixation proteinaceous organelle, the carboxysome (Chapter 3). Finally, in Chapter 4, I showed carbon was partitioned to a heterologous sink (e.g. exported sucrose) from growth by arresting cells through nutrient deprivation or overexpression of a transcriptional regulator which causes a slowed growth. This adds to the growing evidence for sink limitation in algal strains and export of a carbon metabolite in single celled photosynthetic organisms can decrease sink limitations imposed on the cell. These results have implications for our fundamental understanding of how photosynthetic metabolism is naturally limited in photosynthetic microbes. Furthermore, these results suggest new strategies for increasing photosynthetic efficiency in strains of cyanobacteria and algae that have been engineered for bioproduction.

What are the molecular sensors of increased sink capacity?

The introduction of a sucrose export pathway increases metabolic flux into this synthesis pathway, thus requiring more carbon fixation by the CB cycle and energy production by the photosynthetic electron transport chain. Potentially, carbon and energy could merely be rerouted from endogenous pathways without an increase in photosynthetic productivity, but this does not appear to be the case in a sucrose exporting S. elongatus. The photosynthetic response observed when exporting sucrose could be similar in other production strains engineered to produce

compounds that are exported to the extracellular space (Ungerer *et al.*, 2012; Wang *et al.*, 2016). Some exported metabolites elicit a toxic effect on the cell which might diminish photosynthetic (Kato *et al.*, 2016), however, in this dissertation, sucrose export is generally viewed as nontoxic and careful care should be taken in attributing results to metabolite toxicity and/or metabolic sink capacity. Likewise, depending on the particular energetic or carbon demands to produce the final bioproduct, the photosynthetic response might be different.

Photosynthetic sink limitation decreases photosynthetic capacity and efficiency in photosynthetic microbes, as supported by this body of evidence. Export of a sucrose in this dissertation can relieve the limitations of photosynthesis and increase the efficiency of light used by PSII, the first steps in photosynthesis, along with many other photosynthetic responses (Chapter 2 and 3). In this case, sucrose is exported, however sucrose itself is most likely not the direct effector molecule that is sensed and provoking the many cellular responses observed. Most often effector molecules for cellular pathway regulation are charged or phosphorylated carbon molecules. Sucrose that is exported may deplete the cytoplasm of sucrose along with precursor molecules, including sucrose-6-phosphate (S6P) or RuBP, to name a few. These metabolites, among many others, are more likely to be effector molecules. Indeed, S6P is most likely an effector molecule for a sucrose sink directly whereas RuBP might serve as a universal carbon sink effector molecule as it is essential for carbon fixation. Determination of depleted and/or accumulated metabolite pools following induction of a heterologous sink is a dataset that is being pursued currently and these data could provide evidence as to which effector molecules might have the greatest effect on relieving photosynthetic sink limitation

Allosteric regulation can alter metabolic flux but can also directly modulate gene expression. Many of the well-known carbon status transcriptional regulators in plants do not have DNA binding activity or known orthologues in cyanobacteria, such as, hexokinase or sucrose-non-fermenting-1 (SNF1) (Rolland, Baena-Gonzalez and Sheen, 2006; Ryu *et al.*, 2008). Common in most cyanobacteria, CmpR directly binds to DNA which represses expression of CCM genes. Activity of CmpR can be altered by increased RuBP and 2PG cytoplasmic concentrations which abolish DNA binding activity (Nishimura *et al.*, 2008; Daley *et al.*, 2012). RuBP and 2PG are representative metabolites for limited CB flux or rubisco's oxygenation reaction and therefore stimulate expression of several CCM genes through CmpR. Although some information about the carbon status could be gleaned from measuring only RuBP or 2PG over time in strains following induction of a carbon export pathway, the complex metabolic regulation to excreted compounds necessitates a large metabolome dataset. Since multiple metabolites can exhibit effects on the same enzyme, measuring a few metabolites over time will not give the full regulatory scope of the cellular response to heterologous sinks.

Our preliminary data show that sucrose export can increase the amount of rubisco produced within the cell (Chapter 3), but it is unclear how sucrose export elicits this response on the cell. A RbcS-GFP reporter strain shows increased RbcS-GFP fluorescence following induction of sucrose export. Likewise, the relative ratio of RbcL:PsbA (subunit of PSII) increases, suggesting that the increases in the light reactions of photosynthesis observed in chapter 2 are a response to increased carbon fixation. Since CmpR is known to alter expression of several CCM genes it might be an interesting target for future study. Greater CmpR binding to the several promoters of CCM genes might be evident following induction of sucrose which alters rubisco expression (Chapter 3). Likewise, the CCM response includes expression of high

affinity HCO_3^- active transporters to increase Ci concentrations within the cytosol and these might have interesting expression patterns following sucrose export. Therefore, the response induced by CmpR and the expression CCM genes should be studied in careful detail following sucrose export.

The CB cycle is known to be regulated by several mechanisms including, allosteric regulation or redox-mediated disulfide bond formation. CB enzymes can be activated when a reduced cellular environment is detected (dark to light transition) and it is suggested there are 300 putative cellular redox-responsive targets (Lindahl, Mata-Cabana and Kieselbach, 2011). Therefore, redox sensory proteins, or redox activated/inactivated enzymes are critical control mechanisms for photosynthesis. Some of these redox-responsive proteins could be signals for sink capacity as I have shown that increasing the sink size (i.e. sucrose export) oxidizes the plastoquinone pool. It is unclear if the oxidation of NADPH also occurs and kinetics of NADPH production/depletion to a sucrose export pathway is currently lacking. Likewise, the cellular redox state could be measured through a proteomic study of glutathione or thioredoxin disulfide bond linkages in response to heterologous sink induction.

Although photosynthetic regulation by effector molecules, redox activation/inactivation or transcriptional regulation are critical for photosynthesis in a dynamic environment, strict regulation could limit overall photosynthetic productivity in relatively stable bioreactor like conditions. Although an algal culture as a whole can be grown under constant lighting, an individual cell may experience a dynamic lighting environment. The constant shaking or bubbling of cell cultures can alter the light intensity an individual cell perceives within the culture if it is on the outside (HL) or

inside (LL) of a dense culture. The photosynthetic response to effector molecules or the redox state as the cell passes from HL to LL and back and forth might increase and decrease photosynthetic flux. The constant fluctuations in photosynthetic flux could hinder the overall process of photosynthesis. The hindrance would come from brief, yet repetitious, flecks of light and the accumulation of many minute interruptions which could decrease overall photosynthetic productivity. Therefore, mutating or removing some of the allosteric sites or redox sensitive thiol groups of CB cycle enzymes presents a promising potential to increase photosynthetic culture productivity.

How are carbon and redox status reconciled in response to heterologous sinks?

When sucrose is exported it is clear that both a molecular/metabolic and a redox response is observed (Chapter2 and Chapter 3). The metabolic and redox response to sucrose export is expected to be very different at various timepoints following induction of sucrose export. The dynamic response observed in ΦII/qP over time (Figure 2.2d) is a clear indication that the cellular response to sucrose export is dynamic. A delay in the increase in ΦII/qP is observed immediately (<12h) following induction of sucrose export. During this time, metabolite pools may become depleted as a result of cytoplasmic sucrose export and precursor metabolites are consumed. As metabolites are consumed for sucrose synthesis, rubisco expression increases suggesting greater carbon fixation which then increases the demand for ATP and NADPH. Next, increased ΦII/qP is observed (18-48h) due to an imbalance between PET chain constituents and increased energy consumption by the CB cycle due to depleted cellular sucrose (or metabolites for sucrose synthesis) (Figure 2.2). This process oxidizes the PET chain leading to greater ΦII/qP. The oxidation of plastoquinone might then illicit a response to increase expression of photosynthetic complexes to match the energetic demand of the CB cycle. Therefore, it is

possible that the sensing and the response to metabolites and the redox status might occur at different times or regulate different photosynthetic responses, however, both metabolic and redox signals play a role in sensing and responding to exported sucrose, as observed in this dissertation. However, it is unclear at this time which signals, if any, are more important in sensing sink capacity. It is likely both redox and metabolite signals will be critical in perception and response to increased sink capacity in other engineered algal strains.

What is the CCM response to an expanded sink?

When sucrose is exported, the cell responds by increasing rubisco expression and increasing the efficiency of photosynthetic electron transport, however, it is unclear if the metabolic and transcriptomic responses to sucrose export will be similar to the metabolic and transcriptomic responses imposed by stimulation of environmental sensors. Environmental sensors include phytochromes that are known to be stimulated directly by certain wavelengths of light whereby the phytochrome then alters gene transcripts or cell metabolites (Los *et al.*, 2010). The transcriptional changes induced by direct light stimulation of phytochromes should not be a similar mechanism to how the cell responds to sucrose export because sucrose export does not alter light intensity. However, phytochrome stimulation can also lead to changes in metabolic pool sizes and the same metabolite pools might be affected by sucrose export. One metabolite that is affected by phytochromes is cyclic-AMP. cAMP levels are strongly correlated with cellular energy status and ATP levels and ATP levels will most likely be one of the metabolite pools affected by sucrose export. It is clear that the activation of a sucrose sink elicits changes to the rubisco content within the cell and possibly to rubisco localization to the

carboxysome (Chapter 3). I have presented preliminary data supporting these observations, but future work needs to substantiate my observations. These include the noticeable increase in fluorescence intensity and carboxysome size following sucrose export. Alterations to carboxysome size in response to sucrose export could be used as a novel model to study the regulation of carboxysome size. Likewise, an increase in the ratio of CcmM35:M58 suggests a mechanism of increasing rubisco packaging by M35 nucleation and M58 encapsulation (Chapter 3). Altered stoichiometry of M35:M58 presents itself as a relatively fast translational control mechanism for potentially altering carboxysome size. These cellular responses could be confirmed with a detailed proteomics study, with specific attention to protein stoichiometry changes within the carboxysome proteins and between the main photosynthetic complexes that are observed here (Figure 3.4). As proteomics costs continue to decrease, this experiment becomes more practical.

Photosynthetic engineering for more productive strains

The photosynthetic response to a heterologous sink must be confirmed in other bioproduction strains to determine if there are responses that are generalizable across strains engineered to secrete other metabolites versus responses that are specific to sucrose export. Indeed, it is likely that changes in metabolite pools downstream of the CB cycle will be strain specific, but the PET chain and the CB cycle responses will be universal in all expanded sink strains. Likewise, changes in CB metabolites or central metabolic energy molecules (ATP or NADPH) might show similar patterns in all strains engineered with a heterologous sink. For example, an increase in the CB cycle activity would increase the ATP and NADPH consumption rate leading to an increase in photosynthetic electron efficiency observed in this study (Chapter 2).

Finally, an increase in ΦII and qP (Figure 2.2) suggests heterologous sucrose export could be protect the cell in high light conditions (Figure 5.1). Oxygen evolution rates saturate at higher light intensities compared to cultures that are not exporting sucrose suggesting a greater ability for sucrose exporting cells to utilize light energy presumably leading to less photodamage at high irradiances. Indeed, greater photosynthetic inhibition occurs by restricting endogenous sinks (Chapter 4) potentially leading an accumulation of reducing molecules and increased photodamage. A lack endogenous sink capacity allows the heterologous sink to become one of the predominant photosynthetic sinks within the cell. I have shown this by growth arresting cells (Chapter 4.1 and Chapter 4.2) and by showing an increase in photosynthetic efficiency in sucrose exporting cultures.

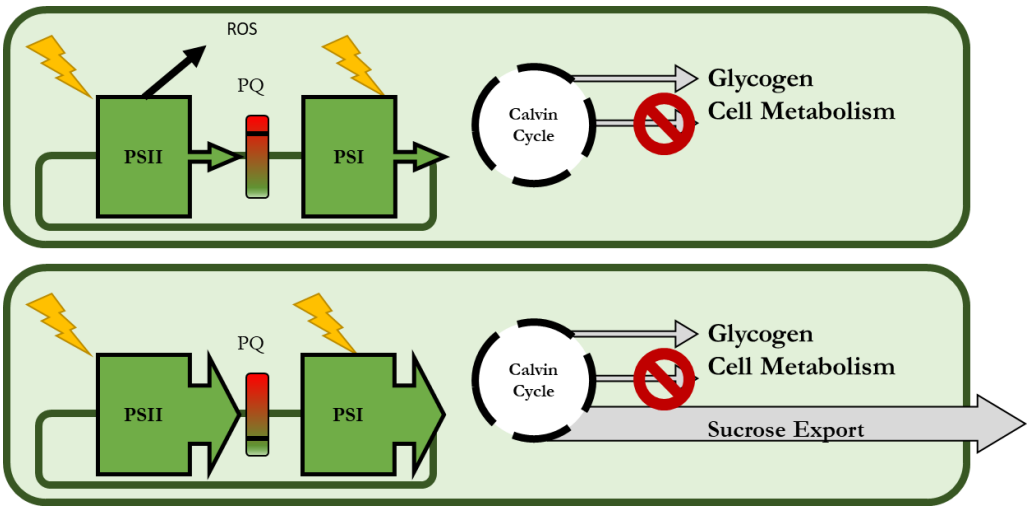

FIGURE 5.1: EVOLUTION AND SELECTION FOR IMPROVED BIOPRODUCTION. When induced to export sucrose, cells have a greater photosynthetic efficiency and oxidized plastoquinone pool. In mutant backgrounds that cause high light stress phenotypes, sucrose export might become beneficial as excess reductant is used predominantly for sucrose export (bottom) as opposed to performing side reactions with oxygen forming toxic ROS (top)

Nitrogen starved, Δ*glgC* strains are known to export high energy metabolites potentially as a photoprotective response (Gründel *et al.*, 2012). This photoprotective response could be mimicked with a heterologous sink by applying high light to the point of photodamage and toxicity. In Δ*glgC* cells starved of nitrogen I showed that less than 10% of the cells survived after 7d of nitrogen starvation (Figure 4.2.1). The cell lethality could be due to high light stress which causes ROS formation when excess electrons are not used (high NADPH or reduced PQ pool) or excitation energy cannot be dissipated effectively (Pospísil, 2009). Measurements of ROS should be performed initially to determine the photoprotective ability of sucrose export and under which light conditions ROS is observed. Similarly, NADPH measurements would be helpful in confirming an increase in excess reductant and an over-reduced cellular environment when endogenous sinks are restricted. Accumulation of NADPH has been shown in Δ*glgC* cells previously (Holland *et al.*, 2016) and might be exacerbated by restricting other endogenous sinks simultaneously. The determination of conditions where accumulation of NADPH, reduced PQ

pool and/or an accumulation of ROS species allows one to compete uninduced and sucrose exporting cells for increased fitness. If sucrose provides protection from high light toxicity, then sucrose exporting cells should survive longer than uninduced cells in high light conditions.

Finally, this body of evidence supports the idea that photosynthesis is feedback limited in ample light and CO_2 conditions. This is evident by the increased photosynthetic capacity and efficiency observed in the engineered strains with an expanded sink highlighted in this dissertation. Understanding the photosynthetic limitations will aid future engineering strategies for increased efficiency and production. This data advances the field by suggesting novel engineering strategies for enhancing strain productivity and efficiency.

REFERENCES

REFERENCES

Abramson, B. W. et al. (2016) 'Increased Photochemical Efficiency in Cyanobacteria via an Engineered Sucrose Sink', Plant and Cell Physiology, 0(October), pp. 1–10. doi: 10.1093/pcp/pcw169.

Ballicora, M. a, Iglesias, A. a and Preiss, J. (2003) 'ADP-glucose pyrophosphorylase, a regulatory enzyme for bacterial glycogen synthesis.', Microbiology and molecular biology reviews: MMBR, 67(2), p. 213–225, table of contents. doi: 10.1128/MMBR.67.2.213-225.2003.

Berepiki, A. et al. (2016) 'Tapping the Unused Potential of Photosynthesis with a Heterologous Electron Sink', ACS Synthetic Biology, 5(12), pp. 1369–1375. doi: 10.1021/acssynbio.6b00100.

Daley, S. M. E. et al. (2012) 'Regulation of the cyanobacterial CO2-concentrating mechanism involves internal sensing of NADP+ and a-ketogutarate levels by transcription factor CcmR', PLoS ONE, 7(7), pp. 1–10. doi: 10.1371/journal.pone.0041286.

Ducat, D. C. et al. (2012) 'Rerouting carbon flux to enhance photosynthetic productivity', Applied and Environmental Microbiology, 78, pp. 2660–2668. doi: 10.1128/AEM.07901-11.

Gründel, M. et al. (2012) 'Impaired glycogen synthesis causes metabolic overflow reactions and affects stress responses in the cyanobacterium Synechocystis sp. PCC 6803', Microbiology (United Kingdom), 158(12), pp. 3032–3043. doi: 10.1099/mic.0.062950-0.

Lindahl, M., Mata-Cabana, A. and Kieselbach, T. (2011) 'The disulfide proteome and other reactive cysteine proteomes: analysis and functional significance.', Antioxidants & redox signaling, 14(12), pp. 2581–2642. doi: 10.1089/ars.2010.3551.

Porchia, A. C., Curatti, L. and Salerno, G. L. (1999) 'Sucrose metabolism in cyanobacteria: Sucrose synthase from Anabaena sp. strain PCC 7119 is remarkably different from the plant enzymes with respect to substrate affinity and amino-terminal sequence', Planta, 210(1), pp. 34–40. doi: 10.1007/s004250050651.

Rolland, F., Baena-Gonzalez, E. and Sheen, J. (2006) 'Sugar sensing and signaling in plants: conserved and novel mechanisms.', Annual review of plant biology, 57, pp. 675–709. doi: 10.1146/annurev.arplant.57.032905.105441.

Ryu, J.-Y. et al. (2008) 'Cyanobacterial glucokinase complements the glucose sensing role of Arabidopsis thaliana hexokinase 1', Biochemical and Biophysical Research Communications, 374(3), pp. 454–459. doi: 10.1016/j.bbrc.2008.07.041.

Ungerer, J. et al. (2012) ‘Sustained photosynthetic conversion of CO2 to ethylene in recombinant cyanobacterium Synechocystis 6803’, Energy & Environmental Science, 5(10), p. 8998. doi: 10.1039/c2ee22555g.

Wang, X. et al. (2016) ‘Enhanced limonene production in cyanobacteria reveals photosynthesis limitations’, Proceedings of the National Academy of Sciences, p. 201613340. doi: 10.1073/pnas.1613340113.